Functional analysis of RAC1B during neuronal development

Thesis

Albertinazzi Chiara

FUNCTIONAL ANALYSIS OF RAC1B DURING NEURONAL DEVELOPMENT

Thesis submitted in partial fulfilment of the requirements of the Open University for the degree of Doctor in Philosophy in Molecular and Cellular Biology

November 2002

DIBIT

Department of Biological and Technological Research-Milan, Italy

Submission date: 31 October 200
Award date: 22 January 20

ProQuest LLC.
789 East Eisenhower Parkway
P.O. Box 1346
Ann Arbor, MI 48106 – 1346

DECLARATION

This Thesis has been composed by myself and has not been used in any previous application for a degree. The microinjection of recombinat ES cells was made by Jose Gonalez in my Institute. All the other results presented here were obtained by myself. Annalisa Bolis, Za Lorena and Sporchia Barbara have helped me with some of the biochemical experiment and with some northen blots. All sources of information are acknowledged by means of reference.

Some of the work presented in this thesis has been published in:

Albertinazzi C., Cattelino A., de Curtis I. (1999)

Rac GTPases localize at sites of actin reorganization during dynamic remodeling of cytoskeleton of normal embryonic fibroblasts.

J Cell Sci. 112, 3821-3831.

Albertinazzi C., Za L., Paris S., de Curtis (2002)

Arf6 and a functional PIX/p95-APP1 complex are required for Rac1B-mediated neurite outgrowth.

Mol. Biol. Cell (in press)

ABSTRACT

Neurite extension requires the concerted action of a number of events including actin polymerization at the growth cone, formation of new adhesive sites to the substrate, and membrane addition, to extend the surface of the elongating neurite. The small GTPase Rac1B, identified from developing chicken retina, is specifically expressed during neural development, and overexpression of Rac1B in embryonic retinal neurons specifically stimulates neurite extension and branching (Albertinazzi et al., 1998). Very little is known about the molecular mechanisms which coordinate Rac1B-mediated neurite extension. In order to study in detail this mechanism in an *in vivo* system, recombinant embryonic stem cells (ES) for the deletion of mouse Rac1B gene were produced. ES cells from four independent clones that resulted positive for the deletion of mouse Rac1B gene were microinjected in blastocysts, and chimeric mice were generated to be used for the generation of Rac1B-null mice.

Recently, p95-APP1 was identified as a protein able to interact with Rac1B in a GTP-dependent manner (Di Cesare et al. 2000). P95-APP1 is an ArfGAP of the GIT family, highly expressed in the developing nervous system. Expression of p95-APP1 with a mutated or deleted ArfGAP domain in retinal neurons prevented Rac1B-induced neuritogenesis, leading to PIX-mediated accumulation of mutant p95-APP1 and associated proteins at large Rab11-positive endocytic vesicles. Analysis of neurons expressing different p95-derived constructs together with wild-type or mutant Arf6 GTPases revealed the requirement of both p95-APP1 and a cycling Arf6 for a normal Rac1B-mediated neuritogenesis.

The data obtained in this thesis show a functional connection between the localization of the p95-APP1 complex at recycling endosomes and Rac1B-dependent

neuritogenesis, and suggest a role of this complex in the regulation of membrane recycling to/from the neuronal surface during neuritogenesis.

CONTENTS

- Chapter 1 -

- *Chapter 2 –*

Chapter 1

INTRODUCTION

1.1 MECHANISMS OF ADHESION AND MIGRATION

Many metazoan cell types, for example fibroblasts or epithelial cells, can become polarized in response to an extracellular stimulus and migrate in a unidirectional fashion. This ability is essential for cells to function in their natural environment. For example, the development of the nervous system in vertebrates requires many complex patterns of cellular migration. Epithelial cells need to migrate in order to close wounds in the epithelial layer, whereas motile fibroblasts are crucial for tissue remodeling. Conversely, improper regulation of cell migration is the basis of many abnormal processes, resulting, for example, in the invasiveness of tumor cells. Not surprisingly, there is considerable interest in understanding the molecular basis of cell migration, since this could lead to new therapeutic strategies for various pathological processes. Cell migration requires the integration and temporal coordination of many different processes that occur in spatially distinct locations in the cell. Migration can be viewed as a multistep cycle. The basic migratory cycle includes extension of a protrusion, the formation of stable attachments near the leading edge of the protrusion, the translocation of the cell body forward, release of adhesions and retraction at the cell rear (Fig.1.1). Polymerization of the actin cytoskeletal network drives the initial extension of the plasma membrane at the leading edge, and promotes extension of lamellipodia. Then it is important to link the growing actin filaments at the leading edge to the substratum with the formation of adhesion sites by the recruitment of adhesion components. The interaction of the integrin family of transmembrane

receptors with the extracellular matrix stabilizes the adhesions by recruiting signaling and cytoskeletal proteins. These small, nascent adhesions may transmit strong forces, and serve as traction points for the propulsive forces that move the cell body forward.

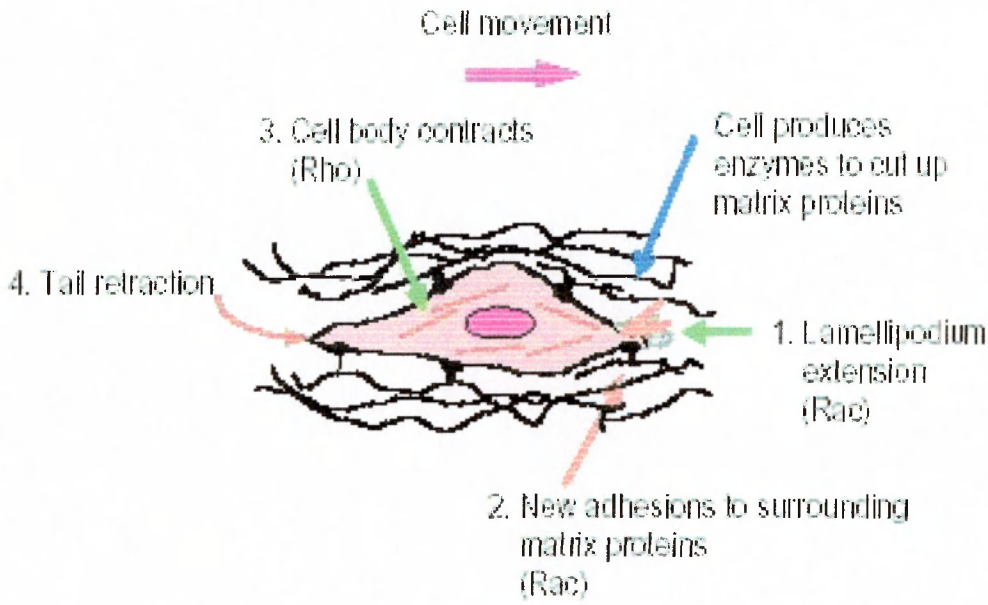

Fig.1.1: A model for the steps of cell migration.

A migrating cell extends a lamellipodium at the front. This extension is stabilized through the formation of new adhesions to the extracellular matrix. The cell body is moved forward by actomyosin-mediated contraction. Finally, the tail of the cell detaches from the substratum and retracts. Migrating cells also secrete proteases that cleave extracellular matrix proteins, and this is important for cell movement through three-dimensional matrices. (From Ridley, A.J., 2001).

Release of adhesions and retraction at the rear completes the migratory cycle, thus allowing the net translocation of the cell in the direction of movement. The formation and disassembly of adhesive complexes are complicated processes and require a coordinated interaction of actin and actin-binding proteins, signaling molecules, structural proteins, integrins, adaptor molecules and microtubules. It is also important the activation of proteases that cleave extracellular matrix proteins.

1.1.1 The Rho family GTP-binding proteins in the process of cell migration.

1.1.1.1 The Rho family of small GTPases

Rho GTPases are members of the Ras superfamily of monomeric 20-30 kDa GTP-binding proteins. At least 20 different Rho GTPases have been identified in human, including multiple isoforms: Rho (A, B, C isoforms), Rac (1, 2, 3/1B isoforms), Cdc42 (Cdc42Hs, G25K, TC10 isoforms), Rnd1/Rho6, Rnd2/Rho7, Rnd3/RhoE, RhoD, RhoG, and TTF. The most extensively characterized members are RhoA, Rac1 and Cdc42 (Table 1.1, from Ridley, A.J. 2001).

Table 1. Rho family members in humans, *Drosophila melanogaster*, *C. elegans* and *Dictyostelium discoideum*

Subfamily	Humans	*Drosophila*	*C. elegans*	*Dictyostelium*
Rho	RhoA, B, C	Rho1	Rho1	None
Rac	Rac1*,2, Rac3/1B	Rac1,2	Rac1/CED10, Rac2	Rac1a,b,c, RacF1,2, RacB
Cdc42h	Cdc42/G25K*, TC10 TCL, Chp1,2	Cdc42	Cdc42	None
Mig2	RhoG	Mtl/Mig2-like	Mig2	None
Rnd	Rnd1,2, RhoE/Rnd3	None	None	None
RhoBTB	RhoBTB1,2	RhoBTB	None	RacA
Others (not classified in subfamilies)	RhoD, Rif, TTF/RhoH	RhoL/Rac3	None	RacC*,D,E, RacG-J,L

*Splice variants known.

These three GTPases are well conserved across a wide range of species. In many cases there has been expansion into a number of closely related isoforms (Table 1.1) that bind to an overlapping set of effectors.

Each of these GTPases act as a molecular switch, cycling between an active GTP-

bound, and an inactive GDP-bound state that have different conformations (Fig. 1.2). In the GTP-bound form they are able to interact with effector or target molecules to initiate a downstream response, while an intrinsic GTPase activity returns the proteins to the GDP-bound state, to complete the cycle and terminate signal transduction. Rho proteins hydrolyze GTP at slow rates in vitro, and this reaction is catalyzed by GTPase-activating proteins (GAPs). At least 53 GTPase-activating proteins (GAPs), which increase the intrinsic rate of GTP hydrolysis of Rho GTPases, have been identified to date (Peck, J et al., 2002). A comparison of the crystal structures of a groundstate complex between RhoGAP and Cdc42 and a transition-state-mimicking complex of Rho- GAP with RhoA-GDP-AIF4-, along with NMR analysis of a Cdc42-RhoGAP complex, has suggested the details of GAP-induced GTP hydrolysis (Rittinger et al., 1997a and b; Nassar et al. 1998). A 20° rotation between GTPase and GAP allows an arginine residue in the GAP protein, the "arginine finger", to enter the GTPase active site and participate in the stabilization of the transition state.

Other regulators of the cycle are guanine nucleotide exchange factors (GEFs) that help the proteins to be reloaded with the GTP. Over 60 guanosine nucleotide exchange factors (GEFs) have been identified that facilitate the exchange of GDP for GTP (Schmidt and Hall, 2002). All Rho GEFs contain a Dbl homology (DH) domain which encodes the catalytic activity (Cherfils et al., 1999; Hart et al., 1996) and most an adjacent pleckstrin homology (PH) domain. The PH domain is thought to mediate membrane localization through lipid binding but, in addition, structural and biochemical evidence suggests that it might directly affect the activity of the DH domain (Rameh et al., 1997). A specific component of the GEF is DOCK180, which contains a novel identified domain, Docker, that specifically recognizes nucleotide-free Rac and can mediate GTP loading of Rac in vitro (Brugnera et al., 2002). Additional domains specific to each GEF

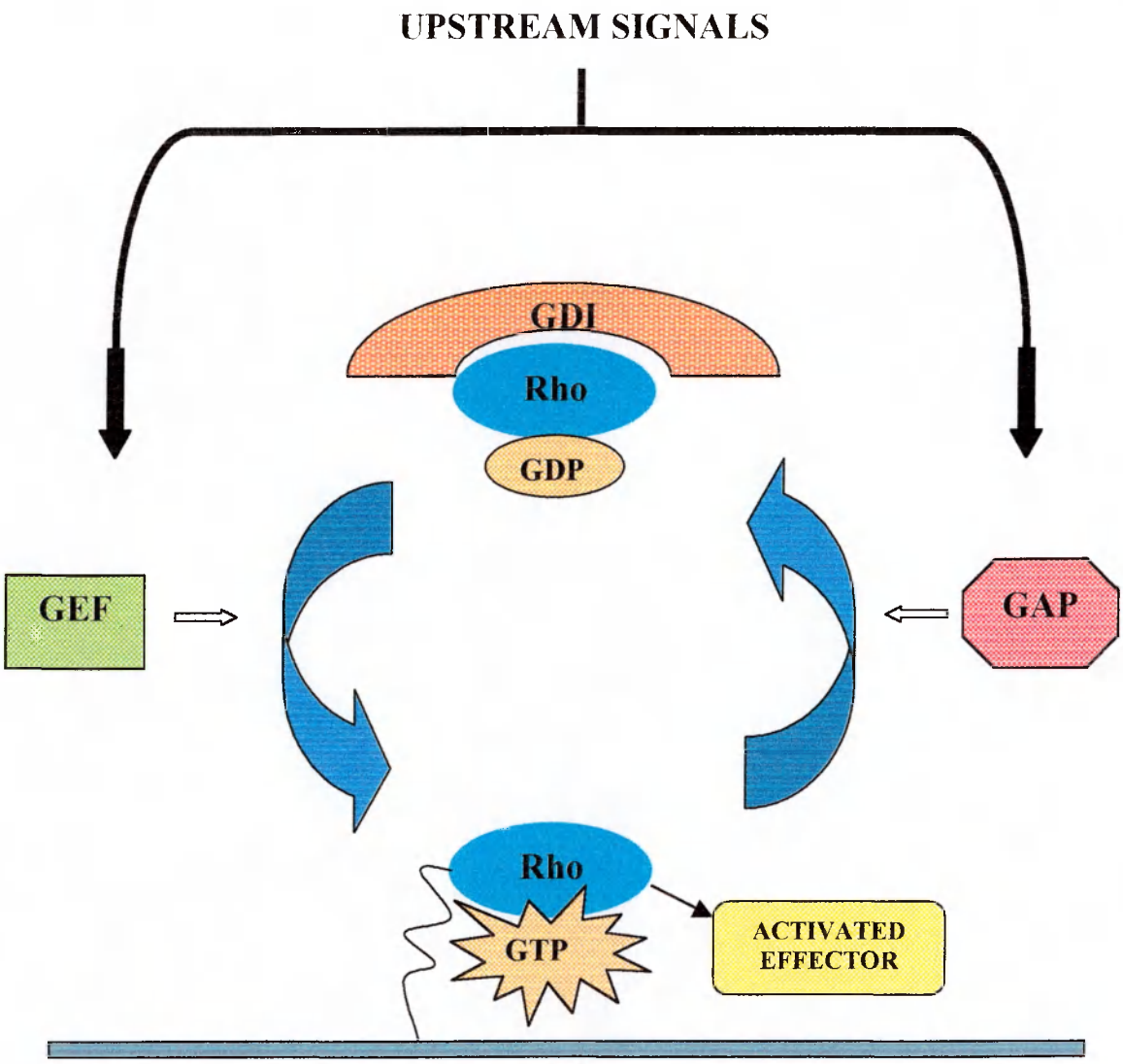

Fig. 1.2. The GTPase cycle: Rho GTPases act as molecular switches**.** Upstream signals transduce signals to Rho GTPases through regulation of the activities of guanine nucleotide exchange factors (GEF) or GTPase-activating proteins (GAP), which facilitate switching on or switching off Rho GTPases. In their GTP-bound state, Rho GTPases bind to and activate their effectors to transduce the signal downstream, and they can associate to the plasma membrane or membrane of internal organelles.

may provide variations in subcellular localization and activation mechanisms. Most Rho proteins are post-translationally modified at their C-termini by prenylation of a conserved cysteine, which is required for their interaction with membranes (Seabra, 1998). In addition, Rho proteins can bind to proteins known
as GDIs (guanine nucleotide dissociation inhibitors) which prevent their interaction with the plasma membrane (but not necessarily with downstream targets) (Carpenter et al., 1999; Hansen and Nelson, 2001).

The major function of Rho GTPases is to regulate the assembly and organization of the actin cytoskeleton (Hall, A., 1998). The effects of Rho, Rac and Cdc42 were initially described using Swiss3T3 fibroblasts, a cell line in which serum starvation creates a low background of organized F-actin structures. Addition of lysophosphatidic acid induces the formation of contractile actin-myosin stress fibres and associated focal adhesions, which can be blocked by C3 transferase which ribosylates and inactivates Rho proteins (Ridley, A. J. and Hall, A. 1992).

Growth factors, such as platelet-derived growth factor (PDGF), insulin or epidermal growth factor (EGF) induce the formation of actin-rich lamellipodia and membrane ruffles associated with focal contacts. The dominant-negative N17Rac specifically inhibits this response (Ridley et al., 1992). Finally bradykinin induces the formation of peripheral microspikes or filopodia, which are also associated with focal contacts. These effects can be inhibited by expression of dominant negative N17Cdc42 (Kozma et al., 1995). These types of experiment have lead to the conclusion that Rho, Rac and Cdc42 regulate three signal transduction pathways linking various membrane receptors to the assembly of actin-myosin filaments, lamellipodia and filopodia respectively. It is not surprising, therefore, that Rho GTPases have been found to play a role in a variety of cellular processes that are dependent on the actin cytoskeleton, such as cytokinesis (Prokopengo et al., 2000), phagocytosis (Caron et al., 1998), pinocytosis (Ridley et al.

1992), cell migration (Nobes and Hall, 1999), morphogenesis (Settleman, J. 1999) and axon guidance (Luo et al., 1997).

One of the most interesting aspects of this family of regulatory proteins is that, in addition to their effects on the actin cytoskeleton, they also regulate a variety of other biochemical pathways including those linked to the c-jun N-terminal kinase (JNK) and p38 mitogen activated protein kinase regulation, the phagocytic NADPH oxidase complex activity, the G1 cell-cycle progression, the assembly of cadherin containing cell-cell contacts, the secretion in mast cells and cell transformation. Therefore, although Rho GTPases are best characterized for their effects on the actin cytoskeleton, there is now much interest in their ability to affect cell proliferation and gene transcription, and the contribution of all of these activities to malignant transformation is an important field of study.

1.1.1.2 Rho GTPases effectors

A great deal of effort has been put into identifying their cellular targets or effector proteins. To date at least 30 potential effectors for Rho, Rac and Cdc42 have been identified, primarily using affinity chromatography and the yeast two-hybrid system. These proteins interact specifically with the GTP-bound form of the GTPase. The conformational differences between the GTP- and GDP-bound forms are restricted primarily to two surface loops, named switch regions I and II (Cdc42/Rac amino acids 26-45 and 59-74 respectively) (Ihara et al., 1998; Wei et al, 1997). Effector proteins must, therefore, utilize these differences to discriminate between the GTP and GDP bound forms, though they also interact with other regions of the GTPase.

Numerous point mutations have been introduced into Switch I of Rho, Rac and Cdc42, often referred to as the "effector region", and have rather interesting effects preventing the binding of some, but not all, target proteins (Lamarche et al., 1996; Joneson et al., 1996; Sahai et al., 1998), suggesting that different effectors interact with different

residues within the switch I region. Further studies using GTPase mutants and chimaeras have implicated regions outside of switch I in the binding of effectors. For instance, an α-helical region present in all Rho-family GTPases, but not in Ras, referred to as the "insert region" (Rac amino acids 123-135), is required for Rac1 activation of the NADPH oxidase complex and for binding to an effector protein called IQGAP, but not for its interaction with PAK. These data indicate that distinct regions of Rac, Cdc42 and Rho outside of switch I are required to make contacts with effector proteins.

The data obtained from the many mutational studies show a complex, and sometimes contradictory, picture of the mechanisms of Rho GTPase effector interactions. However, the recently reported NMR structures of Cdc42 bound to activated Cdc42-associated tyrosine kinase ACK (amino acids 504-545) and WASP (amino acids 230-288) have provided some informations (Mott et al., 1999; Abdul-Manan et al., 1999). ACK and WASP both contain the conserved GTPase-binding consensus site, the CRIB (Cdc42/Rac-interactive binding) motif, which is present in many, though not all, Rac- and Cdc42-binding proteins. This motif is necessary, but not sufficient, for strong binding to the GTPase. These NMR studies show that Asp38 in Switch I interacts with the two His residues conserved in all CRIB proteins. Interestingly Switch I and II are almost identical in Rho, Rac and Cdc42, except for position 38 which is Asp in Rac/Cdc42 and Glu in Rho, and it seems that all CRIB proteins may use Asp38 to distinguish Rac/Cdc42 from Rho.

However, not all Rac/Cdc42 effector proteins contain a CRIB domain (for example IQGAP1), so probably the binding to the GTPase is different in these cases.

Rho binding to its effector proteins also appears, from mutational studies, to require quite different GTPase regions compared with Rac and Cdc42. Some Rho effectors such as protein kinase N (PKN)/PRK1 and PRK2, rhophilin and rhotekin, bind

to Rho via an N-terminal Rho effector homology (REM) region which contains three repeats of a leucine-zipper-like motif named HR1 (Flynn et al., 1998).

The most common mechanism of effector activation by Rho GTPases appears to be the disruption of intramolecular autoinhibitory interactions, to expose functional domains within the effector protein. For example the Rac/Cdc42 targets PAK Ser/Thr kinases, have an intramolecular regulatory domain that inhibits kinase activity. Upon GTPase binding, the inhibitory sequence is displaced, leaving the kinase domain free to bind to and phosphorylate substrates (Bagrodia, S. and Cerione, R. A., 1999; Tu, H. and Wigler, M. 1999). Two kinases that are Rho effectors have also been reported to contain autoinhibitory domains, ROK and PKN. A similar principal may also apply to activation of the many scaffold-like targets of GTPases. Dia is thought to act as a scaffold protein that can be activated by Rho and then interacts with profilin/actin. Recent work has revealed that the N-terminal 389 amino acids interact with a region at the C-terminus which makes Dia inactive. Binding of Rho to the N-terminal sequence relieves this inhibition. WASP and N-WASP, two related Cdc42 targets, also appear to be regulated by an intramolecular interaction. The regions of WASP that bind to each other have recently been identified, as the N-terminal GTPase-binding domain and a cofilin-homology region at the C-terminus (Kim et al., 2000). Cdc42-GTP competes with WASP C-terminus for binding to the N-terminus and induces a conformational change in the WASP N-terminus. Owing to autoinhibitory interactions, full-length N-WASP has decreased ability to activate the Arp2/3 complex compared with the functionally important C-terminal acidic region alone, and Cdc42-GTP can activate N-WASP by releasing intramolecular interactions (Rohatgi et al., 1999). A variation on this mode of effector activation has been suggested for the Cdc42-binding protein IQGAP. In this case a separate protein, calmodulin-Ca^{2+}, binds to IQGAP (via its IQ motif) and inhibits its binding to actin and Cdc42 (Joyal et al., 1997). This might

provide a calcium-sensitive regulatory mechanism for controlling the activation of IQGAP.

Almost all Rho GTPase effectors have multiple domains, and some of these might regulate their activity. Protein-protein interactions can regulate the subcellular localization of GTPase effectors. For example, WASP and PAK contain classic proline-rich SH3-binding motifs which have been reported to bind to the adaptor Nck (Rivero-Lezcano et al., 1995; Bokoch et al., 1996). It is noteworthy that many of the Rho GTPase effector proteins contain coiled-coil regions (ROK, citron, IQGAP, Dia), which in some proteins have been shown to facilitate oligomerization. Effector oligomerization could represent another level of complexity to target activation by Rho GTPases.

1.1.1.3 Rac effectors implicated in actin reorganization

Rho family GTPases are a key regulators of adhesion dynamics. To date there are few examples of unique Rac effectors that have been implicated in actin reorganization. POR-1 (Partner of Rac) has been implicated in Rac-induced lamellipodium formation, since truncations act as dominant negative constructs (Van Aelst et al. 1996; D'Souza Schorey et al., 1997), and p140Sra-1 (Specific Rac1-associated protein) cosediments with F-actin, implying a role in Rac1-induced actin reorganization (Kobayashi et al., 1998). However, little more is known about the cellular functions of these two proteins. A better characterized target of Rac1 is PI(4)P5K. Rac1 interacts directly with PI-4-P5K, though this interaction is not GTP-dependent. It has been established, using permeabilized platelets, that thrombin-induced actin-filament assembly requires actin-filament uncapping, which is absolutely dependent upon an increase in PIP_2 levels, and that this is mediated by Rac1 activation of a type I PI-4-P5K (Hartwig et al., 1998; Tolias et al., 2000).

Interestingly, WASP-like Verprolin-homologous proteins (WAVE1, 2 and 3) can be precipitated with Rac1, though this is not through a direct interaction. WAVE localizes to membrane ruffles, and its overexpression causes actin clusters, an activity which requires the profilin binding and verprolin-homology (actin-binding) domains. A verprolin-homology-domain mutant of WAVE inhibits Rac1 induced ruffling, further suggesting an *in vivo* link between Rac1 and WAVE (Miki et al., 1998). It was shown that activated Rac binds to IRSp53, a substrate for insulin receptor with unknown function, and carboxy-terminal domain of IRSp53 binds to WAVE to form a trimolecular complex. From studies of ectopic expression, it was found that IRSp53 is essential for Rac to induce membrane ruffling, probably because it recruits WAVE, which stimulates actin polymerization mediated by the Arp2/3 complex (Miki et al., 2000). Another mechanism by which Rac WAVE seem to be involved in actin reorganization is through the adapter protein Nck. WAVE1 exists in a heterotetrameric complex that is inactive. Rac1 and Nck cause dissociation of the WAVE1 complex, which releases the active WAVE1 and leads to actin nucleation (Eden et al., 2002).

Some common target proteins appear to be utilized by both Rac1 and Cdc42 in the induction of lamellipodia and filopodia respectively. PAKs are Ser/Thr kinases, related to yeast Ste20 (Manser et al., 1994; Manser et al., 1995; Bagrodia et al., 1995). There have been conflicting reports linking PAKs to actin changes. Activated mutants of PAK1 have been reported to induce both filopodia and membrane ruffles in Swiss3T3 cells, similar to the effects of constitutively active Cdc42 and Rac1 (Sells et al., 1997). PAK1 has been seen to localize to membrane ruffles, as well as phagocytic actin-containing cups, in *N*-formylmethionyl-leucylphenylalanine-stimulated neutrophils (Dharmawardhane et al., 1997). Interestingly, PAK-induced cytoskeletal changes are independent of its kinase activity, but require membrane targeting (Daniels et al., 1998; Lu et al., 1997). Other groups, however, have failed to find any effects of PAK

overexpression on the actin cytoskeleton (Lamarche et al., 1996), and, taken together, these results suggest that PAKs could be capable of affecting the actin cytoskeleton but only in cooperation with other signals that may or may not be present in the cells tested. A variety of substrates for PAKs have been identified that could affect the actin cytoskeleton. Rac1, like RhoA, induces phosphorylation of LIMK (Arber et al., 1998), and PAK1 has been shown to phosphorylate LIMK *in vitro*, which in turn phosphorylates cofilin (Edwards et al., 1999). Moreover, an inactive form of LIMK has been shown to inhibit both Cdc42 and Rac induced actin changes, suggesting that cofilin phosphorylation may be a general requirement in Rho GTPase pathways. PAK has been reported to phosphorylate and inactivate MLC kinase, decreasing MLC phosphorylation and reducing actomyosin assembly (Sanders et al., 1999).

1.2 NEURITOGENESIS: A PARTICULAR FORM OF MIGRATION

The integrity of the nervous system depends on highly specific connections between neurons during development in order to form the correct neuronal circuits that characterize the adult nervous system. This specificity requires neurite extension towards specific directions, a process that is mediated by the growth cone, a specialized structure located at the distal tip of growing neurites. Neurite extension during development can be considered as a particular form of cell migration. It is an important event that requires a significant metabolic effort to sustain the increase in molecular synthesis necessary for plasma membrane expansion. In addition, neurite extension involves changes in the subset of expressed proteins and the reorganization of the cytoskeleton. These events are driven by environmental cues which activate signal transduction pathways inside the cells. In the context of the developing embryo, extracellular guiding cues, cell-cell interactions and soluble factors create a network of interactions that are responsible for neurite outgrowth, polarization, axon guidance to

and from choice points, axonal fasciculation and target selection. The balance between positive and negative signals that produce growth or collapse, attraction or repulsion of the growth cone, is important. In addition, the dynamic regulation of the receptors for the extracellular cues contributes to modify the possible responses of single neurites.

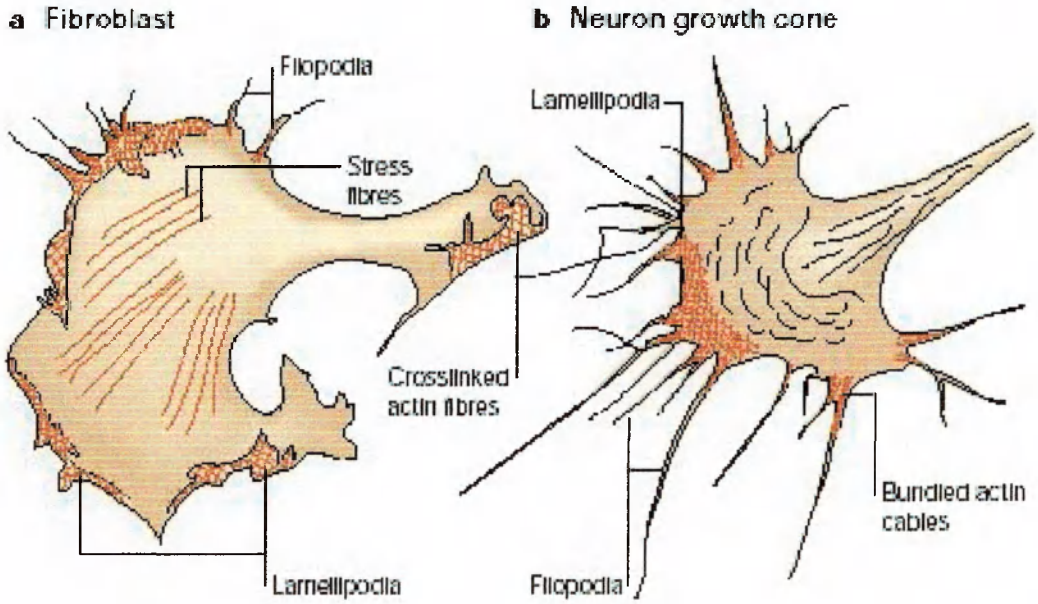

Fig. 1.3. Actin-based structures in a fibroblast and a neuronal growth cone. Prominent F-actin based structures in (**a**) a migrating fibroblast and (**b**) a neuronal growth cone.

Lamellipodia are structures at the edge of cells composed of a crosslinked F-actin meshwork. Filopodia are long, thin protrusions at the periphery of cells and growth cones. They are composed of F-actin bundles. (From Luo L., 2000)

1.2.1 The growth cone

Elongating axons terminate in a protuberance called *growth cone* (fig. 3). This specialized structure is able to explore the environment and to transduce positive and negative signals that regulate intracellular events as the basis of neurite navigation. The structure of the growth cone can be divided into three major parts. First, there is a central core rich in microtubules, mitochondria, and a variety of organelles. Projecting from the core are long membrane extension called filopodia, and between the filopodia, membrane veils

called lamellipodia. Filopodia and lamellipodia are motile structures, and the sensory capability of the growth cone depends in large part on its filopodia. They are thin (0,2-0,4 μm) actin rich spike-like projections up to 40 μm long, that present on their surface membrane receptors for the molecules that serve as directional cues for the axon. Their length allows them to explore the environment far ahead of the central core, and their flexibility allows them to navigate between cells or other obstacles. The shape of filopodia and lamellipodia is determined by the organization of the actin cytoskeleton. At the core of each filopodium is a dense, cross-linked bundle of actin filaments, while the lamellipodium includes long crossed actin filaments. The dynamic properties of these membrane structures are thought to be determined by three main processes: the assembly of actin filaments at the cell membrane, the disassembly of actin filaments at sites in the growth cone centre, and the translocation of the F-actin network from the leading edge toward the centre in a process called retrograde flow (Forscher and Smith, 1988). It has been proposed that when cell surface receptors bind extracellular matrix ligands, they recruit a multiprotein complex that links the receptor to the actin cytoskeleton. This retards the retrograde flow of F-actin relative to the substrate, allowing the continued assembly of F-actin at the leading edge, and the action of actin-

based motors to cause protrusion of the lamella, and consequently cell movement in that direction. Probably, a myosin-type motor is responsible for retrograde flux. Many forms of myosins was found in growth cones (Ruppert et al., 1993).

The final step involves the microtubules: they are also prominent cytoskeletal components in the neurites. They elongate and provide support for the extending neurite and are substrate for axonal organelle transport. At the level of the growth cone they remain in the central core of this structure, but they are also characterized by assembly and disassembly in the actin-rich peripheral domain. Pharmacological studies using drugs that inhibit dynamic instability of microtubules reveal that both axonal advance and growth cone guidance depend on dynamic microtubules (Yamada et al., 1970; Tanaka et al., 1995).

1.2.2 Substrate-cytoskeleton coupling in growth cones

It is established that growth cone motility involves cytoskeleton dynamics and cell-substrate adhesion. Growth cones can move forward if they are capable of coupling intracellular actomyosin-based motility to an extracellular substrate via cell surface receptors. These receptors must form a strong linkage between the substrate and the actin cytoskeleton allowing actomyosin contractions to pull the growth cone forward. The classical neuronal cell adhesion molecules belong to three distinct structural families: integrins, cadherins and IgCAMs.

Integrins are important heterodimeric receptors that interact with extracellular matrix molecules. They are widely expressed in the nervous system and play a role in different processes such as neuronal migration, axonal growth and guidance by attaching to matrix proteins such as laminin, fibronectin and tenascin. Informations about the proteins that link integrins to the actin cytoskeleton come largely from studies on focal adhesions formed by nonneuronal cells in culture. Several cytoskeletal associated components, such as vinculin, talin, and paxillin, and signalling molecules

(Fak, Src and Rho) participate in this process. Many of these proteins have been detected in growth cones, in support of a role for integrin-cytoskeletal coupling in growth cone motility.

Cadherins are Ca^{2+}-dependent molecules involved in homophilic interactions that play important roles in morphogenesis both in neuronal and nonneuronal cells. The linkage between cadherins and the actin cyoskeleton is described. The general structure of the linkage involves either β-catenin or γ-catenin binding to the cytoplasmic domain of cadherin as well as to α-catenin, which is thought to link the cadherin/catenin complex to the actin cytoskeleton (Aberle et al., 1996). Several studies *in vitro* have demonstrated the function of N-cadherin in promoting neurite outgrowth, either when presented as purified protein substrate or when expressed on the surface of cells (Neugebauer et al., 1988; Payne et al. 1992).

The Ig superfamily is the largest family of structurally related proteins all characterized by the presence of at least one Ig domain. The first neuronal member identified as a mediator of cell adhesion of retina cells is NCAM (Hoffman et al., 1982). Several neuronal IgCAMs have been demonstrated to undergo multiple homophilic and heterophilic interactions, but the details of their interaction with the cytoskeleton are less known. Most is known about ankyrin and its role in linking L1 family members to spectrin/actin cytoskeleton (Davis and Bennet, 1994).

1.2.3 Families of attractive and repulsive guidance molecules

Genetic, biochemical and molecular approaches have identified four conserved families of neuronal guidance cues with prominent developmental effects: the netrins, Slits, semaphorins and ephrins (Table 1.2). Netrins, Slits and some semaphorins are secreted molecules that associate with cells or extracellular matrix, whereas ephrins and other semaphorins are expressed at the cell surface.

The signaling pathways in axon guidance are not fully understood, but it is likely that they act locally and they are converted into local changes in the actin cytoskeleton of the growth cone, which modulate the stability of the growth cone.

GUIDANCE MOLECULES	*RECEPTORS*
Netrins	UNC40, UNC5
Slits	Robos
Semaphorins	Neuropilin, Plexins
Ephrins	Eph receptors

Table 1.2. Families of guidance molecules and receptors for neurite navigation.

The activity of guidance pathways is regulated both by transcriptional modulation and by post-transcriptional mechanisms that influence the availability of receptors and ligands. These include receptor downregulation, ligand-induced inactivation of receptors, alternative splicing, and regulated proteolysis.

1.2.4 Role of Rho GTPases in the process of neuritogenesis

Neurons are terminally differentiated cells with specialized cytoskeletal extensions. Therefore, the role of Rho GTPases in neuronal function is expected to be more complicated than in fibroblasts. Over the past several years, Rho GTPases have been implicated in many different aspects of neuronal development, ranging from the initiation of neurite, to neurite elongation, establishment of axon dendrites (cell polarity), and growth cone in response to guidance molecules.

1.2.4.1 Neurite extension

The first investigations of Rho GTPases in neurons identified their function in regulating outgrowth and retraction of neurites (Luo et al., 1994; Jalink et al. 1994).
In *Drosophila melanogaster* embryonic sensory neurons, expression of either constitutively active or dominant negative Drac1 results in selective defects in axonal outgrowth (both initiation and elongation), without notably affecting dendrite growth. Similar mutations in Dcdc42 affected both axons and dendrites (Luo et al., 1994). Expression of constitutively active Rac1 had a similar selective effect on the growth of axons (but not dendrites) in cerebellar Purkinje cells in transgenic mice (Luo et al., 1996). RhoA is thought to mediate neurite retraction, because activation of RhoA in neuronal cell lines led to neurite retraction, whereas expression of dominant negative RhoA prevented neurite retraction in response to extracellular stimuli (Jalink et al., 1994). Later studies in systems from neuron-like cell lines and primary neurons, to *in*

vivo systems, support the following general scheme. Rac1 and Cdc42 seem to be positive regulators (Kozma et al., 1997; Lamoureux et al., 1997; Albertinazzi et al. 1998; Ruchhoeft et al., 1999; Brown et al., 2000), whereas RhoA seems to be a negative regulator (Jalink et al., 1994; Kozma et al., 1997; van Leeuwen et al., 1997; Kalman et al., 1999; Yamashita et al., 1999) of process outgrowth, although there are exceptions (Jin and Strittmatter, 1997; Vastrik et al., 1999). These distinct effects of different Rho GTPases, as well as the differential effects of each Rho GTPase in different neuronal compartments, indicate that the function of Rho GTPases may be more complex in neurons than in fibroblasts. Often, the expression of constitutively active and dominant-negative GTPase mutants produce similar, rather than opposite, phenotypes (Luo et al, 1994; Ruchhoeft et al., 1999; Zipkin et al., 1997). This might mean that the Rho GTPase signalling pathway has a cyclic mode of action. For example, if filopodia are required to cycle between extension and retraction during axonal growth for the growth cone to advance, then blocking filopodia in either state (with either constitutively active or dominant negative GTPase mutants) would have the same net outcome of decreased neurite outgrowth.

Rho GTPases are also involved in guiding growing axons. As axons grow, their growth cones encounter many cues that guide them towards or away from specific cells or pathways. Guidance cues act by causing the selective stabilization or destabilization of actin-based filopodia and lamellipodia. Accumulating evidence indicates that Rho GTPases participate in mediating these actions. In *Caenorhabditis elegans*, mutations in a Rho-like GTPase *mig-2* (*migration 2*) caused both outgrowth defects and guidance defects (Zipkin et al., 1997). Similarly, in *Drosophila*, expression of dominant-negative Rac1 caused motor axon guidance errors at specific choice points (Kaufmann et al., 1998). In addition, overexpression of dominant-negative Rho or wild-type Cdc42

caused axon guidance defects in *Xenopus laevis* retinal ganglion neurons *in vivo* (Ruchhoeft et al., 1999).

Genetic loss-of-function mutants in GEFs for Rho GTPases or in downstream effectors have also been shown to result in axon guidance defects (Steven et al., 1998; Awasaki et al., 2000; Bateman et al., 2000; Liebl et al., 2000, Newsome et al., 2000), further supporting the role of Rho GTPases in axon guidance.

1.2.4.2 Dendrites growth and remodeling

Dendrites and dendritic branches are highly dynamic and they might contribute to the structural basis of neural plasticity.

The functions of Rho GTPases have been examined by expressing dominant-negative and constitutively active mutants in several systems, including Purkinje cells of transgenic mice (Luo et al., 1996), rat cortical neurons (Threadgil et al., 1997), *Xenopus* retinal ganglion cells (Wong et al., 2000) and tectal neurons *in vivo* (Li et al., 2000), and pyramidal neurons in hippocampus slices (Nakayama et al., 2000). The role of Rho was further supported by genetic analysis of RhoA using null mutations in mosaic *Drosophila* brains, in which RhoA mutant neurons overextended their dendrites (Lee et al., 2000)). As for the regulation of axonal outgrowth, the results identify Rac1 and Cdc42 as positive regulators of dendrite growth and dynamics, whereas RhoA is a negative regulator.

Another special feature of dendrites that might contribute to neural plasticity is dendritic spines, which are special protrusions that are the primary sites of excitatory synapses and might be the basic unit of synaptic integration. Perturbation of Rac activity in cerebellar Purkinje cells or hippocampal pyramidal neurons resulted in an increase in the formation of dendritic spines, smaller than in normal mice, with minimal effect on dendrite growth and branching (Luo et al., 1996). This indicates that regulation of Rac1

activity might be crucial for the morphological development and plasticity of dendritic spines.

1.2.4.3 Neuronal polarity

There is evidence for a possible involvement of Rho GTPases in establishing neuronal polarity. Hippocampal pyramidal neurons in primary culture have long been a model system of the initial events leading to the establishment of neuronal polarity (Bradke, F. and Dotti, C.G., 2000). Shortly before axon formation, the actin cytoskeleton in the growth cone of future axons becomes selectively dynamic and unstable compared with growth cones of future dendrites. Treatment of cultured hippocampal neurons with the Rho GTPase inhibitor toxin B mimicked the actin destabilization in growth cones to generate several axon-like processes (Bradke, F. and Dotti, C.G., 1999). However, because toxin B inactivates several Rho GTPases, it is not clear which of the GTPases is/are involved in this process. Some evidence indicates that Rac1 might be involved in establishing polarity, since perturbation of Rac1 function preferentially affects the outgrowth of axons *in vivo* (Luo et al., 1994; Luo et al., 1996). The formation of highly specialized presynaptic terminals and postsynaptic specializations is another example of the highly specialized morphology of neurons that seem to be regulated by Rho GTPases. One important step in the formation of the neuromuscular synapse is the clustering of acetylcholine receptors in the muscle fibre, which is induced by neuronal expression of agrin (Weston et al., 2000). Recent evidence shows that agrin induces the expression of Rac and Cdc42 in myotubes, and that these two proteins are necessary to cause acetylcholine receptor clustering in response to agrin (Weston et al., 2000). Other evidence pointing to the involvement of Rho GTPases in synapse development includes the concentration of RhoGEFs in pre- and postsynaptic terminals (Awasaki et al., 2000; Sone et al., 1997), and the reduction

of the postsynaptic density marker 95 (PSD-95) in dominant negative Rac-expressing hippocampal pyramidal neurons (Nakayama et al., 2000).

1.2.4.4 GEFs and GAPs involved in neuronal development

The common view is that Rho GTPases are regulated by upstream signals through the regulation of GEFs and GAPs. The best-studied RhoGEF in the nervous system is the triple functional domain protein Trio. Originally identified in mammals as a binding partner of the receptor tyrosine phosphatase Lar (Debant et al., 1996), Trio contains two GEF domains that probably act on Rac and Rho. Recent evidence indicates that the *Drosophila* Trio homologue is genetically required for the growth and guidance of sensory, motor and central nervous system neurons (Awasaki et al., 2000; Bateman et al., 2000; Newsome et al., 2000). The *C. elegans* homologue, uncoordinated-73 (UNC-73), is also required for cell migration and axon guidance (Steven et al., 1998). Although the physical interaction with Lar might not be conserved in worms or flies, the amino-terminal SH3 domain and the ankyrin repeats are conserved in mammals, flies and worms, and might allow Trio to be linked to conserved axon guidance receptors.

So far, the only RhoGAP studied extensively in the context of neuronal morphogenesis is N-chimaerin. This was shown to co-operate with Rac and Cdc42 to induce the formation of lamellipodia and filopodia in neuronal cell lines (Kozma et al., 1996). GAPs, like GEFs, might transduce signals from receptors to the Rho GTPases. The tissue distribution and subcellular location of different GEFs and GAPs might well be responsible for fine regulation of the Rho GTPases in different neurons at different developmental stages and in specific cellular compartments. It is also possible that different GEFs and GAPs in the same growth cone integrate signals from different receptors, which converge for the regulation of Rho GTPases. These possibilities might, in turn, explain why Rho GTPases are so versatile, regulating seemingly different

processes of neuronal development, in different developmental contexts. Although GEFs and GAPs are important regulators of GTPases, not all upstream signals must proceed through GEFs and GAPs. The low-affinity neurotrophin receptor p75 has been shown to bind directly to Rho and to activate its activity. This binding and activation is abolished when neurotrophin binds to the receptor, inactivating Rho and so permitting process outgrowth (Yamashita et al., 1999). Plexin-B1, a receptor for Semaphorin4D, can bind directly Rac. This interaction seems to be bidirectional, Rac modulates plexin-B1 activity and plexin-B1 modulates Rac function (Vikis et al., 2002).

1.2.4.5 Other Rho family members in neuronal development.

In neurons, the less well studied members of the Rho family, such as RhoG, Rnd1 and TC10, have also been implicated in regulating neurite formation. Overexpression of RhoG in PC12 cells induces neurite outgrowth (Katoh et al., 2000). It is thought that RhoG may function upstream of Rac and Cdc42 because dominant negative mutants of these proteins can block the cytoskeletal rearrangements induced by RhoG (Gauthier-Rouviere et al., 1998). Whether or not RhoG acts immediately downstream of guidance receptors in regulating Rac and Cdc42 activity in the growth cone remains to be determined.

TC10, another ubiquitously expressed member of the Rho family, was recently implicated in nerve regeneration. It has been found that upon severing peripheral nerves, the expression of TC10 was preferentially induced compared with that of RhoA, Rac1 and Cdc42 (Tanabe, K., et al., 2000). Expression of a constitutively active form of TC10 induces neurite extension in rat DRGs. TC10 shares greater sequence similarity with Cdc42 than with Rac1 and RhoA. Consistent with this is the observation that in fibroblasts TC10 stimulates filopodial extensions similar to those generated by activated Cdc42 (Murphy et al., 1999; Neudauer et al., 1998). It is not known whether TC10 is

necessary and sufficient for nerve regeneration or whether it functions as a redundant molecule in nerve cells.

Rnd1 is a constitutively GTP-bound protein that induces loss of stress fibers and cell rounding in fibroblasts (Nobes et al., 1998). Like RhoG, overexpression of Rnd1 promotes neurite process formation (Aoki et al., 2000), and the GTPase has also been implicated in Semaphorin signaling (Rhom et al., 2000).

1.3 cRAC1B/RAC3

We have identified a novel member of the Rho family of small GTPases from chicken E6 developing retinal neurons called cRac1B, which is highly and specifically expressed in the neural tissue of developing chick embryos (Malosio et al., 1997). cRac1B is highly homologous to Rac1, and is the orthologue of mammalian Rac3 (fig.1.4) Comparison of the polypeptide sequences derived from the chick clones with the human sequences confirmed that the cRac1B polypeptide is 93.7% identical to human Rac1 whereas the chicken Rac1 polypeptide (cRac1A) is 100% identical to the human Rac1 protein.

The mammalian Rac3 was isolated from the human cell line k562 cDNA library (Haataja et al., 1997). The gene is located on human chromosome 17q23-25, which is a region frequently deleted in breast cancer (Haataja et al., 1997). Rac3 is expressed at mRNA level in a variety of different cell lines: it is relatively abundant in the chronic myeloid leukemia cell line K562 and also expressed, albeit at a lower level, in the Ewing sarcoma cell line 5838, the promyelocytic cell line HL60, and the breast cancer cell line DU4475. Among human tissues, the highest Rac3 expression levels have been found in brain, although it has also been detected in heart, placenta, and pancreas.

Constitutively active V12Rac3 is able to induce the activation of JNK in COS1 cells (Haataja et al., 1997), indicating that Rac3 is involved in the stress activation pathway.

By using a GST-PBD pull-down assay (Mira et al., 1999) from cell lysates it has been revealed the presence of hyperactive Rac3 in highly proliferative cell lines (MDA-MB 435, T47D, and MCF 7), but not in normal breast cell lines or in less proliferative breast cancer epithelial cells. Additionally, as indicated by the absence of Rac3 in the supernatant of the PBD pull-down, all the Rac3 protein present in these cell lines was active. Mira et al. have also shown that endogenous, active Rac3 is essential for breast cancer cell proliferation via a Pak-dependent pathway. Since cDNA cloning and sequence analysis of full-length Rac3 did not reveal any mutations in the breast cell lines studied and did not explain the observed Rac3 activation, they suggest that a Rac3 regulatory protein could be altered or deleted in highly proliferating cancer cells, and that its specificity toward Rac3 could results from the adjacent location of both proteins at the membrane, given the distribution of Rac3 only at the plasma membrane in the cell lines used.

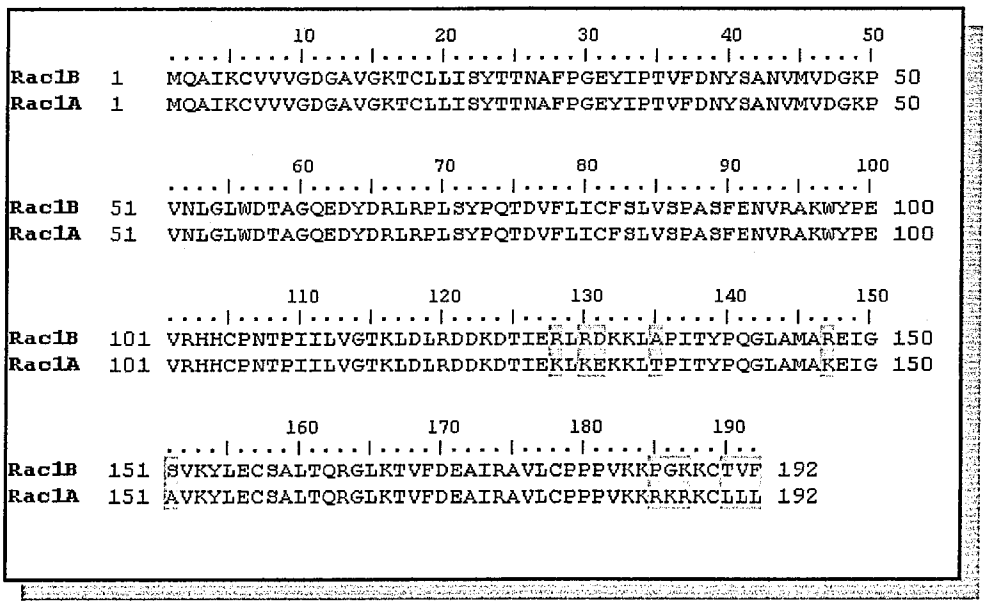

Fig 1.4. Aminoacid sequence comparisons of cRac1A and cRac1B. In green are indicated the residues that distinguish the two GTPases.

In normal Chicken Embryo Fibroblasts (CEFs), while cRac1A transcripts is abundant, cRac1B mRNA is almost not detectable. The actin cytoskeleton of CEFs is characterised by the presence of abundant stress fibers. As previously reported by us (Albertinazzi et al., 1998), expression of either the wild-type cRac1A or wild-type cRac1B has similar effects on actin reorganization in CEFs. The majority of the cells transfected with either of the wild-type cRac GTPases showed a dramatic change in cell shape one day after transfection, which was accompanied by a radical reorganization of the cytoskeleton. Several transfected cells showed numerous, highly branched membrane protrusions rich in F-actin. The distribution of microtubules was also affected by Rac expression. Microtubules were found in the membrane protrusions and their major branches. (Albertinazzi et al., 1999). Also the distribution of both wild-type Rac proteins is similar. Ventral plasma membrane (VPMs) from CEFs transfected with wild type cRac1A or cRac1B were used. VPMs contain well preserved focal adhesions and stress fibers, as defined both by morphological and biochemical criteria (Cattelino et al., 1997). This system is particularly useful because the distribution of antigens on the membrane appears much clearer in VPM preparations as compared to intact cells, due to the elimination of the fluorescent signal from the dorsal cell membrane, and from the cytoplasm. Analysis of VPMs from transfected CEFs has shown association of both Rac1A and Rac1B GTPases with the ventral portion of the plasma membrane, and in particular along VPM-associated stress fibers. (Albertinazzi et al., 1999).

1.3.1 The role of cRac1B in neuronal development

Northern blot analysis and in situ hybridization experiments have shown that cRac1B expression is restricted to the nervous system of the chicken embryo (Malosio et al., 1997). We have also shown that it is regulated during the development of the chicken brain (Albertinazzi et al., 1998). While the related cRac1A is highly expressed

throughout the development, the amount of cRac1B transcript increases between E4 and E15, and decreases thereafter, to be only weakly expressed in the adult brain. At E6, the endogenous level of Rac1B is low. One major finding from our study is that overexpression of cRac1B in E6 retinal neurons, specifically affects the morphology of transfected cells, by inducing the formation of an increased number of neurites, and by dramatically increasing neurite branching (Albertinazzi et al., 1998). These effects are specific for Rac1B, since Rac1A-transfected neurons show a morphology similar to that of non-transfected neurons, characterized by the presence of one long, poorly branched neurite.

A second major finding is the strong inhibition of neuritogenesis upon expression of the inactive mutant N17Rac1B. A large fraction (about 60%) of the N17Rac1B transfected neurons had no, or very short neurites, suggesting that not only is the inactive GTPase unable to induce the dramatic morphological modifications caused by the wild-type GTPase, but also that it has a negative effect on neuritogenesis. A significantly different effect was obtained by expressing the dominant-negative form of the cRac1A GTPase (Albertinazzi et al., 1998). More than two-thirds of the transfected neurons had a morphology similar to that of nontransfected cells, with one or two long neurites, indicating a specific dominant negative effect of the N17Rac1B on neuritogenesis induced by the endogenous protein.

At the protein level, cRac1A and cRac1B differ in 12 aminoacid residues, concentrated in the rho insert region (4 residues), in the effector loop (2 residues) and in the carboxy terminal region containing the CAAX box (6 residues). By expressing chimeric cRac1A/cRac1B constructs, the region containing the last eight COOH-terminal amino acid residues of Rac1B was shown to be necessary for Rac1B-mediated enhancement of neuritogenesis and neurite branching. Neurons expressing chimeras including the carboxyterminal eight residues from cRac1B show enhanced neuritogenesis and

branching while the substitution of this region with the corresponding region of cRac1 abolishes these effects.

In contrast to CEFs (Albertinazzi et al., 1999), in retinal neurons cRac1B shows a specific effect, not detectable with the highly homologous cRac1A. This implicates a cell type–dependent specificity of Rac protein action. It has been found that the activity of Rac3 can be regulated in vitro by Bcr (Haataja et al., 1997), a GTPase-activating protein highly expressed in the brain (Heisterkamp et al., 1993). These data, together with the finding that Tiam1, a guanine nucleotide exchange factor highly expressed in the brain (Habets et al., 1995), affects neurite outgrowth in neuroblastoma cells in a Rac-dependent fashion, suggest that neuritogenesis may be modulated by specific Rac regulators during development (van Leeuwen et al., 1997).

Moreover, the differences existing between the cRac1A and cRac1B polypeptides may be sufficient to allow their interaction with distinct sets of neuronal effectors and/or regulators, which may be responsible for the different effects observed on the neuronal cytoskeleton.

1.3.2 Specific Rac3/cRac1B interacting proteins

Regarding molecules specifically interacting with Rac3, it has been shown, by the yeast two-hybrid system, that mammalian Rac3 can bind CIB (Calcium and Integrin Binding Protein). CIB is a protein that interacts with the αIIbβ3 fibrinogen receptor, and it has been shown to bind exclusively with activated V12Rac3 but not Rac1 or Rac2 (Haataja et al., 2002). Binding of V12Rac3 to CIB is mediated by the C-terminal end of Rac3 and by Rac3 membrane localization. Adhesion of CHO cells on fibrinogen is accompanied by a specific increase in the levels of Rac3 in the cytoskeleton-bound fraction of the cell. Expression of V12Rac3 and CIB stimulated αIIbβ3 -mediated adhesion and spreading on fibrinogen. Moreover, it has been shown that adhesion

through αIIbβ3 causes a marked increase in the levels of endogenous GTP-bound Rac3. The results implicate Rac3 and CIB in integrin-associated cytoskeletal reorganization during αIIbβ3 -mediated adhesion.

Using the yeast two-hybrid system, another Rac3-interacting protein has been isolated from a human placenta cDNA library. Sequence analysis revealed that this protein is C1D, the human homologue of the murine SUN-CoR protein which acts as a corepressor for the thyroid hormone receptor (Hataaja et al., 1998). In yeast cells, C1D binds to constitutively activated but not to GDP-bound Rac3. The C1D gene was mapped to human chromosome 2, which frequently shows deletions in human follicular thyroid carcinomas.

Another component that has been shown to interact with activated V12Rac3 is human NRBP, a protein containing a kinase-homology domain and that exhibits an associated kinase activity. The overexpression of NRBP in COS1 cells causes a dramatic redistribution of the Golgi-associated marker p58 to more peripheral locations within the cell, consistent with an impairment of the ER to Golgi transport (De Langhe et al., 2002). The authors also showed that NRBP and activated Rac3 colocalize to endomembranes and at the cell periphery in lamellipodia, suggesting that NRBP functions in subcellular trafficking and may be directed to specific subcellular locations through interaction with small GTPases Rac3.

By affinity chromatography of cRac1A and cRac1B GTPases, using brain lysates from chicken embryos, p95-APP1 (p95-ArfGAP, Paxillin interacting, Pix interacting Protein1), was identified as a protein interacting indirectly with the GTP-bound (and not with the GDP-bound) form of both cRac proteins (Di Cesare et al., 2000). P95-APP1 is a member of a recently discovered family of proteins that are characterized by a GAP domain for the Arf GTPases (table 1.3).

1.4 THE ARF GTP-ASES AND THE ARFGAP PROTEINS.

During cell migration, it has been hypothesized that membrane internalized from the cell surface is recycled to the front of migrating cells to contribute to the extension of the cell border. The molecular mechanisms underlying this process are not known. Recent findings have shown that a number of multi-domain proteins containing an ArfGAP domain interact with both actin-regulating and integrin-binding proteins, and affects Rac-mediated protrusive activity and cell migration (de Curtis I., 2001). Some of these proteins have been shown to localize to endocytic compartments and have a role in regulating endocytosis (de Curtis et al., 2001). Given the participation of Arf (ADP-ribosylation factor) proteins in regulating membrane traffic, one hypothesis is that the ArfGAPs act as molecular devices that coordinate membrane traffic and cytoskeletal reorganization during cell motility.

Like Rho proteins, Arf small GTPases cycle between the GTP- and GDP- bound form under the control of specific GAPs and GEFs (Donaldson, J.G. and Jackson, C.L., 2000). They are involved in the regulation of membrane traffic in cells, and they can be divided into three classes, depending on sequence homology: class I (Arf1, 2 and 3), class II (Arf4 and 5), and class III (Arf6). It is well known that class I Arfs are involved in the regulation of membrane traffic between endoplasmic reticulum and the Golgi apparatus, while the function of class II GTPases is still not clear. Regarding Arf6, its subcellular localization is quite different from that of class I and class II Arf proteins. Arf6 is localized to the plasma membrane, especially to membrane ruffles in spreading cells (Radhakrishna et al., 1996). Arf6 is involved in membrane recycling at the plasma membrane, and has been implicated in remodeling the actin cytoskeleton underlying the plasma membrane. Activation of Arf6 induces remodeling of the actin cytoskeleton and cell spreading, and expression of a dominant negative mutant of Arf6 blocks cell spreading (Radhakrishna, H.O. et al., 1999). Arf6 seems to be involved in the traffic

between a recycling endosomal compartment and the plasma membrane because of the localization of Arf6 in these compartments and the effects of its overexpression on transferrin uptake and recycling to the cell surface (D'Souza-Schorey et al., 1995; Peters et al., 1995). Moreover, Arf6 colocalizes with transferrin receptor at the recycling compartment (D'Souza-Schorey et al., 1998).

Arf6 seems to be functionally linked to Rac1: the two proteins colocalize at the plasma membrane and on recycling endosomes, and Rac1-induced ruffling can be blocked by the inactive mutant N27Arf6. Recent studies indicate that Arf6 and Rac1 may also share effectors called Arfaptins (D'Souza-Schorey et al., 1997), including POR1 (arfaptin 2) which has been implicated in the cytoskeletal rearrangements induced by either Rac1 (D'Souza-Schorey et al., 1997) or Arf6 (Van Aelst et al., 1996).

Considering these data, it has been proposed that Arf6 could be a good candidate for mediating membrane traffic toward the cell front during migration. The ArfGAP proteins could be required for the regulation of the activity of Arf6-mediated membrane recycling. The ArfGAP proteins identified can be divided in three groups (table 1.3). The first is the family of ASAP1/DEF-1 (differentiating enhancing factor) (Brown et al., 1998; King et al., 1999), PAPα (Pyk2 carboxyl-terminus-associated protein)/PAG3 (Paxillin-associated ARF GAP) (Kondo et al., 2000; Andreev et al., 1999), and PAPβ. They have a centrally located ArfGAP and ankyrin repeats domain flanked by a PH domain. ASAP1 and PAPα show in vitro GAP activity toward Arf1, Arf5 and Arf6. They interact with Src and Pyk2, respectively (Brown et al., 1998; Andreev et al., 1999), two tyrosine kinases involved in the regulation of integrin-mediated adhesion. Asap1 localizes into focal contacts and is implicated in actin remodeling during cell migrations. (Randazzo et al., 2000). PAPα can recruit paxillin to focal complexes by a GAP activity-dependent mechanism (Kondo et al., 2000). These data support the

hypothesis that important molecules such as paxillin and tyrosine kinases are recruited to the leading edge through ArfGAPs.

ACAP1 and ACAP2 (Arf GAP with coiled-coil, ANK repeat and PH domains) belong to the second group. Their molecular structure is very similar to the organization of the components of the first group. Both proteins belong to the centaurin family and they show strongest GAP activity towards Arf6 (Jackson et al., 2000). Their GAP activity is stimulated by the interaction of the PH domain with PIP_2 and by phosphatidic acid. Overexpression of ACAPs blocks the formation of Arf6-mediated protrusions, and leads to redistribution of ACAPs and activated Arf6 to endosomes (Radhakrishna and Donaldson, 1997).

The Git (G-protein-coupled receptor kinase interacting protein) family is the third group. They are components of complexes that include the RhoGEF Pix (Oh et al., 1997; Bagrodia et al., 1998; Manser et al., 1998), the Rac effector Pak (Daniels and Bokoch, 1999) and the adaptor Nck (McCarty, 1998; Turner et al., 1999). As well as other ArfGAPs, they are multidomain proteins characterized by an N-terminal ArfGAP domain followed by at least three ankyrin repeats. They can bind paxillin through a region that has been mapped in the C-terminal part, and the SHD domain of Git1 has also been shown to bind focal adhesion kinase (FAK) (Zhao et al., 2000). Their GAP activity seems to be regulated by phosphoinositides. Git1 and Git2 are regulated by PIP_3 (Vitale et al., 2000). These proteins seems to be involved in the regulation of adhesion and motility. Overexpression of Git1 causes a loss of paxillin from focal complexes and stimulates cell motility (Zhao et al., 2000) while inhibition of the interaction between PKL/Git2 and paxillin prevents lamellipodium formation. Recently, Git1 has been identified as a potential substrate for the receptor tyrosine phosphatase PTPζ (Kawachi et al., 2001). This phosphatase has been implicated in the control of neurite outgrowth and neuronal cell migration.

FAMILY	SUB-FAMILY	NAME	DOMAIN ORGANIZATION
ASAP	***ASAP1***	Centaurinβ4	PH, ArfGAP, ankyrin repeats (3), SH3
	PAPα	Centaurinβ3	PH, ArfGAP, ankyrin repeats (3), SH3
ACAP	***ACAP1***	Centaurinβ1	PH, Arf GAP, ankyrin repeats (2)
	ACAP2	Centaurinβ2	PH, Arf GAP, ankyrin repeats (2)
	ACAP3	Centaurinβ5	PH, Arf GAP, ankyrin repeats (2)
GIT	***GIT1***	Git1/Cat1/p95APP1	N-term. ArfGAP, ankyrin repeats (3)
	GIT2	Git2/Cat2/p95APP2/ PKL	N-term. ArfGAP, ankyrin repeats (3)

Table 1.3. The families of Arf-GAP proteins.

These data raise the possibility that PTPζ activity may facilitate motility in these cells by reversing the integrin-mediated tyrosine phosphorylation of Git1 that occurs in response to cell adhesion (Bagrodia et al., 1999).

P95-APP1 is the chicken homologue of GIT1/Cat1. In figure 1.5 is shown a schematic representation of the protein. The dissection of the multidomain p95-APP1 has been useful to identify possible distinct functions for the different domains (Di Cesare et al., 2000). Both wild-type p95-APP1 and the truncated p95C (the carboxy-terminal portion including the paxillin binding domain) shown on figure 4.4 induce actin-rich protrusions mediated by Rac and Arf6 (Di Cesare et al., 2000). By contrast, the aminoterminal portion of p95-APP1 (including the ArfGAP domain and the three ankyrin repeats) colocalizes with the inactive mutant N27Arf6 in an endosomal compartment. By further dissection of this multi-domain protein, the truncated p95-C2 (Fig. 4.4), including both PIX- and paxillin-binding domains, accumulates via PIX around large vesicles. Paxillin is recruited from the focal adhesions to these vesicles. Consistent with this findings, the paxillin reduction observed at focal adhesion in response to Git1 overexpression is accompanied by the localization of paxillin to large perinuclear vesicles (Zhao et al., 2000). These vesicles are distinct from the smaller endocytic structures where the amino terminal truncated polypeptides including the ARF-GAP domain and the ankyrin repeats accumulate by a PIX-independent mechanism. The characterization of this membrane compartment has revealed that it is a Rab11-positive recycling compartment, suggesting that p95-APP1 could be involved in the regulation of membrane recycling to the cell surface (Matafora et al., 2001). In addition Rac activation induces the localization of p95-APP1 complex at the periphery of the cell, with the formation of large lamellipodia where V12Rac colocalizes with the components of the p95-APP1 complex.

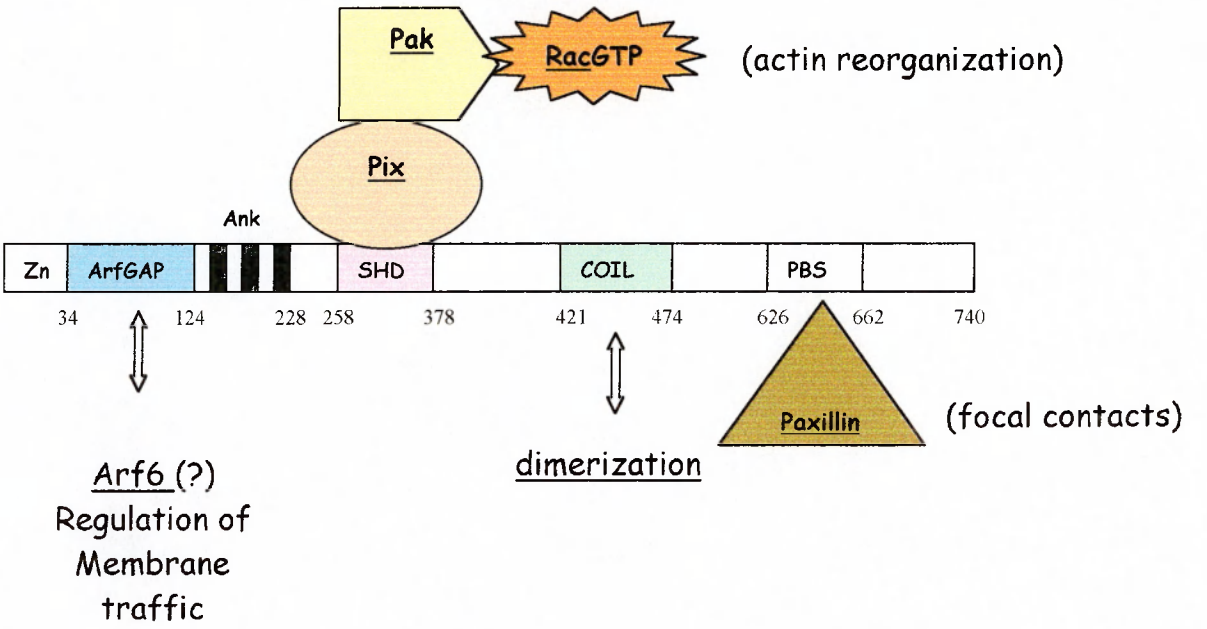

Fig 1.5. Schematic representation of the p95-APP1 polypeptide.

P95-APP1 is a multidomain protein. Zn (zinc finger), GAP (ArfGAP domain), ANK (ankyrin repeats), SHD (Spa2 homology domain), COIL (coiled coil region), PBS (paxillin binding subdomain).

1.5 AIM OF THE WORK

Most of the information that we have about neuritogenesis concerns the extracellular mechanisms driving growth cone migration and neurite elongation. Large gaps still exist in understanding the sequence of intracellular events leading to this process. Many attempts have been made in the last few years to investigate the role of Rho family GTPases in these processes, but still the information that we have is largely fragmentary. This is probably due to the complexity of the cross-talk between different signalling pathways occurring in the cell at the same time. The complexity is further increased by peculiarities that may be present in the different cell types studied.

In our laboratory, Rac1B was identified as a Rac expressed during neural development (Malosio et al., 1997). In the first part of my thesis I will describe the preparation of recombinant mouse embryonic stem cells (ES cells) to generate Rac1B knock-out mice. It was shown that avian Rac1B plays an important role in the process of neuronal development (Albertinazzi et al., 1998), by overexpression experiments in primary retinal neurons. A better understanding of the role played by Rac1B in this process could come from studies in an "in vivo" system. Today, transgenic animals provide one of the most potent research tools in the biological sciences, that allow us to explore the regulation of gene expression as well as the regulation of cellular and physiological processes. For these reasons, our purpose is to obtain knock-out mice for Rac1B, in order to analyse possible defects in the development of the nervous system of mice lacking this neurospecific small GTPase.

Since Rac1B is specifically expressed in the chicken developing nervous system (Albertinazzi et al., 1998), in the first part I describe the characterization of a polyclonal antibody used to investigate Rac1B expression pattern also in mice during development.

The aim of the second part of my thesis was to analyze the role played by Arf6 and the p95-APP1 complex in Rac1B-induced neurite extension in primary neurons,

and investigate the components required for the recruitment of p95-APP1 complex at the membrane of the recycling compartment.

Chapter 2

MATERIALS AND METHODS

2.1 GENE TARGETING IN MOUSE EMBRYONIC STEM CELLS

2.1.1 Preparation of Mouse Embryo Fibroblasts as Feeder Layers

Embryonic stem (ES) cells were grown on mitotically inactive mouse embryo fibroblasts. They provide a basal level of Leukemia Inhibitory Factor (LIF) and a number of yet unidentified factors that sustain ES cell growth in the totipotent state. E13,5 mouse embryos were dissected in PBS, and heads, livers and internal organs were removed. The embryos were minced into small pieces in 10 ml of Trypsin/EDTA (GIBCO, 0,5 mg/ml Trypsin, 0,2 mg/ml EDTA)with 1 mg/ml Dnase type I. The suspension was incubated for 10 min at 37°C, and the tissue pieces were triturated by pipetting up and down. After another incubation of 10 min at 37°C, the suspension was triturated by pipetting up and down with a smaller pipette, and the suspension above the debris was taken and split into two 50 ml tubes and 25 ml of complete medium (DMEM containing 10% FCS, 100 U/ml penicillin and streptomycin, 20 mM glutamine) was added. After a 5 min spin at 1500 rpm, the pellet containing cells was resuspended in 2 ml of complete medium, and disaggregated by pipetting up and down with a pasteur, and cells were counted. About 80 millions cells were plated in one 15 cm diameters plate and cultured at 37°C, 5% CO2. When confluent, cells were trypsinized and frozen. The plates were washed with 20 ml PBS and 7 ml of trypsin were added to each plate. The trypsin was removed and the plates were incubated at 37°C for 5 minutes. Cells were resuspended in 8 ml of medium, centrifugated for 5 min at 1500 rpm and

resuspended in 1 ml per dish of 25% FCS, 65% complete medium and 10% DMSO and placed at –80°C for 2 days. Vials were then conserved in liquid nitrogen. When used, each aliquot was thawed and added to 8 ml of complete medium, and plated in a 100-mm diameter culture dish which reached confluence in 2 days. When cells were confluent, they were treated with mitomycin C, in order to block mitosis and mantain cells as a monolayer. 50 µl of 1mg/ml mitomycin C were added to 5 ml of complete medium. After 2 h of incubation, cells were washed two times with PBS, and fresh medium was added to the plate. Mitomycin treated cells can be kept in culture for one week.

2.1.2 Culture and electroporation of ES cells.

Before transfection, ES cells must be expanded and kept growing minimizing passages. One vial of R1 ES cells was thawed at 37°C, and cells were dilute in 10 ml of complete medium (DMEM containing 15% FCS, 100 U/ml penicillin and streptomycin, 20 mM glutamine, 0,1 mM non-essential aminoacids, 1mM sodium pyruvate, 0,1 mM β-mercaptoethanol, 1000 U/ml LIF). After a 5 min spin at 1200 rpm, cells were resuspended in fresh medium and plated in a 6 cm diameter dish with a monolayer of mitomycin C treated fibroblasts. After the cells were thawed, they must be trypsinized every two days. Cells were expanded by washing them with trypsin-EDTA 1X (GIBCO) and by incubating 15 min at 37°C with fresh trypsin-EDTA. To obtain single cell suspension, cells were separated by pipetting up and down, and an excess of fresh complete medium was added. After a spin of 5 min at 1200 rpm, cells were resuspended in fresh medium and plated at the appropriate dilution.

The plasmid for the transfection were linearized by digesting 300 µg of DNA with 150 Units of the restriction enzyme XhoI at 37°C for 5 h, and the linearized plasmid was purified with phenol-chlorophorm and precipitated with the addition of 3M

Na acetate and two volumes of ethanol. The pellet was washed with 70% ethanol and resuspended under sterile hood in 150 µl of autoclaved H2O.

For the electoporation, 7 millions of ES cells were centrifuged 5 min at 1200 rpm, resuspended in 800 µl of PBS, and 20 µl of linearized plasmid were added. The suspension was transferred into the electroporation cuvette (BIORAD), and the cuvette was placed in the cuvette holder of the Bio Rad Gene Pulser. The electric pulse was delivered setting up the Gene pulser with 0,24 kV and 500 µF. The cuvette was incubated on ice for 20 min and the cell suspension was diluted in 20 ml of complete medium. Cells were plated on two 10 cm dishes pre-coated with sterile 0,1% gelatine. Twenty-four h after the electroporation the medium was replaced with fresh medium, and after two days the medium was replaced with complete medium supplemented with 325 µg/ml of G418, and after 3 days with complete medium with 325 µg/ml G418 and 2 µM gancyclovir.

G418 can be inactivated by the neomycin phosphotransferase which is one of the most used genes that confers antibiotic resistence in mammalian cells. This positive selection eliminates cells in which the construct was not integrated into the genomic DNA, since the enzyme is produced only when the construct is integrated. The presence of thymidine kinase in the construct downstream the long arm represents the negative selection. During targeted gene replacement events, this sequence is lost and degraded, whereas clones in which the vector has integrated at random will typically incorporate the sequence. For this reason this selection kills most clones of cells which have integrated the vector at random location, while targeted clones survive. Thymidine kinase phosphorylates gancyclovir, a nucleotide analogous that upon phosphorylation can be incorporated into the DNA during replication. Incorporation of the phosphorilated nucleotide analouge causes the block of DNA replication and cell death.

The medium with the selection was changed every day, and the first resistant clones appeared after 8 days.

2.1.3 Picking the colonies

Starting 8-9 days after electroporation 300 colonies were picked over 4-5 days and transferred to 96-well-feeder plates containing complete ES cells medium without selection. After one day, the medium in the plates of the collected clones was sucked off and each well was washed with 150 µl PBS. 30 µl of trypsin were added to each well and the plate was incubated 10 min at 37°C, 5% CO2. The cells of each clone were resuspended in the trypsin by pipetting up and down to get single cells, and 150 µl of complete medium were added to each well.

2.1.4 Passage of 96-well plates

For each original feeder plate containing the clones, two fresh feeder plates were prepared and one plate coated with 0,1% gelatine. Each well was washed with PBS and 30 µl of trypsin were added. The plate was incubated for 15 min at 37°C, 5% CO2 and cells were resuspended to obtain single cells. Trypsin action was blocked by the addition of 150 µl of complete medium, and 70 µl of cell suspension were distributed in the two feeder plates, and 40 µl in the gelatine plate. Each clone was treated individually, because the rate of the growth of the different clones was different.

2.1.5 Freezing of 96-well-feeder-plates

Once the clones have grown enough, the two copies are frozen in the two 96 well plates. Each well was washed with PBS, and 30 µl of trypsin were added for 15 min at 37°C. Cells were resuspended to obtain single cells, and 70 µl of complete cold

medium were added. Subsequently, 100 µl of cold 2X concentrated freezing medium were added (for 10 ml: 6 ml of complete medium, 2 ml FCS and 2 ml DMSO). The plates were transferred on ice, the edges were wrapped with parafilm and the plates were transferred into a box at –80°C.

2.1.6 Genomic DNA extraction

Cells of each clone growing on gelatine were trypsinized with 30 µl of trypsin for 10 min at 37°C and transferred into 24 well plates. When confluent, cells were lysed with 500 µl/well of lysis buffer (100 mM Tris pH 8,5, 5 mM EDTA, 0,2% SDS, 200 mM NaCl, 200 µg/ml proteinase K). The plates were transferred at 56°C o.n., and then 500 µl/well of isopropanol were added to precipitate DNA, and the plate was incubated for 15 min at room temperature on an orbital shaker. The precipitated genomic DNA of each clone was transferred to an eppendorf tube and centrifuged for 5 min at room temperature at 13000 rpm. In order to eliminate the excess of isopropanol, the eppendorf tubes were left opened for 1 h at 37°C. To resuspend DNA, 150 µl of TE were added and the eppendorf tubes were left at 65°C in waterbath. After one night, DNA was dissolved by pipetting up and down, and it has been stored at 4°C.

2.1.7 Southern blot analysis

30 µl of genomic DNA of each clone were digested overnight at 37°C with 20 U of *EcoRI* and 20 U of *XbaI* in a final volume of 40 µl. The DNA fragments were separated on a 0,8% agarose gel. The DNA was then denaturated by incubating the gel in 0,4 N NaOH, 0,6 M NaCl for 30 min, and neutralized by incubating it in 1,5 M NaCl, 0,5 M Tris-HCl pH 7,5.

A nylon membrane (Genescreen Plus, NEN) was incubated it in deionized water and

then in 10X SSC. The digested DNA was transferred on the membrane by capillary action in 10X SSC for one night. The filter was first denaturated by incubation in 0,4 N NaOH for 1 min, and then neutralized by incubation in 0,2 M Tris-HCl pH 7,5 and 2X SSC. DNA was fixed on the filter with UV crosslinker, and the membrane was prehybridized with 10 ml of the prehybridization solution (5 ml formamide, 2 ml H2O, 2 ml of 50% dextrane sulphate, 1 ml of 10% SDS and 0,58 g NaCl) at 42°C for at least 2 h. The probe and salmon sperm DNA were denaturated for 10 min at 95°C, placed on ice for 10 min and added to the tube containing the filter and the prehybridization solution. After one night of incubation at 42°C, the filter was washed twice with 2X SSC at room temperature for 5 min, twice with 2X SSC, 1% SDS at 65°C for 30 min, and twice with 0,1X SSC at room temperature for 30 min. X-ray films were exposed to the hybridized filters.

2.1.8 Thawing the 96-well plate and expanding positive clones.

The 96 well plates containing the positive clones were immediatly thawed in 37°C waterbath and centrifuged for 5 min at 1200 rpm. The medium containing DMSO was removed and new fresh medium was added to the wells of interest. The resuspended cells were transferred in new fresh 96well feeder plate. After two days cells were trypsinized and transferred to a 24 well plate, and after two more days they were trypsinized with 200 µl of trypsin and transferred into one well of a 6 well feeder plate. After two more days, cells were incubated with 500 µl of trypsin, resuspended in 5 ml of complete medium and centrifuged for 5 min at 1200 rpm. Cells were resuspended in fresh medium and plated in one 10 cm feeder plate. When ready, cells were frozen by preparing 6 vials for one 10 cm plate.

2.2 CELL CULTURES

2.2.1 Culture and transfection of primary neurons

Neural retinal cells were prepared from E6 chick neural retinas. After dissection, E6 retinas were incubated for 6 minutes at 37°C in 0,1% trypsin in 6 ml of phosphate-buffered saline (PBS). Digestion was stopped by adding 1 ml of fetal calf serum. After a 3 min spin at 700 rpm, the pellet was washed in F12 nutrient mixture and triturated in F12 containing 125 µg/ml DNase I. Cells were cultured on coverlips covered with 0,2 mg ml^{-1} poly-D-lysine and 40 µg ml^{-1} laminin-1 (Albertinazzi et al., 1998) in Retinal Growth Medium (RGM), composed of F12 with 20 mM glutamine, 100 U/ml penicillin and streptomycin, and Bott's additives (5 µg/ml insulin, 0,1 mg/ml human transferrin and 3 µM selenic acid). For transfection by electroporation, retinal cells were resuspended in cytomix pH 7.6 (120 mM KCl, 0.15 mM CaCl2, 10 mM K2HPO4/KH2PO4, 25 mM Hepes, 2 mM EGTA, 5 mM MgCl2) to a final concentration of 65 millions of cells ml^{-1}. 200 µl of cell suspension were placed in a Gene Pulser Cuvette (Biorad) and 50 µg of plasmid were added (40 µg of each plasmid in cotransfection experiments). After an incubation on ice for 5 minutes, cuvettes were subjected to 2 sequential pulses at 0.4 KVolts and 125 µFarad, resuspended in 10 ml of RGM, and plated on coverlips. Cells were cultured for 20-24 h at 37°C, 5%C02 and fixed for immunofluorescence. Quantification of the effects of the overexpression of the constructs in retinal neurons were made by examining transfected, neurofilament-positive neurons, or cotransfected neurons. For each type of transfection, at least 50 neurons were morphologically examined from at least two distinct experiments (total of 100 neurons / experimental condition). Long neurites were equal or longer than 3 cell body diameters, short neurites were shorter than 3 cell body diameters. For measures of total neurite length and of number of neurite terminals, a total of 30 neurons from two independent experiments were examined by using the Image-Pro® Plus Program.

2.2.2 CEFs culture and transfection

Chicken Embryo fibroblasts (CEFs) were isolated from 10-day-old embryos. The head, legs, wings and internal organs were removed and the embryo was squirted through a 10 ml syringe without a needle and trypsinized with 5 ml 0.1 trypsin in PBS for 15 min at room temperature. The suspension above the debris was taken and 10 ml of complete medium (DMEM containing 5% fetal calf serum (FCS), 1% chicken serum, 100 U/ml penicillin and streptomycin, 20 mM glutamine) was added. After a 5 min spin at 800 rpm, the pellet containing cells was resuspended in 10 ml complete medium, filtered through a nylon membrane and the cells were counted. 0.5-2.0 x 10^6 cells were plated on each 100 mm diameter petri dish at 37°C, 5% CO_2. Each dish reached confluence in 2-3 days. A confluent dish of CEFs was washed twice with 10 ml of PBS and trypsinized by approximately 2 min with shaking in 1 ml trypsin-EDTA (Bio-Whittaker, 0,5 mg/ml Trypsin, 0,2 mg/ml EDTA) at room temperature. The trypsin digestion was blocked by addition of 9 ml of complete medium, cells were resuspended and plated at a dilution of 1:5-1:10. After the second passage, CEFs were frozen and conserved in liquid nitrogen in 1 ml aliquots containing 0.5-2.0 x 10^6 cells in 50% FCS, 40% complete medium and 10% DMSO. When used, each aliquot was thawed and added to 10 ml of complete medium, and plated in a 100-mm diameter culture dish which reached confluence in 2-3 days. CEFs up to the fifth passage were used for experiments. For CEFs transfection, cells were plated in 6 cm diameter plates and cultured 18 h. Subconfluent cells were transfected with the calcium phosphate method. 20 µg of plasmid DNA and 20 µl of 2,5 M CaCl2 were diluted in TE to reach a final volume of 200 µl (for cotransfection experiments, 10 µg of each plasmid were used). The DNA/CaCl2 solution was added dropwise to 200 µl of HBS 2X solution (280 mM NaCl, 50 mM Hepes, 1,5 mM Na2HPO4, pH 7,12) under the vortex. The precipitates

were allowed to sit 30 min at room temperature, and the final solution was added to the plates containing 3 ml of fresh medium. After 20 hours from the transfection, cells were lysed.

2.2.3 COS7 cells culture and transfection

COS7 cells were cultured in DMEM containing 10% fetal calf serum, 100 U/ml penicillin and streptomycin and 20 mM glutamine. For transfection experiments, cells were plated in 6 cm diameter dishes and cultured for 18 h. Subconfluent cells were transfected with the Fugene reagent (Roche). For each plate, 9 μl of Fugene were diluted in 300 μl of serum-free DMEM, and the solution was added drop by drop to 10 μl of TE containing 6 μg of plasmid DNA (3 μg of each plasmid in the case of cotransfection). After 15 min incubation at room temperature, before the solution was added to the plate containing 3 ml of fresh complete medium. Cells were lysed 20 h after transfection.

2.3 ANTIBODIES

The pAbs against Pix (Manser et al., 1998), Arf6 (Gaschet and Hsu, 1999), Rab11 (Sonnichsen et al., 2000), and Early Endosomes Antigen 1 (EEA1; Simonsen et al., 1998) have been previously described. Other antibodies included: anti-neurofilament 3A10 mAb (Serafini et al., 1996), obtained by the Developmental Studies Hybridoma Bank (The University of Iowa, IA). Mab anti-FLAG M5 (Kodak), pAb anti-FLAG (Santa Cruz Biotechnology, Inc., Santa Cruz, CA), mAb anti Rac1 and anti-paxillin (Transduction Laboratories); anti-HA-Tag pAb (Babco); anti-Myc mAb 9E10 (Sigma-Aldrich, Milano, Italy). MAb against LEP100 (Fambrough et al., 1988); anti-βCOP mAb (Sigma). The 64S pAb specific for p95-APP1 was raised against the GST-P95-C

fusion protein (including amino acid 347 to 740 of p95-APP1), prepared from bacteria transformed with the pGEX-p95-C construct (Di Cesare et al., 2000).

2.4 CONSTRUCTS

The pBK-Arf6, pBK-N27Arf6, and pBK-L67Arf6 plasmids were obtained by subcloning the cDNAs corresponding to avian Arf6, Arf6(N27), and Arf6(L67) into the pBK-CMV vector (Stratagene). The cDNA for chicken Arf1 and Arf5 were amplified by PCR from an E15 chick brain cDNA library. The cDNAs were cloned into a pBK-CMV vector modified to include a sequence coding for a HA tag at the carboxyterminus of the Arf proteins. The obtained pBK-Arf1-HA and pBK-Arf5-HA plasmids were used to produce pBK-N31Arf1-HA, pBK-L71Arf1-HA, pBK-N31Arf5-HA, and pBK-L71Arf5-HA, using degenerate oligonucleotides in combination with the QuickChange^{TM} site-directed mutagenesis kit (Stratagene Gmbh). The pcDNA-I-HA-Rac1B, pGEX-p95-C, pFLAG-p95, pFLAG-p95-C, pFLAG-p95-C2, pFLAG-p95-K39, pFLAG-p95-N, and pFLAG-LacZ plasmids were described elsewhere (Malosio et al., 1997; Di Cesare et al., 2000; Matafora et al., 2001). The pGEX-cRac1B plasmid was obtained by cloning the cDNA coding for cRac1B into the pGEX-4T-1 vector (Pharmacia Biotech). The resulting pGEX-cRac1B plasmid was used to obtain a GST fusion protein by expression into *Escherichia coli* BL21 cells. The pGEX-p95-C2 plasmid was prepared by cloning the cDNA fragment corresponding to the C-terminal amino acids 229-740 of p95-APP1 into the pGEX-4T-1 vector (Amersham Pharmacia Biotech). The pFLAG-p95-LZ was obtained by site directed mutagenesis with the QuickChange^{TM} site-directed mutagenesis kit (Stratagene), starting from the pFLAG-p95 plasmid, and using the primers 5' GTGAACAACAGCCCGAGCGATGAGCTGCGCCGGCCGCAGCGCGAGATC 3' and 5' GATCTCGCGCTGCGGCCGGCGCAGCTCATCGCTCGGGCTGTTGTTCAC

3'. The pFLAG-p95-C2-LZ was obtained from the pFLAG-p95-LZ plasmid. The pBK-HA-p95 plasmid was obtained by cloning the fragment coding for the full length p95-APP1 protein into the pBK-HA vector, derived from the pBK-CMV vector from Stratagene by removing the LacZ gene and inserting a sequence coding for an HA tag between the starting ATG codon and the multiple cloning site of pBK-CMV. The pCMV6m/PAK1 plasmid coding for the Myc-tagged PAK1, and the pXJ40-HA-βPIX plasmid coding for the HA-tagged βPIX polypeptide were described elsewhere (Bernard et al., 1999; Manser et al., 1998).

The pXJ40-HA-βPIX-ΔLZ plasmid was prepared by digesting pXJ40-HA-βPIX with Hind III and Bgl II to remove the carboxyterminal coiled coil region, and by ligating the paired oligonucleotides ΔLZ (AGCTTACTGCACAAGTGCAAAGACGAGGCAGACCCTGAACTCAAGTTCAC GCAAAGAGTCTGCTCCACAAGTGCCCGGGTAGA) and ΔLZ2 (GATCTC TACCCGGGCACTTGTGGAGCAGACTCTTTGCGTGAACTTGAGTTCAGGGTCT GCCTCGTCTTTGCACTTGTGCAGTA) to introduce a stop codon. The pXJ40-HA-βPIX-PG mutant (in which Trp-43 and Trp-44 have been changed into Pro-43 and Gly-44, respectively) was prepared by site-directed mutagenesis with the QuickChange™ site-directed mutagenesis kit (Stratagene GmbH), starting from the pXJ40-HA-βPIX plasmid, and using the primers PIXBIS-5 (GGAAGGAGGCCCGGGGGAAGGCACAC) and PIXBIS-3 (GTGTGCCTTCCCCCGGGCCTCCTTCC). The pXJ40-HA-βPIX-ΔPH plasmid was obtained by PCR on pXJ40-HA-βPIX with the oligonucleotides PIXΔPH5 (GGGGTACCTCTGTGAGCAACCCCACC) and PIXΔPH3 (GGGGTACCACTGCCCAACGTCTTTATG). PXJ40-HA-βPIX-C was obtained by PCR with the PIX-C5 (TGGATCCTCTGTGAGCA ACCCCACCATC) and PIX-C3 (GAAGATCTGCGCCTATAGATTGGTCTCATCCC) oligonucleotides. The PCR

fragment was then ligated into pXJ40-HA. The procedure to obtain plasmids pXJ40-HA-βPIX-PG-ΔLZ, pXJ40-HA-βPIX-ΔPH-ΔLZ, and PXJ40-HA-βPIX-C-ΔLZ was the same as the one described to obtain pXJ40-HA-βPIX-ΔLZ, but starting from pXJ40-HA-βPIX-PG, pXJ40-HA-βPIX-ΔPH, and PXJ40-HA-βPIX-C, respectively.

2.5 BIOCHEMICAL METHODS

2.5.1 Preparation of lysates from CEFs, COS7, embryonic chicken retinas and embryonic mouse brain.

Transfected CEFs and COS 7 cells were transferred on ice, washed twice with 10 ml of ice-cold TBS (20 mM Tris-HCl, pH7.5,150 mM NaCl), and solubilised with lysis buffer (0,5% Triton X-100, 150 mM NaCl, 20 mM Tris-Cl, pH 7,5, 2 mM MgCl2, 1 mM Na-orthovanadate, 10 mM NaF, 0,1 mM DTT, 20 μg ml^{-1} each of antipain, chymostatin, leupeptin and pepstatin). Lysates were transferred to tubes, and rotated for 15 min by end-over-end mixing at 4°C. The insoluble material was removed by centrifugation at 4°C for 15 min at 13000 rpm in a refrigerated centrifuge. For the preparation of lysates from embryonic chick retina, E6 retinas were dissected, cooled on ice, washed with ice-cold TBS, and solubilised with 9 volumes of lysis buffer containing 1% Triton X-100, 150 mM NaCl, 20 mM Tris-Cl, pH 7,5, 2 mM MgCl2, 1 mM Na-orthovanadate, 10 mM NaF, 0,1 mM DTT, 20 μg ml^{-1} each of antipain, chymostatin, leupeptin and pepstatin. Lysates were then transferred to tubes, and rotated for 15 min at 4°C. The insoluble material was removed by centrifugation at 4°C for 15 min at 13000 rpm.

For the preparation of lysates from mouse brain, the brain of mouse embryos at different stages of development were dissected in PBS and solubilized in 9 volumes of lysis buffer containing 1% Triton X-100, 150 mM NaCl, 20 mM Tris-Cl, pH 7,5, 2 mM

MgCl2, 1 mM Na-orthovanadate, 10 mM NaF, 0,1 mM DTT, 20 μg ml^{-1} each of antipain, chymostatin, leupeptin and pepstatin. Lysates were then transferred to tubes, and rotated for 30 min at 4°C. The insoluble material was removed by centrifugation at 4°C for 15 min at 13000 rpm.

2.5.2 Immunoprecipitation

Lysates prepared from transfected CEFs and COS7 were incubated for 2 h with 40 μl of Protein-A Sepharose beads (Pharmacia) with or without preadsorbed 10 μg of anti-FLAG M5 mAb. The beads were washed twice with 0,5 ml of lysis buffer and resuspended in SDS-PAGE loading buffer for SDS-PAGE analysis.

Lysates prepared from embryonic mouse brain were incubated 2 h with 40 μl of Protein-A Sepharose beads with or without preadsorbed pAb anti-Rac1B (10 μl) or pre-immune serum (20 μl). The beads were washed twice with 0,5 ml of lysis buffer and resuspended in SDS-PAGE loading buffer for SDS-PAGE analysis.

2.5.3 SDS-PAGE and immunoblotting

Immunoprecipitates, lysates and unbound fractions were used for SDS-PAGE, according to Laemmli (1970). Gels were electrophoretically transferred to 0.2 mm nitrocellulose filters and stained with Ponceau S (0.2% in 3% TCA, destain with dd-water) to visualise molecular weight standards and proteins. After blocking the nitrocellulose with 50 mM Tris-Cl, 150 mM NaCl , 5% BSA , pH 7.5, for 1h at room temperature, filters were incubated for 2 h in the same buffer containing the primary antibodies at the following dilutions: pAb anti-HA 1:1000; mAb anti-paxillin 1:250; mAb anti-Rac1 1:2000; pAb anti-Rac1B 1:500; pAb anti-Pix 1:400; pAb anti p95 64S 1: 500; mAb anti-Flag 1μg/ml.

For the detection of primary antibodies, blots were incubated with horseradish peroxidase-conjugated secondary antibodies and revealed by enhanced chemiluminescence (Amersham Pharmacia Biotech). Alternatively, blots were incubated 1 h at room temperature with 0.2 μCi ml^{-1} of either ^{125}I-anti-mouse Ig, or ^{125}I-protein A (Amersham Pharmacia Biotech), washed, and exposed to Amersham Hyperfilm-MP.

2.5.4 Affinity chromatography

The pGEX-cRac1B and pGEX-p95-C2 plasmids were used to obtain GST fusion protein by expression into *Escherichia coli* BL21 cells. After induction of the expression with isopropyl-β-D-thiogalactopyranoside (Sigma-Aldrich) for 18 h at 23°C, cells were resuspended in PBS, and then lysed by sonication. Lysates were centrifuged for 10 min at 11,000 *g* and GST fusion proteins were purified from the supernatants on glutathione–agarose beads (Sigma-Aldrich). 0,5 mg GST-Rac1B bound to 50 μl aliquots of glutatione-agarose beads (Sigma) were loaded for 10 minutes at 37°C with 0,1 mM GTP-γ-S or GDP-β-S in 20 mM Hepes-NaOH pH 7,5, 50 mM NaCl, 1 mM EDTA and 1 mM DTT. Loading was stopped by adding $MgCl_2$ to 5 mM final concentration. Protein (3-3,5 mg) from E6 retinas extracts in lysis buffer were added to beads and incubated for 1 h at 4°C with rotation. Beads were washed 3 times with 0,5 ml of lysis buffer, loaded onto 7,5% polyacrylamide gel for SDS-PAGE, and immunoblotted with the indicated antibodies. For affinity chromatography with GST-p95-C2, 25 μl of beads were loaded with the purified fusion protein, and incubated for 1 h at 4°C with 2 mg of E6 chicken retina lysate. Beads were washed 3 times with 0,5 ml of lysis buffer, loaded onto 7% polyacrilamide gel for SDS-PAGE and analysed by immunoblotting with the indicated antibodies.

2.6 IMMUNOFLUORESCENCE

After transfection, cells were fixed for 15 min with 3% paraformaldehyde in PBS, at room temperature. After two washes with PBS, paraformaldehyde was blocked by 10 min incubation with 2.5 mg/ml NH_4Cl. After two washes with PBS, cells were permeabilised with 0.1% Triton X-100 in PBS for 4 min, washed again with 2xPBS, and incubated 10 min with 0.2% gelatine in PBS. Coverslips were then incubated for 60 min at room temperature with the following primary antibodies diluted in 0.2% gelatine in PBS: mAb anti-Flag 1:300; mAb anti-Myc 1:300; pAb anti-Flag 1:300; anti-paxillin antibody, 40 µg/ml; pAb anti-HA 1:2000; mAb 3A10 1:5; pAb anti-Arf6 1:2000; pAb anti Rab11 1:100; mAb LEP100 1:100; pAb anti-EEA1 1:50; mAb anti-βCOP 1:50. After two washes with 0.2% gelatine in PBS, the samples were incubated for 40 min with FITC-conjugated sheep anti-rabbit IgG and TRITC-conjugated sheep anti-mouse IgG (Boehringer, Mannheim, Germany), or with FITC-conjugated donkey anti-mouse IgG and TRITC-conjugated donkey anti-rabbit IgG (Jackson Immunoresearch Laboratories, Inc., West Groove, PA). All coverslips were mounted with 1 drop of Gelvatol solution (20% polyvinyl alchool, 2% propylgallate, in PBS) and observed using a Zeiss-Axiophot microscope. Fluorescent images were collected using the Image-Pro® Plus software package (Media Cybernetics, L.P.), and processed using Adobe Photoshop 5.0.

2.7 NORTHERN BLOT ANALYSIS

Total RNA was prepared from different organs from E10 chicken embryos, and from E10 CEFs, by a single-step RNA isolation method (Chomczynski and Sacchi, 1987). Northern blot analysis of total RNA (20 µg/lane) was performed as previously

described (Lehrach et al., 1977). Blots were hybridised with a 1 kb probe corresponding to the 5' region of the cDNA for p95-APP1. Hybridisation took place in hybridisation buffer supplemented with ^{32}P-labelled probes (1-2 x 10^6 cpm ml^{-1}) for 21 h at 65°C. Following high stringency washes at 65°C, X-ray films were exposed for 3-7 days to the hybridised filters.

Chapter 3

RESULTS I

3.1 RAC1B KNOCK-OUT: THE GENERATION OF RECOMBINANT EMBRYONIC STEM CELLS Rac1B+/-

Transgenic animals represent an important tool in the biological sciences to investigate the regulation of gene expression and the of cellular and physiological processes.

The null mutants of mouse Rac1 and of mouse cdc42 have been shown to be lethal (Sugihara et al., 1998; Chen et al., 2000), because the development stops at the very early stages . But Rac1 and Cdc42 are ubiquitously expressed, and they play important roles in cell migration which is a central event during the first stages of development. Rac2 is a component of the family specifically expressed in the haematopoietic cells. The knock-out mice for Rac2 have been generated (Roberts et al., 1999) and they are viable, but with specific defects in the migration and functions of haematopoietic derived cells.

Rac1B is specifically expressed in the developing nervous system, and it is possible that Rac1B knock-out may results in mice with affected neural development. The analysis of the phenotype due to the absence of Rac1B gene will be fundamental in order to understand the mechanisms mediated by the GTPase in the nervous system development.

3.1.1 Characterization of the polyclonal antibody for Rac1B

In order to study the expression of mouse Rac1B, a polyclonal antibody was produced by immunizing rabbits with a peptide specific for Rac1B, corresponding to the

carboxy terminal part of the protein: Cys Pro Pro Pro Val Lys Lys Pro Gly Lys Lys Cys Thr Val Phe.

The antibody was specific, since it was able to recognize only GST-Rac1B fusion proteins, and not the highly homologous GST-Rac1A (Fig. 3.1). The polyclonal antibody was also able to immunoprecipitate the endogenous protein from a lysate of E13 chicken brain. The specific band was not recognized when the immunoprecipitation was performed with the pre-immune serum, or when the antibody was preincubated with the peptide that was used for the immunization of the rabbit (Fig. 3.2).

3.1.2 The expression of mouse Rac1B protein is regulated during brain development.

In order to study the expression of Rac1B in mouse brain development, the polyclonal antibody specific for this GTPase was used to immunoprecipitate endogenous protein from lysates prepared from mouse brain at different stages of development (Fig. 3.3). The level of Rac1B protein was regulated during development: it started to increase at E13.5, reached a maximum after birth at stage P7, and then it decreased, and was almost absent in the adult brain. These data support the hypothesis that Rac1B plays a specific role during neural development.

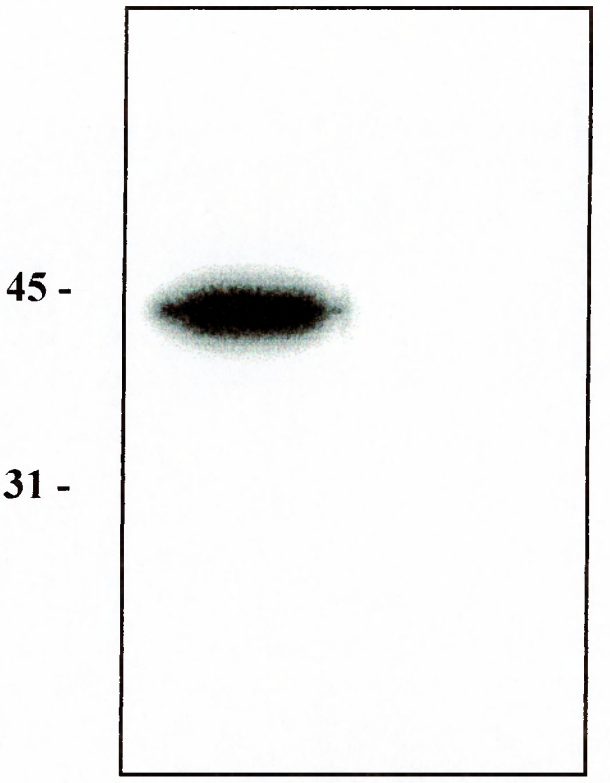

Fig. 3.1. The anti-Rac1B pAb specifically recognizes the GST-Rac1B fusion protein.

Equal amounts of GST-Rac1A and GST-Rac1B (2 μg) were loaded on a 12% SDS-PAGE, and immuno-blotted using the anti-Rac1B pAb (1:500). The antibody was specific for Rac1B, since it did not recognize GST-Rac1A.

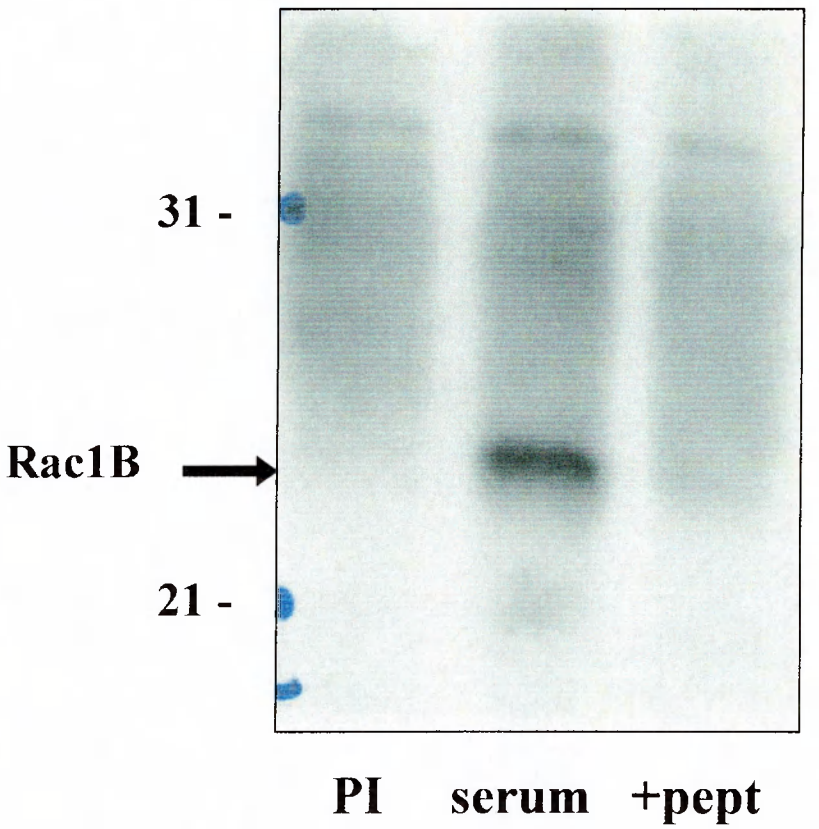

Fig. 3.2. The anti-Rac1B pAb can immunoprecipitate the endogenous protein.

Preimmune serum (PI, 20 μl), anti-Rac1B antibody (serum, 10 μl), and anti-Rac1B preincubated with the peptide used for the immunization (+pept), were used to precipitate the endogenous Rac1B from brain lysate of E13 chicken embryos (2 mg/lane). Proteins were resolved by SDS-PAGE and western blotting performed using anti-Rac1 mAb antibody (1:2000) (Transduction Laboratories) which recognizes both the GTPases Rac1A and Rac1B. A specific band was detected only when the serum without peptide was used.

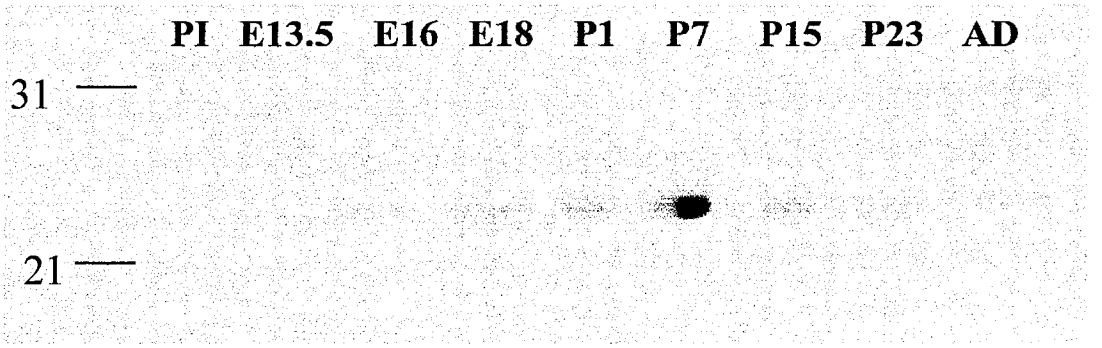

Fig. 3.3. The expression of mouse Rac1B protein in the brain is regulated during development.

The anti-Rac1B pAb was used to immunoprecipitate endogenous protein from equal amounts (2 mg/lane) of brain lysate prepared at different stages of development. Western blotting was performed using anti-Rac1 mAb (1:2000), which recognizes both Rac1A and Rac1B. Rac1B protein is almost absent in the adult brain, and its expression peaks at P7. (AD: adult, PI: preimmune serum).

3.1.3 Strategy used to generate Rac1B knock-out mice.

Mouse Rac1B is composed of 6 exons and 5 short introns. The region of the gene covering the translated sequence is very short: 2 kb from the initial ATG to the stop codon (Fig. 3.4). To generate a null mutation of Rac1B, the strategy was to remove in R1 ES cells the entire translated sequence of mouse Rac1B, from the first codon to the stop codon, and to replace it with the β-galactosidase sequence, and with a *loxP*-flanked PGK-Neo cassette to be used for the selection. The *loxP* sites ensure that the neomycine-resistance selection marker (Neo) can be deleted via Cre-mediated recombination to generate a 'clean' deletion (Lakso et al., 1996).

The neomycin phosphotransferase enzyme can inactivate the drug G418, that is added to the medium of the transfected ES cells. Only transfected cells that express the neomycin phosphotransferase can survive in the presence of G418.

In order to induce the homologous recombination to replace the sequence of Rac1B, a construct was prepared where the sequence of the β-galactosidase and the neo cassette were flanked by two genomic sequences: the short arm of 1,6 kb, which is the region immediately upstream the ATG of the gene, and the long arm of 5 kb immediately downstream the stop codon.

The plasmid included the gene encoding thymidine kinase, which represents another way of selection for the transfected cells. The sequence of the enzyme was located downstream of the long arm, and it can be integrated in the genome only when the recombination is not homologous. In this case the enzyme is produced and it is able to phosphorylate and activate gancyclovir, a nucleotide analogue which is added to the selection medium. Once converted in the triphosphate form, this analogue can be incorporated in the DNA during cell division, causing a block of DNA replication. When the recombination is homologous, the sequence of the thymidine kinase is not integrated in the genome, and the enzyme is not produced.

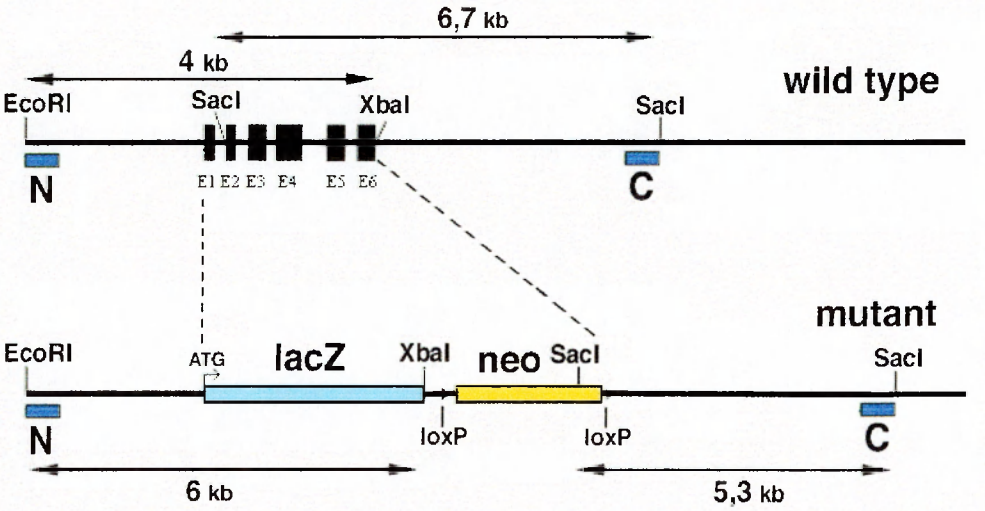

Fig. 3.4. The strategy used for the generation of Rac1B knock-out mice.

Scheme of the organization of the mouse Rac1B gene (upper panel), and of the construct used for the transfection of ES cells (lower panel). LacZ (β-galactosidase sequence), neo (neomycin phosphotransferase), N (aminoterminal probe used for Southern blotting after digestion of genomic DNA with *EcoRI* and *XbaI*), C (carboxyterminal probe used for Southern blotting after digestion of genomic DNA with *SacI*). Double arrows and numbers indicate the fragments and their size, obtained by enzymatic digestion of genomic DNA from wild-type (top) and recombinant (bottom) cells.

3.1.4 Transfection and screening of recombinant ES clones

R1 ES cells were used for electroporation. Cells were thawed, amplified and transfected by electroporation using the linearized plasmid with the modified genomic DNA, as described in the chapter Materials and Methods. After 8 days of selection in the presence of G418 and gancyclovir, 320 clones were picked, amplified and frozen for screening by Southern Blotting. Two types of DNA digestion and two different probes were used. As shown in Fig. 3.5, by digesting the genomic DNA with *EcoRI* and *XbaI*, and using an aminoterminal probe (N), it was possible to detect a fragment of 4 kb if no homologous recombination occurred , and a fragment of 4 kb together with a fragment of 6 kb in the case of homologous recombination (Fig. 3.4, 3.5). The second type of digestion was with *SacI*, using a carboxy terminal probe (C), which gave a band of 6,7 kb in the clones where no homologous recombination had occurred, and a 6,7 kb together with one of 5,3 kb in the case of homologous recombination (Fig. 3.4, 3.5).

Four independent clones in which homologous recombination had occurred were identified: the clone numbers 215, 239, 313 and 314.

The cells of each clone were microinjected in blastocysts, and the clones 215 and 314 were able to colonize the embryos to give chimeric mice with good percentages of chimerism (from 30% to 95%) (Table 3.1). Chimeras were subjected to the breeding programme with C57-BL6/J in order to identify possible germ-line transmission of the mutation. The most used genetic marker is coat colour. Chimeric combinations of strains which differ at one coat colour locus allow a simple appreciation of the degree of tissue contribution in terms of the proportion of the coat that expresses the ES cell allele. In general, the degree of coat colour chimerism correlates with the degree of germline contribution. In these case, ES cells give an agouti color, but the progeny was

composed of black mice, so until now no germ-line transmission was obtained (Table 3.2).

As no germ-line trnsmission was obtained, a second transfection of ES cells was carried out using cells of an earlier number of passages. ES cells that are subjected to too many passages, start to loose their totipotency, and the probability to be involved in the germ-line colonization decreases. After the selection in the presence of the drugs G418 and gancyclovir, 300 clones had been picked, and the screening by Southern blot is now in progress.

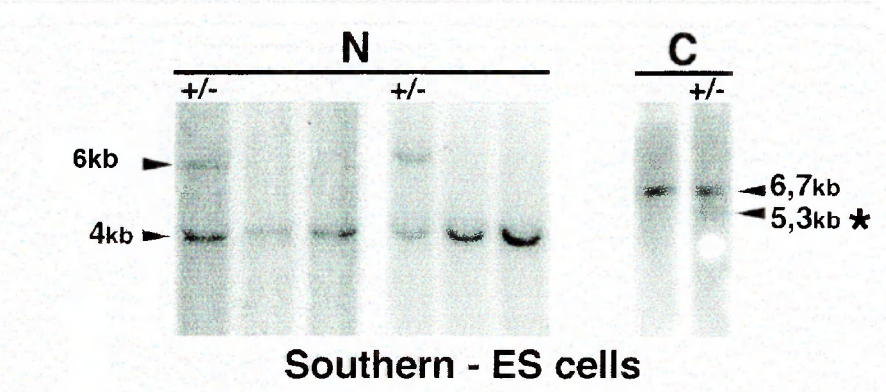

Fig. 3.5. Example of Southern Blot on recombinant and non recombinant ES clones.

Left panel: 6 clones were analysed by digesting the DNA with *EcoRI* and *XbaI*, followed by Southern using the aminoterminal probe (N). Two positive clones are present, with two bands of 4 and 6 kb. Right panel: two clones were analysed by digesting the DNA with *SacI*, followed by Southern with the carboxyterminal probe (C). One positive clone is present, with two bands of 6,7 and 5.3 kb.

CLONE NUMBER	CHIMERAS	% OF CHIMERISM
215	215A	70%
	215B	30%
	215C	30%
239	/	/
313	/	/
314	314A	95%
	314B	95%
	314C	95%

Table 3.1. Scheme of the chimeras obtained by the microinjection of the recombinant clones of ES.

The chimeras with the best percentage of chimerism were obtained by the microinjection of the clone number 314 (95%), while no chimeric mice were obtained with the clones number 239 and 314.

CLONE NUMBER	CHIMERA	NUMBER OF LITTERS	COAT COLOUR
215	215A	3	Black (1 eaten)
	215B	3	Black (1 eaten)
	215C	4	Black (1 eaten)
314	314A	9	Black (2 eaten)
	314B	9	Black (4 eaten)
	314C	1	eaten

Table 3.2. Scheme of the litters obtained from the chimeras.

The chimeras 215A, B and C, and 314A, B, and C were crossed with C57-BL6/J. In the table are indicated the numbers of littermates and the coat colour, that is an indication of the germline transmission. Several events of cannibalism made impossible to analyze the coat colour.

3.2 DISCUSSION

In this chapter I have described the production of recombinant Rac1B +/- ES cells in order to obtain mice null for the small GTPase Rac1B. It has been shown that Rac1-deficient embryos cannot survive because several defects of gastrulation induce death (Kazuhiro et al, 1998), suggesting that Rac1 is required for the formation of the three germ layers, which is the most prominent event during the early mouse embryogenesis. During this period, the embryonic mesoderm and definitive endoderm are both generated from the epiblast by cell migration through the primitive streak, in which coordinated changes in cytoskeletal organization, cell adhesion and motility are critical. Thus, Rac1-mediated cytoskeletal reorganization, cell adhesion and migration are essential for early development. Similar to Rac1, Cdc42-null embryos also die at E7,5. The embryos were smaller than normal, disorganized in structure and largely lacking embryonic primary ectoderm, with defects in post-implantation development probably due to an inability to properly form and reorganize actin-based cellular structures crucial for further gastrulation (Chen et al., 2000).

Rac1B, in contrast to Rac1 and Cdc42, shows a more restricted expression pattern and it is highly concentrated in the nervous system. For this reason Rac1B-null mice could represent a very good model in order to study the mechanisms of neural development. Unfortunately, until now, I have not identified germ-line transmission from the chimeras obtained from the recombinant Rac1B +/- ES cells. One possible explanation could be the R1 ES cells used in this experiment. I used a vial of cells that were at the passage number 13. Germ-line colonization of the embryos is a very important and delicate event, and cells that have been subjected to many passages start to loose their totipotency and they can differentiate. The state of ES cells is very critical for the colonization of the germ-line, and this could have been the reason why it was not possible to obtain the germ-line transmission. Another problem was cannibalism, in fact

several litters were eaten by females immediately after birth (see Table 3.2). This problem, which is probably due to stressed conditions of females, prevented analysis of possible germ-line transmission. I transfected another vial of R1 ES cells at an earlier passage (number 10), that were used by other groups and that gave germ-line transmission and the generation of transgenic or knock-out mice, and the screening of the clones resistant to the selections is now in progress.

An important point is to characterize in details the expression pattern of Rac1B in the nervous system of mice, in order to facilitate the analysis of the future null-Rac1B mice. The polyclonal anti-Rac1B was used in immunohistochemical analysis on brain sections of P7 mice, since at this stage the endogenous protein is highly expressed (Fig. 3.3), and the project is still in progress. The data has shown that Rac1B is highly expressed in the layers I and II/III of the cortex, and also in the cerebellum, where it is concentrated in the granular layer, in Purkinjie cells, and also in the deep nuclei and in medulla oblungata (unpublished data). Rac1B expression pattern indicates that it could be involved in nervous system development.

Chapter 4

RESULTS II

Actin dynamics during growth cone navigation evolve into stabilization of the cytoskeleton and neurite elongation. While a large amount of information exists about the extracellular mechanisms driving these processes, large gaps still exist in the comprehension of the corresponding intracellular events. With the aim of investigating the molecular mechanisms at the basis of Rac1B-mediated neurite extension, by affinity chromatography of GTP-bound RAC GTPases it was identified p95-APP1 (Di Cesare et al., 2000), and the role of the protein was analysed in neurite extension of E6 chicken retinal neurons.

4.1 ANALYSIS OF THE EXPRESSION OF P95-APP1

4.1.1 P95-APP1 is expressed in neural tissue

P95-APP1 was isolated from E15 brain lysates of chicken embryos. In order to investigate in detail the expression pattern of p95-APP1 in chicken embryonic tissues during development, northern blot analysis was carried out. A 2,8 kb transcript was detected by hybridising filters with total RNA isolated from various tissues of embryonic day 10 (E10) avian embryos (Fig.4.1) with a cDNA probe of 970 bp located in the 5' end, immediately downstream the ATG. P95-APP1 was particularly abundant in neural tissues, including neural retina, and was present also in E10 CEFs. In embryonic day 6 (E6) neural retinas, the source of neurons utilized in this study, the level of the transcript was low, compared to the stage E10, suggesting a regulation of the expression of the transcript during development (Fig.4.2).

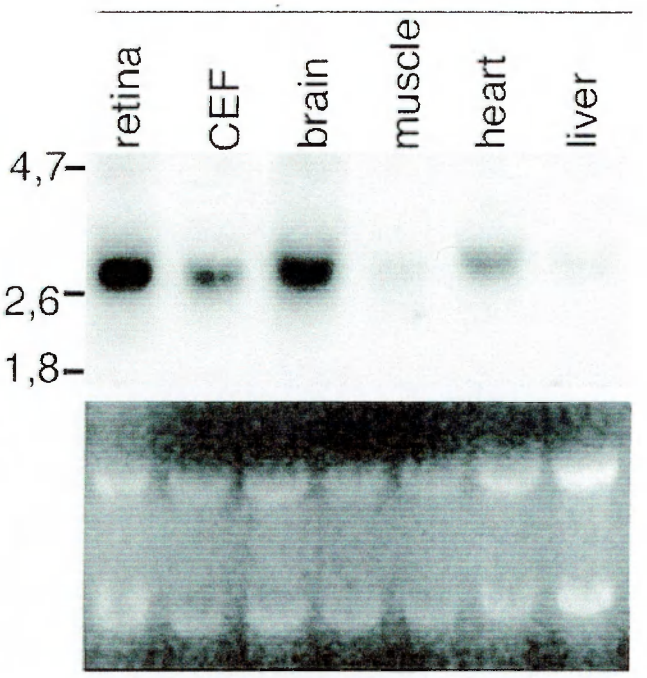

Fig. 4.1. Expression of p95-APP1 in E10 chicken tissues

Northern blot analysis (upper panel) on total RNA (lower panel) prepared from different chick E10 tissues and from CEFs. The filter was incubated with a cDNA probe specific for p95-APP1. 20 μg of total RNA were loaded in each lane. P95-APP1 was highly expressed in neural tissues, including neural retina.

Fig. 4.2. The expression of p95-APP1 in the chicken retina is regulated.

Northern blot analysis on total RNA prepared from chicken retina at two different stages of development. The level of the transcript increases between E6 and E10, indicating a regulation of the expression of p95-APP1 during the development.

4.1.2 Characterization of the p95-APP1 complex in neural cells

Since p95-APP1 has been shown to interact with PIX and paxillin (Di Cesare et al., 2000), the presence of this complex in E6 neural retinas was investigated by immunoblotting after affinity chromatography on Rac1B columns loaded with a lysate from E6 neural retinas. P95-APP1, βPIX, and paxillin were specifically detected after chromatography on Glutathione-S-transferase (GST)-Rac1B-GTPγ-S, but not on GST-Rac1B-GDPβ-S protein (Fig.4.3), confirming the existence of an endogenous p95-APP1/PIX/paxillin complex in E6 neural retinal cells which binds Rac1B in a GTP-dependent manner.

4.2 ANALYSIS OF THE EFFECTS OF OVER-EXPRESSION OF WILD-TYPE AND MUTANT P95-APP1 ON NEURITE EXTENSION

The molecular dissection of the function of this multidomain protein in non-neuronal cells has shown that, while the carboxy terminal portion of p95-APP1 has a diffuse distribution and induces protrusive activity in fibroblasts (Di Cesare et al., 2000), ArfGAP-deficient mutants specifically accumulate at large Rab11-positive vesicles, suggesting a role for this ArfGAP in membrane recycling (Matafora et al., 2001).

To look at the effects of p95-APP1 on neurite extension, I transfected E6 retinal neurons with a number of p95-APP1-derived constructs (Fig. 4.4), in order to uncouple different domains of the protein, and to analyse the effects on cellular organization and subcellular distribution. The transfected cells were cultured for 20-24 h on laminin-1, a potent inducer of neurites in these neurons (Adler et al., 1985).

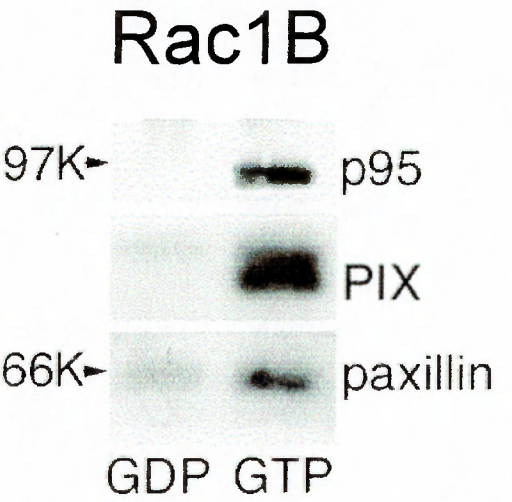

Fig. 4.3. Analysis of the p95-APP1 complex in E6 neural retina.

A lysate from E6 retinas was incubated with agarose beads bound to GST-Rac1B loaded with GDP-β-S (left lane) or GTP-γ-S (right lane). Eluates were immunoblotted with anti-p95-APP1 (upper), anti-PIX (centre) and anti-paxillin (lower) antibodies. The complex can be eluted only from Rac1B bound to GTP.

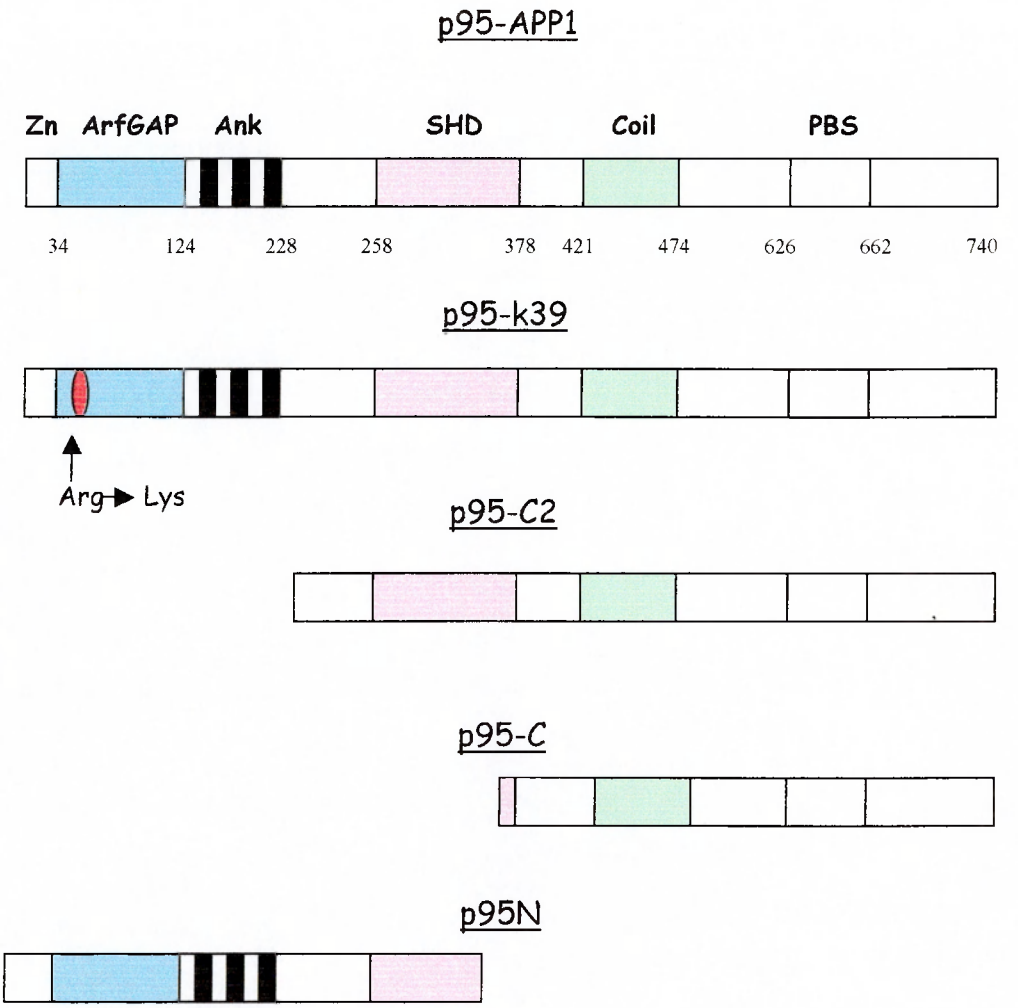

Fig. 4.4. Scheme of p95-APP1 constructs used in the transfection experiments.

Zn (zinc finger), GAP (ArfGAP domain), ANK (ankyrin repeats), SHD (Spa2 homology domain), COIL (coiled coil region), PBS (paxillin binding subdomain).

4.2.1 Overexpression of full-length p95-APP1 does not affect neuronal morphology

Non-transfected E6 retinal neurons, or neurons expressing a control protein (β-galactosidase), usually extend one long, poorly branched neurite after 24 h on laminin (identified by anti-neurofilament staining in Fig. 4.5b). Overexpression of the wild-type p95-APP1 did not affect the overall morphology of retinal neurons (Fig. 4.5c). In Fig. 4.6 is shown a quantitative analysis. The graph shows the percentage of transfected neurons lacking a neurite, with a short neurite (with length less than three cell body diameters), or with a long neurite. Quantification and comparison between neurons expressing the control protein confirmed the lack of effects of p95-APP1 overexpression on neuritogenesis.

4.2.2 The truncated protein p95-C shows a mild effect on neuronal morphology

It has been previously shown that the expression of the carboxyterminal p95-C polypeptide, that includes the paxillin-binding domain, enhances the formation of membrane protrusions in CEFs (Di Cesare et al., 2000). The expression of p95-C did not have such a dramatic effect in neurons, although neurons with two neurites were more frequently observed (60%) when compared to neurons expressing the β-galactosidase (Fig. 4.7). The quantification showed that the percentage of transfected neurons characterized by a normal process of neuritogenesis was not affected (Fig. 4.8).

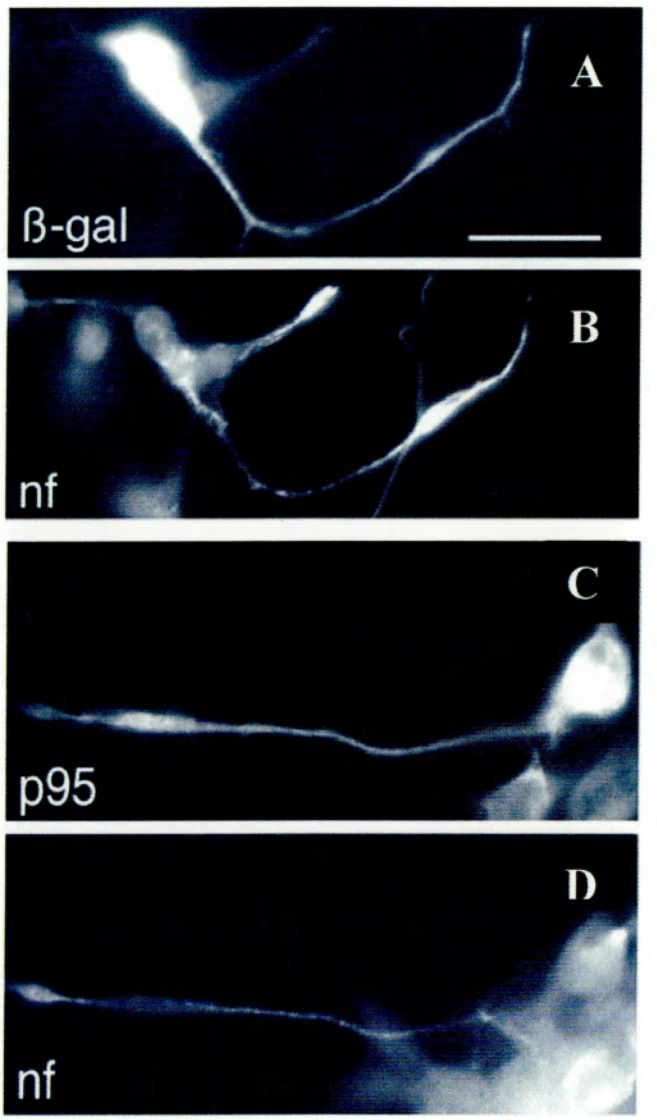

Fig. 4.5. The overexpression of p95-APP1 does not affect neuronal morphology.

Retinal neurons were transfected with pFLAG-LacZ (A) and pFLAG-p95-APP1 (C) and cultured overnight on polylysine- and laminin-coated coverslips. One day after transfection, cells were processed for immunofluorescence using the anti–FLAG mAb (A, C) and the polyclonal antibody against the 200-kDa neurofilament protein (B, D). The same cells are shown in A and B; in C and D. P95-APP1 overexpression showed no effect on neuritogenesis (Bar, 10 μm).

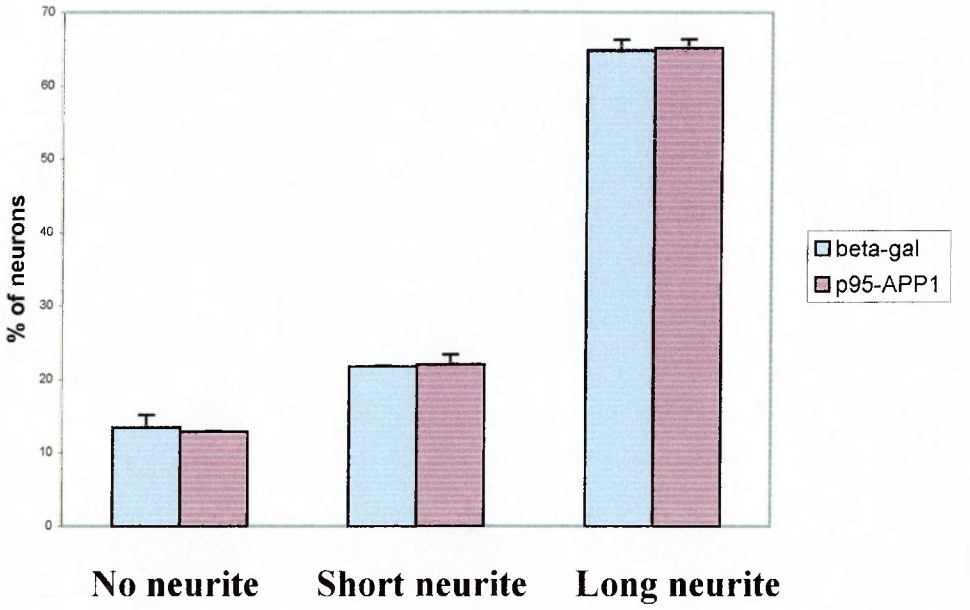

Fig. 4.6. Quantitative analysis of the effect of p95-APP1 overexpression on neuritogenesis.

Data are expressed as percentage of transfected neurofilament-positive neurons with no, short (less than three cell body diameters in length), and long neurite. Values are means +/- s.d. from two experiments. As for neurons transfected with the β-galactosidase, neurons expressing p95-APP1 show normal neurite extension.

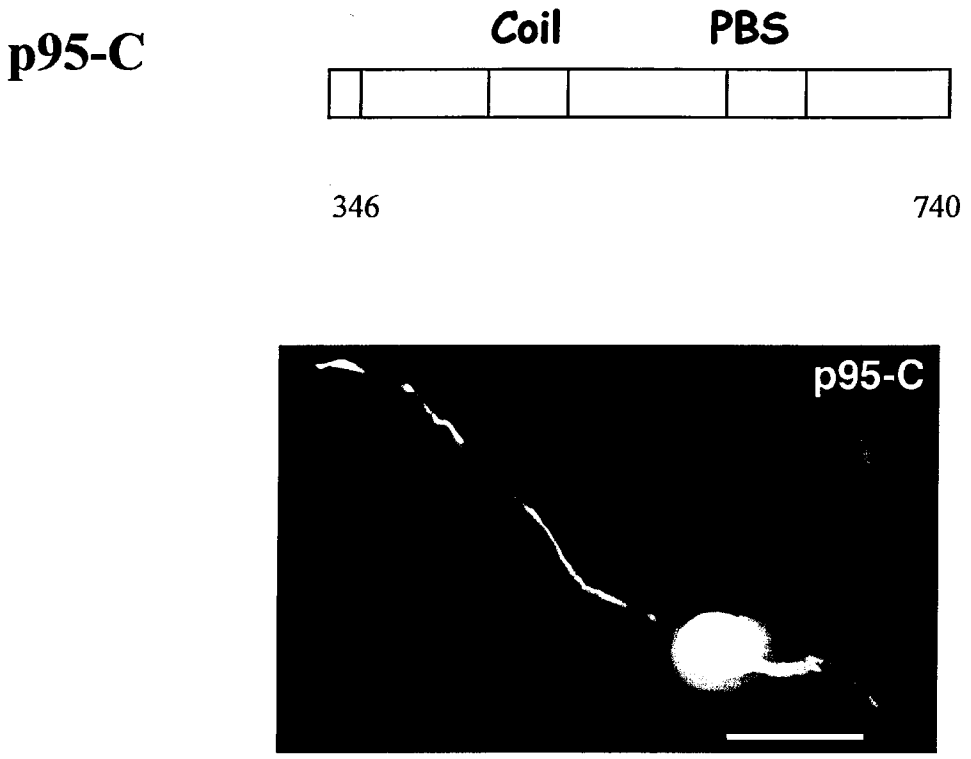

Fig. 4.7. Analysis of the expression of p95-C.

Retinal neurons were transfected with pFLAG-p95-C and processed for immunofluorescence using the anti–FLAG mAb. Some transfected neurons had two neurites per cell. In the upper panel is shown a schematic representation of the deleted construct p95-C, containing the PBS (Paxillin Binding Subdomain) domain and the coiled-coil region (Bar, 10 μm).

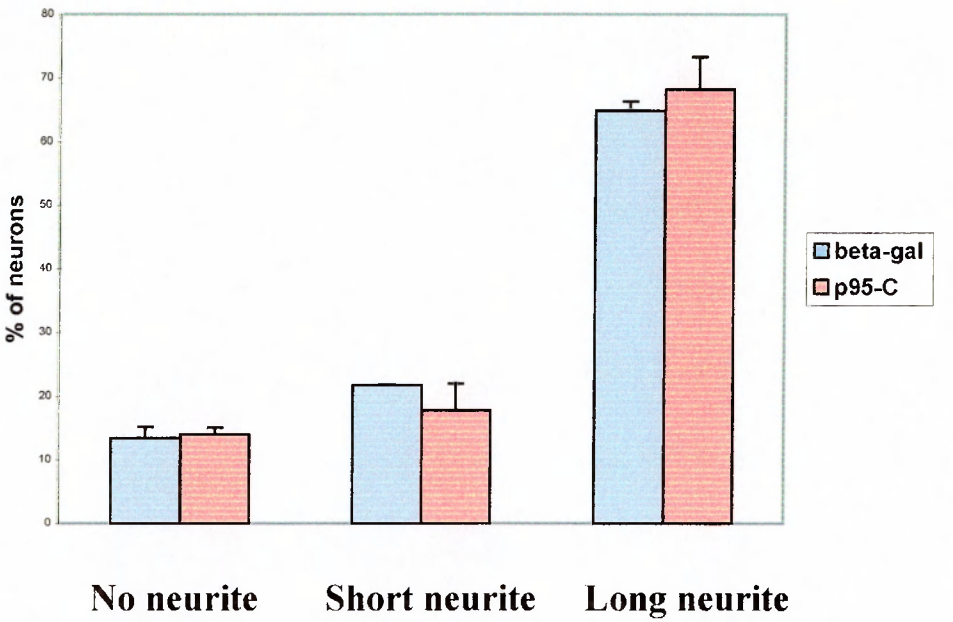

Fig. 4.8. Quantitative analysis of the effect of p95-C overexpression on neuritogenesis.

Data are expressed as percentage of transfected neurofilament positive neurons with no, short (less than three cell bodies diameters in length) and long neurite. Values are means +/- s.d. from two experiments. As for neurons transfected with the β-galactosidase, neurons expressing p95-C showed normal neurite extension.

4.2.3 Mutants of p95 lacking a functional ArfGAP domain inhibit neuritogenesis

The process of neurite formation was strongly affected by the expression of p95-C2 (Fig. 4.9), a truncated mutant of p95-APP1 which lacks the entire ArfGAP domain and the three ankyrin repeats. P95-C2 differs from p95-C in that it includes the Spa2 homology domain (SHD), required for the binding to Pix (Fig. 4.4). About 60% of the p95-C2-transfected neurons showed complete inhibition of neurite extension (Fig. 4.11).

In several ArfGAPs, mutation of a conserved arginine in the GAP domain, corresponding to arginine 39 in p95-APP1, is known to drastically reduce the GAP activity (Mandiyan et al., 1999; Randazzo et al., 2000; Szafer et al., 2000; Jackson et al., 2000). To test whether the effects observed upon p95-C2 expression could be attributed to the absence of the ArfGAP activity, the epitope-tagged p95-K39 protein, in which arginine 39 is substituted by a lysine (Fig. 4.10) was expressed. P95-K39 clearly inhibited neurite extension, leading to lack of neurites in about 50% of the transfected neurons (Fig. 4.11). These data indicate the requirement of an intact ArfGAP domain in p95-APP1 for neurite outgrowth on laminin.

Both p95-C2 and p95-K39 mutants induced the formation of large vesicles in the cell body of transfected neurons (Fig. 4.9 and 4.10). These proteins are able to interact with PIX and paxillin in fibroblasts (Matafora et al., 2001). In retinal neurons endogenous paxillin redistributed from the diffuse punctate pattern observed in non-transfected neurons, to the large p95-C2/K39 positive vesicles (Fig. 4.12). Concentration at large vesicles was also observed in cells cotransfected with PIX or PAK (Fig. 4.12, 4.13). Therefore, mutations affecting the ArfGAP domain of p95-APP1 induce the

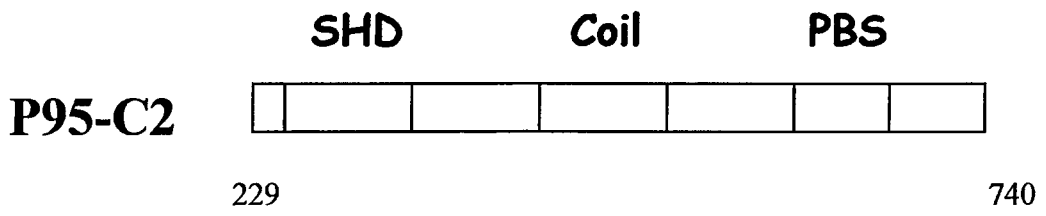

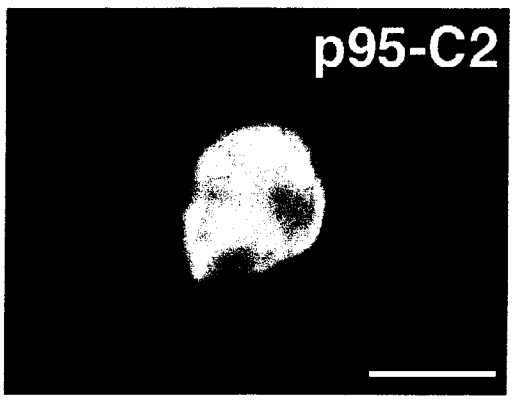

Fig. 4.9. Analysis of the expression of p95-C2.

Retinal neurons were transfected with pFLAG-p95-C2 and processed for immunofluorescence using the anti–FLAG mAb. Most of the transfected neurons did not extend neurites, and large vesicles were present in the cell bodies. In the upper panel is shown a schematic representation of the deleted construct p95-C2, containing the PBS domain, the coiled-coil region and the Spa2 homology domain required for the interaction with PIX. (Bar, 5 μm)

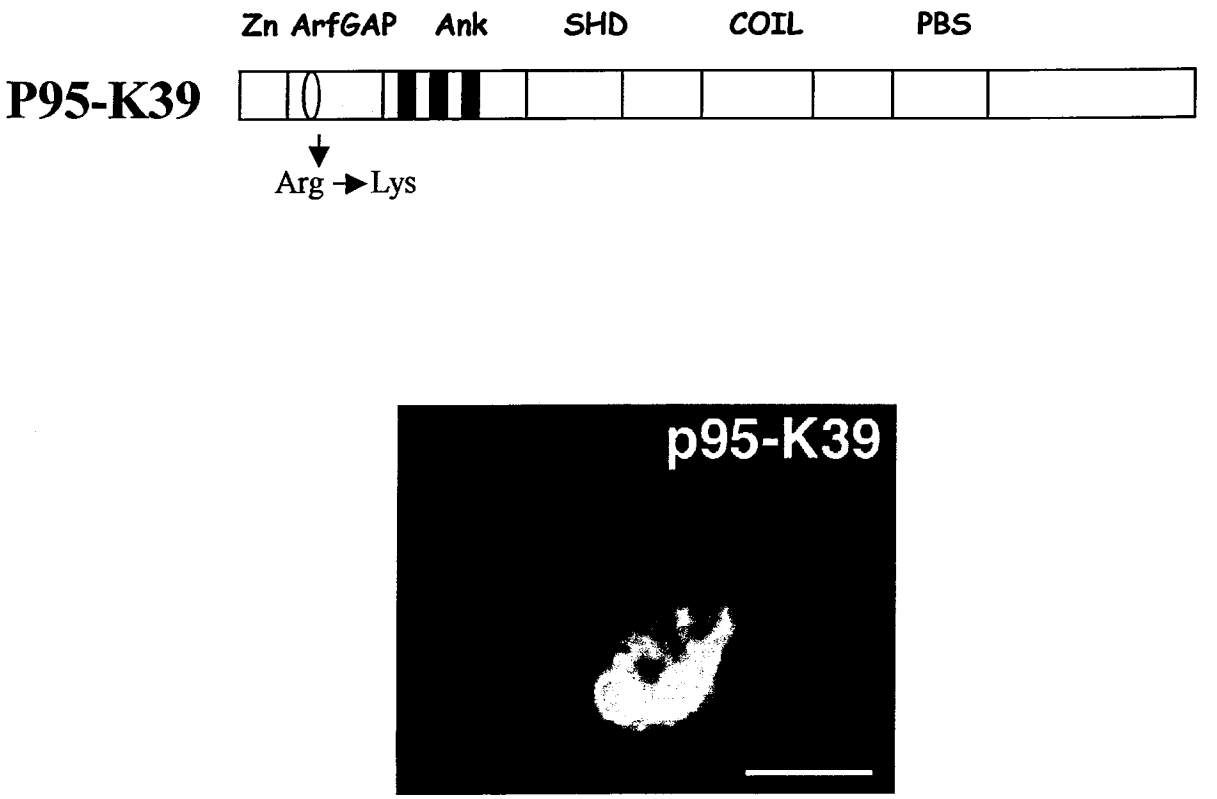

Fig. 4.10. Analysis of the expression of p95-K39 mutant.

Retinal neurons were transfected with pFLAG-p95-K39 and processed for immunofluorescence using the anti–FLAG mAb. As for neurons expressing p95-C2, most of the transfected neurons did not extend neurites, and large vesicles were present in the cell bodies. In the upper panel is shown a schematic representation of construct p95-K39, characterized by a single aminoacid substitution in the GAP domain (Arg 39 is substituted by Lys). (Bar, 5 μm).

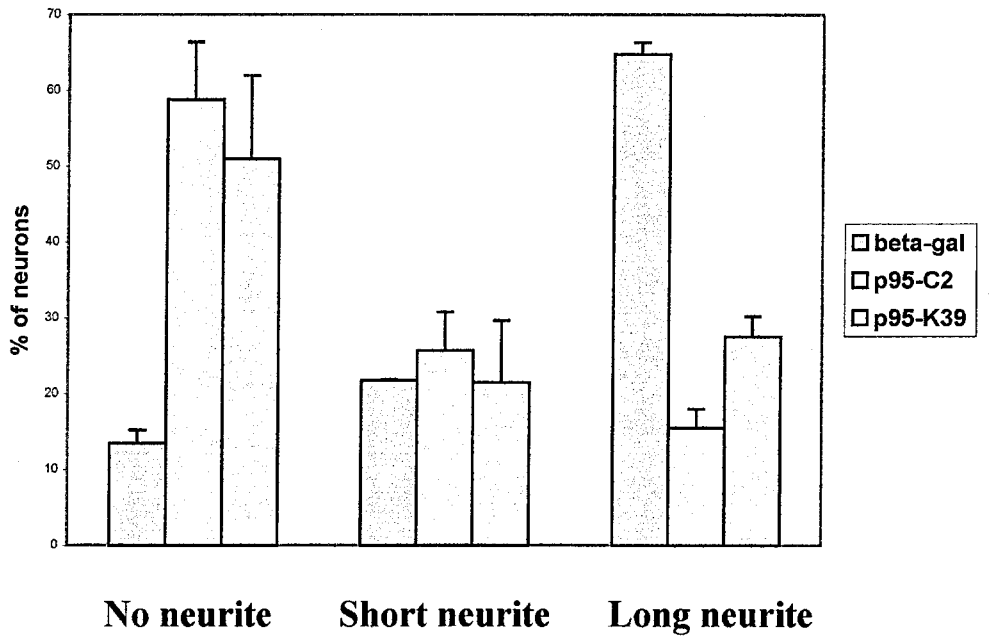

Fig. 4.11. Quantitative analysis of the effect of p95-C2 and p95-k39 overexpression on neuritogenesis.

Data are expressed as percentage of transfected neurofilament positive neurons with no, short (less than three cell body diameters in length) and long neurite. Values are means +/- s.d. from two experiments. The overexpression of the two constructs lacking a functional ArfGAP domain inhibited neurite extension.

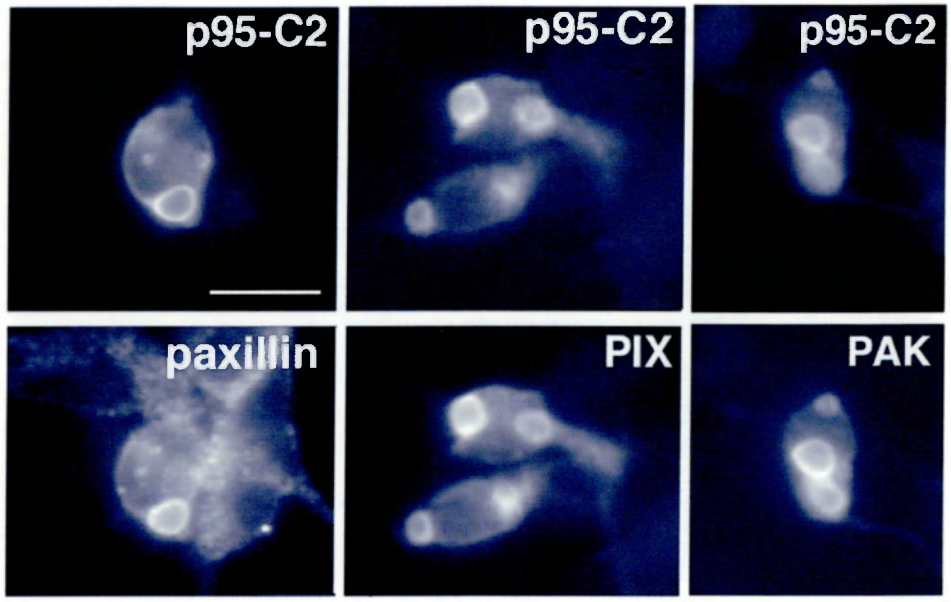

Fig. 4.12. Endogenous paxillin, and transfected PIX and Pak colocalize with p95-C2 at the large vesicles.

Retinal neurons were transfected with pFLAG-p95-C2 (left panels) or cotransfected with pFLAG-p95-C2 and pXJ40-HA-βPIX or pCMV6m/PAK1 (middle and right panels, respectively), and processed for immunofluorescence using the anti–FLAG mAb (upper panels) and with the anti-paxillin (left), anti-HA (middle) and anti-Myc (right) antibodies. Endogenous paxillin and exogenously expressed PIX and Pak colocalized at the large vesicles induced by the expression of the mutant p95-C2. (Bar, 7 μm).

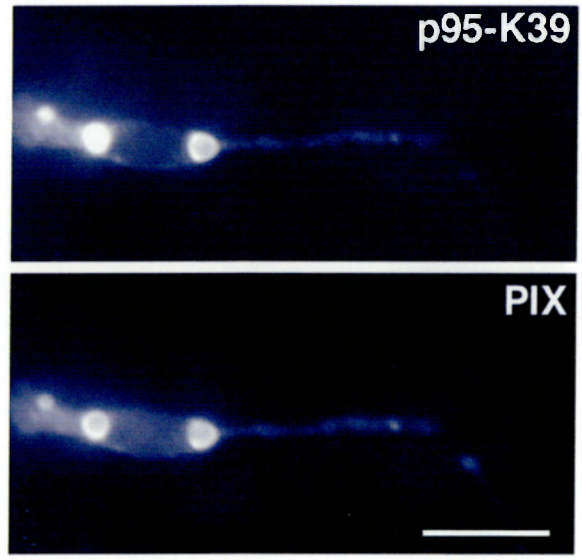

Fig. 4.13. Transfected PIX colocalizes with p95-K39 at vesicles.

Retinal neurons were cotransfected with pFLAG-p95-K39 and pXJ40-HA-βPIX, and processed for immunofluorescence using the anti–FLAG mAb (upper panel) and with the anti-HA antibodies (lower panel). PIX and p95-K39 colocalize at the large vesicles. (Bar, 7 μm).

accumulation of the entire p95 complex on large vesicles. These data indicate a correlation between the formation of the large vesicles and the inhibition of neuritogenesis. The different subcellular distribution of p95-C2 compared to p95-C suggests the requirement of the PIX-binding domain of p95-APP1 for the accumulation of the p95 complex on the large vesicles.

4.3 P95-C2 SPECIFICALLY ACCUMULATES AT RECYCLING ENDOSOMES IN RETINAL NEURONS.

In order to characterize the nature of the large vesicles induced by the overexpression of p95-C2, the transfected neurons were analysed by immunofluorescence using antibodies specific for various intracellular compartments. The data indicated that the large vesicles positive for p95-C2 are positive for Rab11 (Fig. 4.14), a functional marker of the endocytic recycling compartment (Ullrich et al. 1996). The accumulation of p95-C2 at this compartment is specific, since the subcellular distribution of both the early endocytic marker EEA1, of the Golgi marker βCOP and of the lysosomal marker LEP100 did not show any overlap with the p95-C2 positive vesicles (Fig. 4.15 and 4.16).

For comparison, in non-transfected neurons, Rab11 was distributed in a cytoplasmic punctated pattern along neurites and at the growth cone (Fig. 4.17). This indicates that the overexpression of ArfGAP-defective p95 proteins induced a specific alteration of the morphology of the neuronal recycling compartment, and suggests a correlation between the recycling of vesicles and the process of neurite extension.

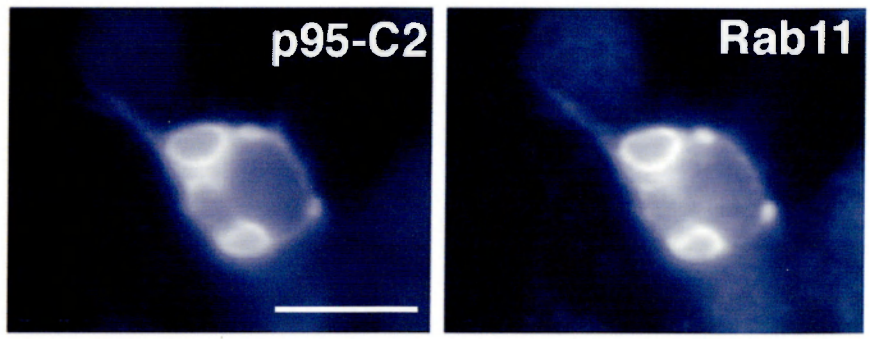

Fig. 4.14. Specific localization of p95-C2 at large Rab11-positive vesicles.

Neurons expressing p95-C2 were fixed after 24 h and costained with the anti-Flag antibody and the recycling endosomal marker Rab11. There was a clear colocalization of p95-C2 with endogenous Rab11 at the vesicles. (Bar, 5 μm).

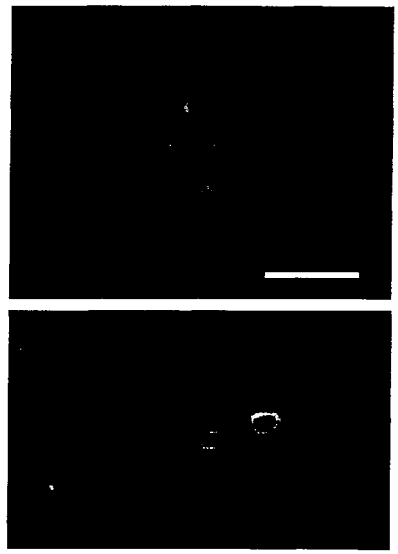

Fig. 4.15. Early endosomal and Golgi markers do not colocalize with p95-C2.

Confocal microscopy analysis of retinal neurons transfected with pFLAG-p95-C2 and stained after 24 h with anti-FLAG (green) and for the Golgi marker βCOP (red) in the upper panel, and with anti-FLAG (green) and for the early endocytic marker EEA1 (red) in the lower panel. The analysis does not show overlap of these markers at the large vesicles with the ArfGAP domain-deficient mutant. (Bar, 5 μm).

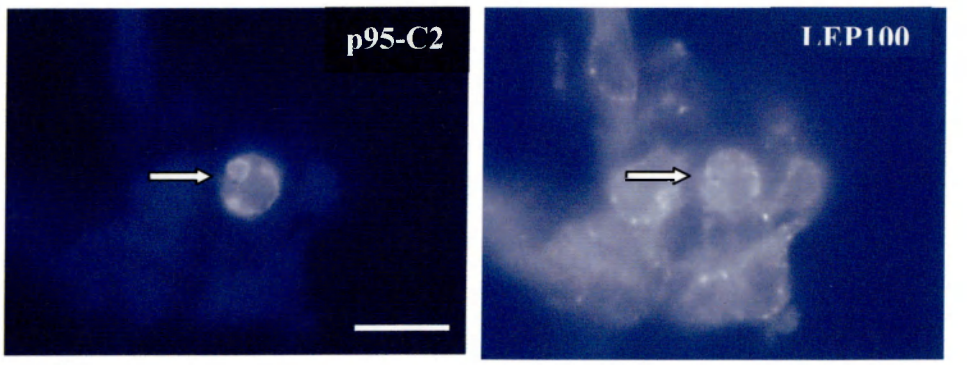

Fig. 4.16. The large vesicles induced by p95-C2 are not lysosomes.

Retinal neurons were transfected with pFLAG-p95-C2 and stained with the anti-FLAG antibody and with the lysosomal marker LEP100. The arrow indicates a transfected neuron. The analysis shows no colocalization of LEP100 with the large vesicles. (Bar, 5 μm).

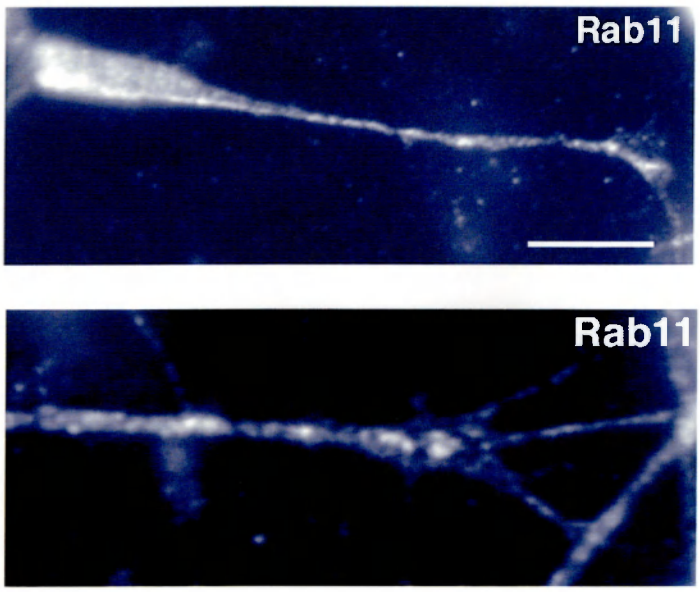

Fig. 4.17. Rab11 distribution in non transfected neurons.

Retinal neurons were analysed by immunofluorescence with the anti-Rab11 antibody. The recycling endosome marker is distributed in the soma, along the neurite and also in the growth cone (lower panel) of neurons, in a punctate pattern. (Bar, 7 μm in upper panel; 10 μm in lower panel).

4.4 LOCALIZATION OF DISTINCT ARF GTP-ASES SUGGESTS A ROLE OF P95-APP1 AS REGULATOR OF ARF6 AND ARF5, BUT NOT ARF1.

GIT proteins have GAP activity for different Arf proteins in vitro, including Arf6 (Vitale et al., 2000). The Arf substrate for p95-APP1 in vivo has not been identified yet. The truncated mutant p95-N including the ArfGAP domain (Fig. 4.4) colocalizes at endocytic vesicles with the inactive mutant N27Arf6 in CEFs (Matafora et al., 2001). These data were confirmed in retinal neurons, as shown by confocal microscopy analysis (Fig. 4.18). The expression of the truncated construct p95-N, which contains the GAP domain and the three ankyrin repeats, and an incomplete SHD domain, induced the formation of small vesicles in the cytoplasm that were different from the ones induced by p95-C2 or p95-K39. P95N and N27Arf6 colocalized at the small vesicles (Fig. 4.18a). Arf6 is the only known member of class III Arfs. For comparison the distribution of Arf1, a class I Arfs, and of Arf5, a class II Arf, was determined. The inactive mutant N31Arf1 did not show colocalization with p95-N (Fig. 4.18b), while the corresponding N31Arf5 mutant colocalized with the p95-N construct (Fig. 4.18c). These data suggest that p95-APP1 may interact functionally with Arf6 and Arf5 in vivo.

When overexpressed, wild-type Arf6 and Arf5 showed a diffuse distribution in the cell body and neurites, and cell morphology was not affected (Fig. 4.19). In contrast, the transfected Arf1 showed a perinuclear staining overlapping with the distribution of the Golgi marker βCOP (Fig. 4.19, 4.20). It has been shown that overexpression of GIT2, a GAP for Arf1, causes the redistribution of βCOP, whose distribution is regulated by Arf1 and not by Arf6 (Mazaki et al., 2001). The overexpression of p95-APP1 did not affect the distribution of βCOP in retinal neurons (Fig. 4.21), suggesting that Arf1 is not a substrate for p95-APP1 in these cells.

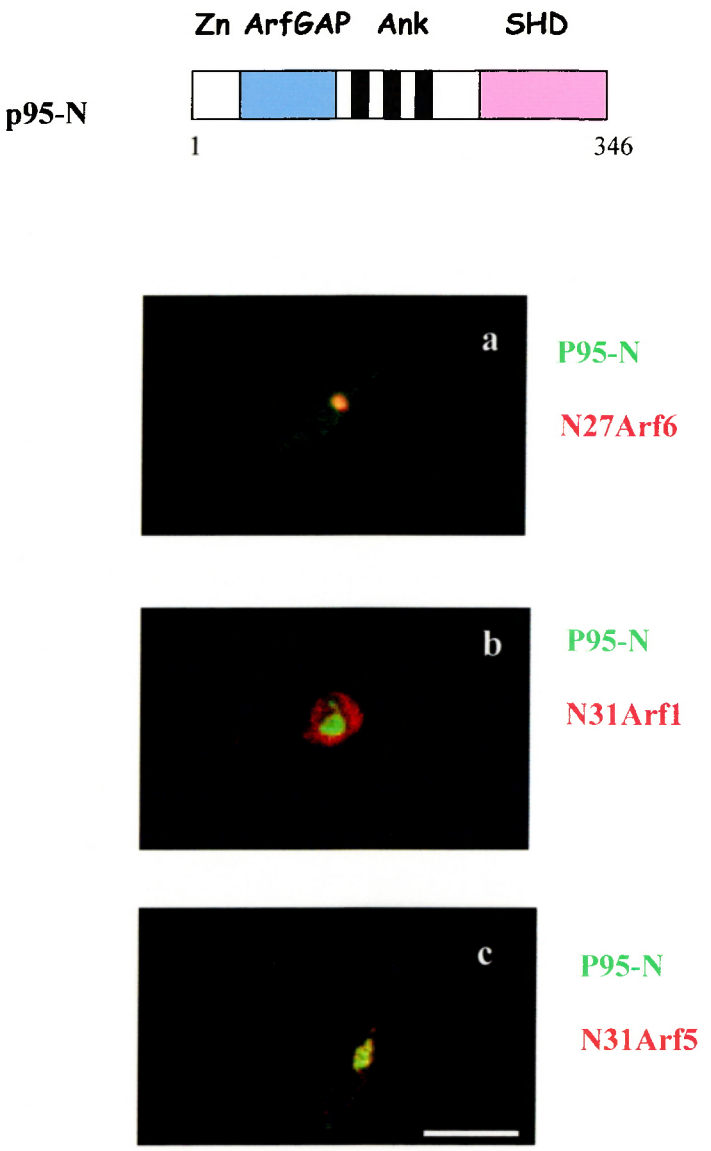

Fig. 4.18. N27Arf6 and N31Arf5, but not N31Arf1, colocalize at p95-N small vesicles Confocal microscopy analisys of neurons cotransfected with pFLAG-p95-N and pBK-N27Arf6 (a), pBK-N31Arf1 (b) and pBK-N31Arf5 (c). As shown in the overlays, p95-N (green) colocalizes with N27Arf6 and N31Arf5, but not with N31Arf1. In the upper panel is shown a schematic representation of the aminoterminal construct p95-N. (Bar, 5 μm).

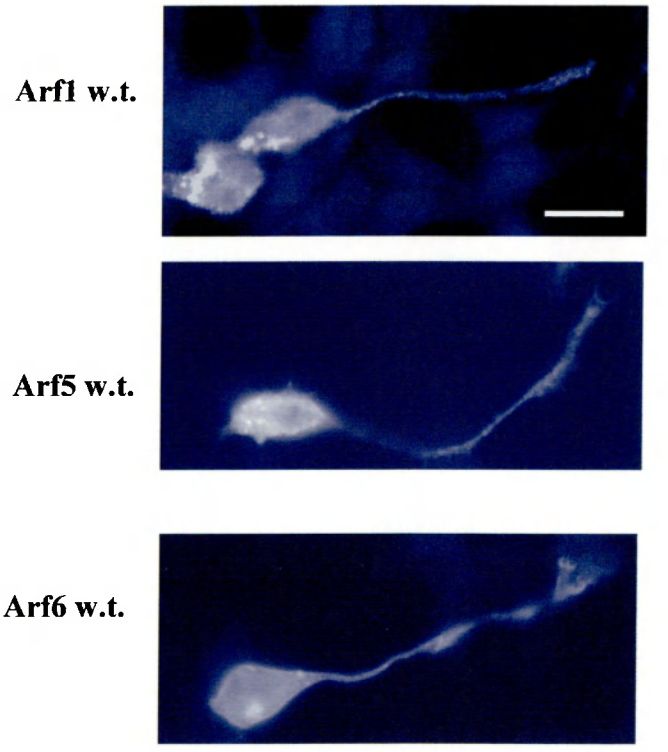

Fig. 4.19. Analysis of the distribution of w.t. Arf1, Arf5 and Arf6.

Retinal neurons were transfected with pBK-Arf1, -Arf5 or Arf6 –HA and analyzed by immunofluorescence with the anti-HA antibody. Arf5 and Arf6 show a diffuse distribution, while Arf1 is mainly concentrated in the perinuclear region. (Bar, 5 μm)

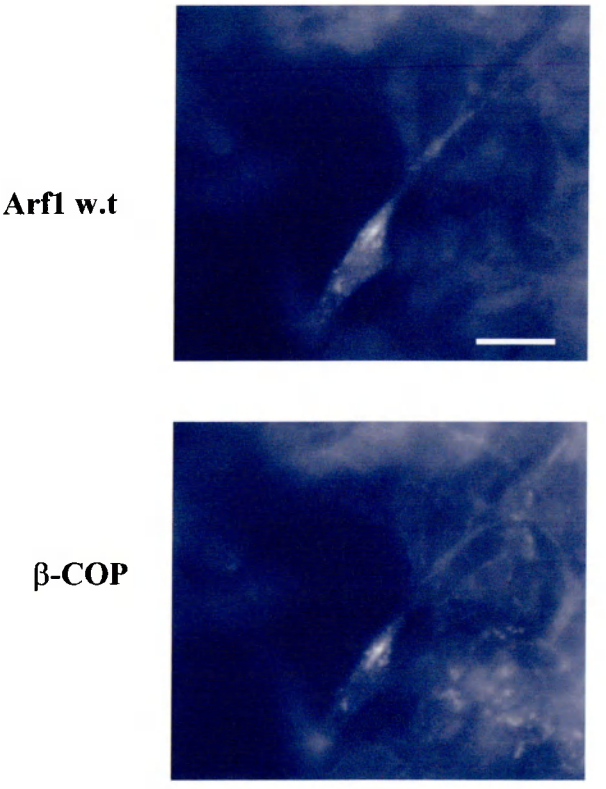

Fig. 4.20. Localization of w.t. Arf1 with the Golgi marker βCOP.

Retinal neurons were transfected with pBK-Arf1-HA and stained with the anti-HA (upper panel) and the anti-βCOP (lower panel) antibodies. The analysis shows colocalization of Arf1 with the endogenous Golgi marker βCOP. (Bar, 5 μ).

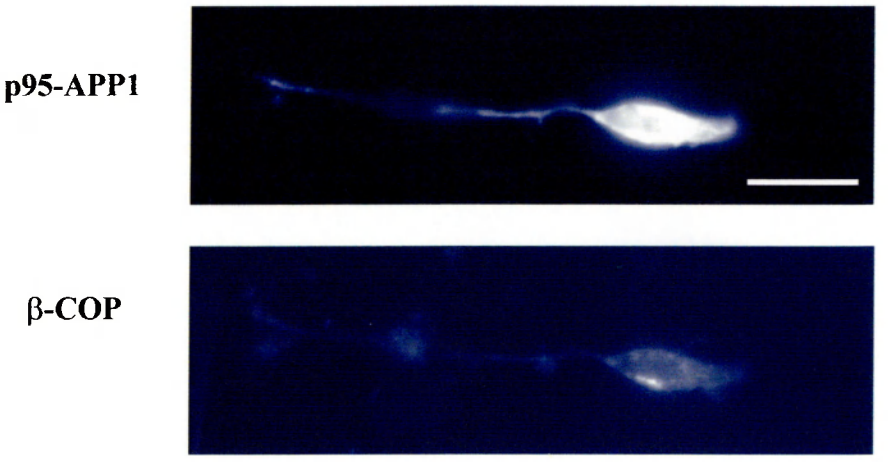

Fig. 4.21. Overexpression of p95-APP1 does not affect the distribution of βCOP.

Neurons were transfected with pFLAG-p95-APP1 and stained with the anti-Flag (upper panel) and anti-βCOP (lower panel) antibodies. The expression of p95-APP1 did not modify the distribution of the Golgi marker βCOP, indicating that Arf1 is not a substrate of p95-APP1 in these cells. (Bar, 7 μm).

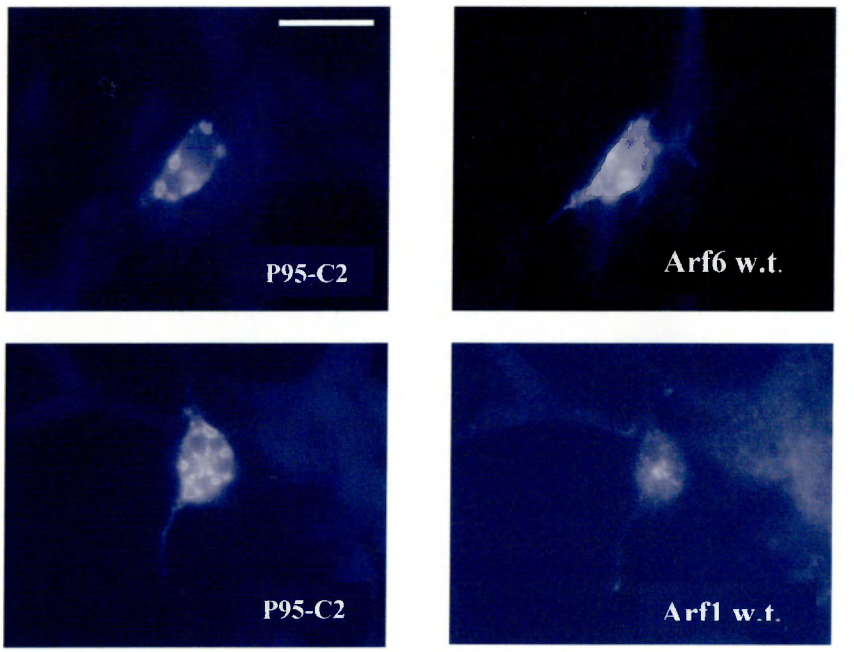

Fig. 4.22. W.t. Arf6, but not Arf1, colocalizes with p95-C2 at the large vesicles.

Neurons cotransfected with pFLAG-p95-C2 and pBK-Arf6 (upper panel) or pBK-Arf1 (lower panel) were analysed with the anti-Flag antibody and with anti-HA antibody. Arf6 and p95-C2 are localized at the large vesicles, while Arf1 remains differently distributed in the cotransfected cells. (Bar, 7 μm).

Moreover, in contrast to wild-type Arf1, wild-type Arf6 clearly colocalized with the truncated mutant p95-C2 at the large vesicles (Fig. 4.22), and Arf5 distribution partially overlapped with p95-C2 (not shown).

These data suggest that p95-APP1 is not a regulator of Arf1 in vivo, and point to a role of p95-APP1 as a possible regulator of Arf5 and Arf6.

4.5 ARF6 ACTIVITY IS NECESSARY FOR NEURITE EXTENSION

In order to investigate which Arf GTPases could be a substrate for p95-APP1 in the process of neurite extension, the effects of overexpressing wild-type and mutant Arf1, Arf5 and Arf6 GTPases on neuritogenesis were analysed. Overexpression of the three wild-type proteins did not affect the percentage of neurons having a single long neurite (Fig. 4.19, 4.23). In contrast, the GTP-binding defective N27Arf6, when overexpressed, strongly inhibited the formation of neurites, with over 70% of the transfected cells lacking neurites (Fig. 4.24, 4.26). In comparison, weaker effects on neuritogenesis were observed in cells expressing the corresponding inactive mutants N31Arf1 and N31Arf5 (Fig. 4.24, 4.26). A strong inhibition of neurite formation was observed also when constitutively active mutant L67Arf6 was expressed, while the corresponding active mutants L71Arf1 and L71Arf5 showed weaker reduction in neurite elongation (Fig. 4.25, 4.26). This indicates that Arf6 plays an important role among the tested Arfs during neurite elongation.

The possible functional relationship between Arf6 and p95-APP1 during neuritogenesis was investigated. Interestingly, coexpression of wild-type Arf6 with the truncated mutant p95-C resulted in a potentiation of neuritogenesis. The neurites extended by the cells were often much longer, often branched, and sometimes more than one per neurons. As a control, coexpression of p95-C with Arf1 or Arf5 did not affect neurite length (Fig. 4.27). This effect was quantified by measuring the total neurite length/neuron in cotransfected neurons (Fig. 4.29). The quantification clearly shows that

the potentiation of neuritogenesis observed by the overexpression of p95-C with wild-type Arf6 was not observed by coexpression of p95-C with either wild-type Arf1 or Arf5. As a control, coexpression of the inactive mutant N27Arf6 with p95-C not only prevented the potentiation, but also inhibited basal neurite extension when compared to control neurons (Fig. 4.28, 4.29). This functional analysis shows a predominant role of Arf6 on neurite extension in retinal neurons with respect to other Arfs, and indicates a specific functional connection between Arf6 and p95-APP1.

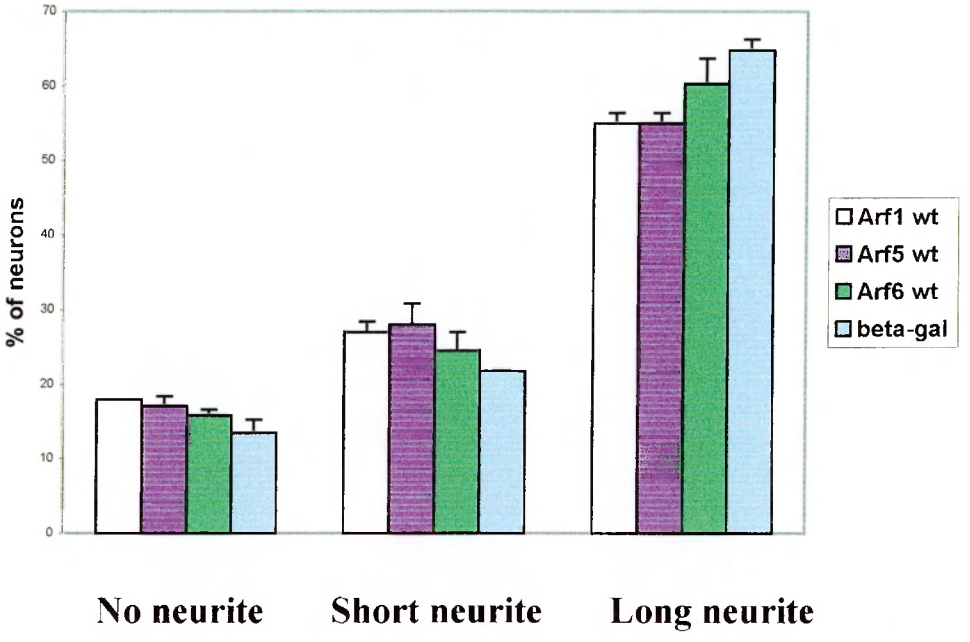

Fig. 4.23. Quantitative analysis of the effect of the w.t. Arf1, Arf5 and Arf6 overexpression on neuritogenesis.

Data are expressed as percentage of transfected neurofilament positive neurons with no, short (less than three cell body diameters in length), and long neurite. Values are means +/- s.d. from two experiments. As for neurons transfected with the β-galactosidase, neurons expressing the indicated w.t. Arf GTPases show normal neurite extension.

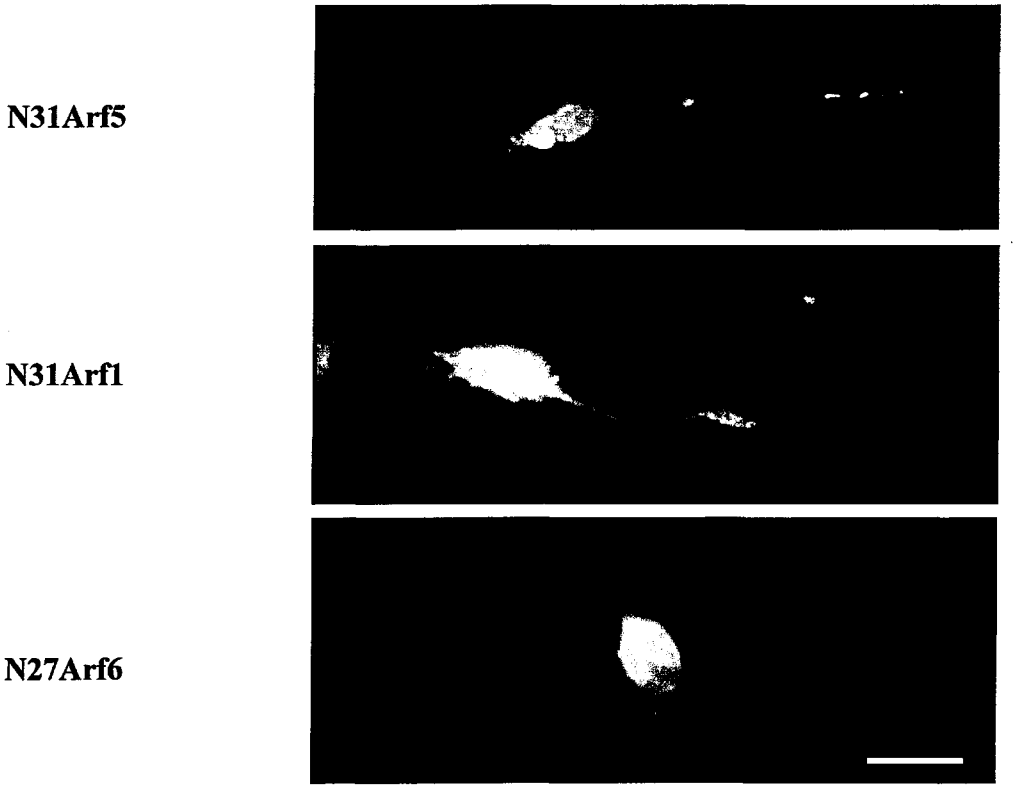

Fig. 4.24. The overexpression of the inactive mutant N27Arf6 inhibits neuritogenesis.

Neurons were transfected with pBK-N31Arf5, -N31Arf1 and -N27Arf6 and stained with the anti-HA antibody. N27Arf6 overexpression reduced neurite extension. In the same conditions, N31Arf5 or N31Arf1 overexpression did not show the same effect, implicating Arf6 in the process of neuritogenesis. (Bar, 5 μm).

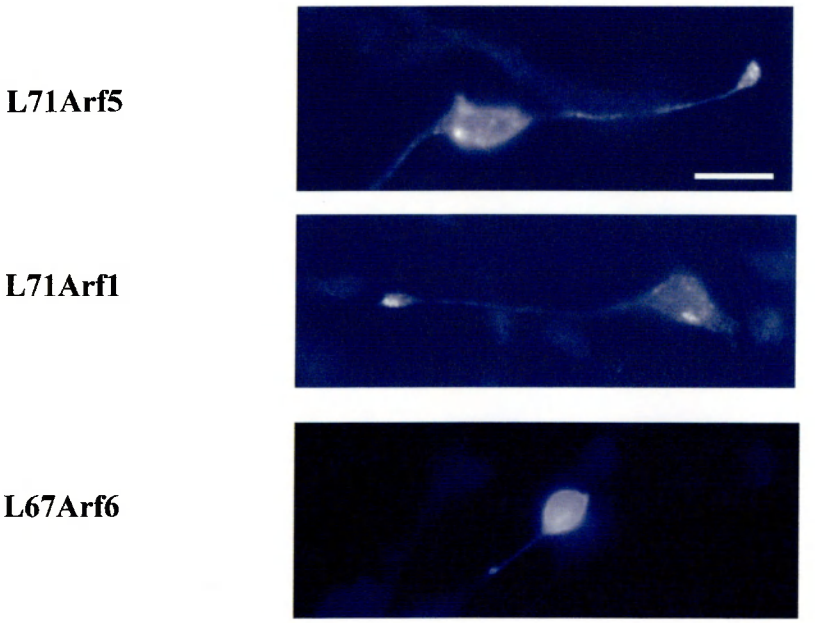

Fig. 4.25. The overexpression of the active mutant L67Arf6 inhibits neuritogenesis. Neurons were transfected with pBK-L71Arf5, -L71Arf1 and -L67Arf6, and stained with the anti-HA antibody. Overexpression of L67Arf6 reduced neurite extension. Under the same conditions, L71Arf5 or L71Arf1 overexpression did not show the same effect. These data suggest the requirement of Arf6 activity and cycling in the process of neuritogenesis. (Bar, 5 μm).

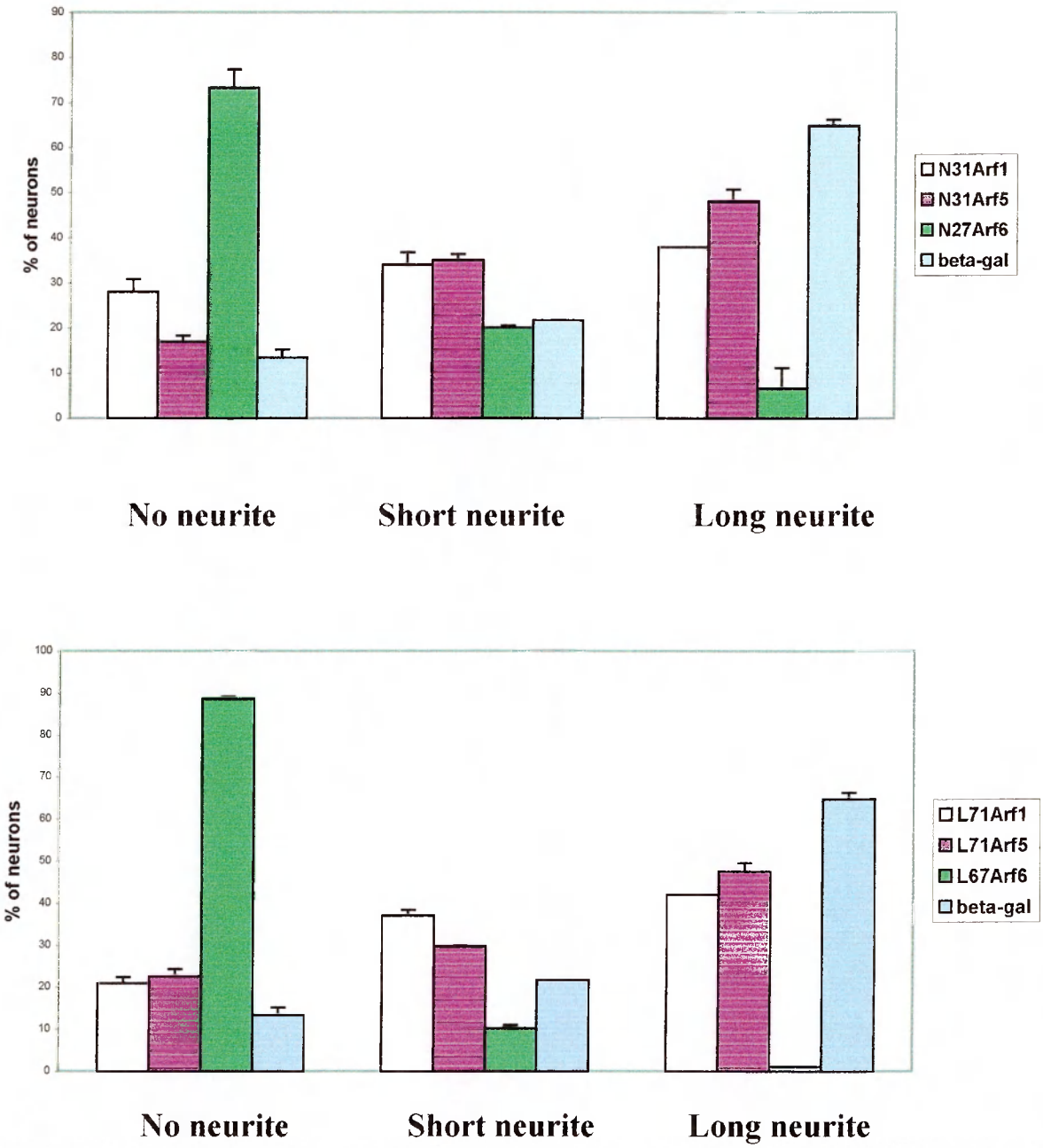

Fig. 4.26. Quantitative analysis of the effect of the overexpression of the dominant negative and constitutively active mutants of Arf1, 5 and 6 on neuritogenesis.

Data are expressed as percentage of transfected neurofilament positive neurons with no, short and long neurite. Values are means +/- s.d. from two experiments with a total 100 neurons. The overexpression of dominat negative N27Arf6 and constitutively active L67Arf6 inhibits neuritogenesis. The correspondent mutants of Arf1 and Arf5 have limited effects on neurite extension.

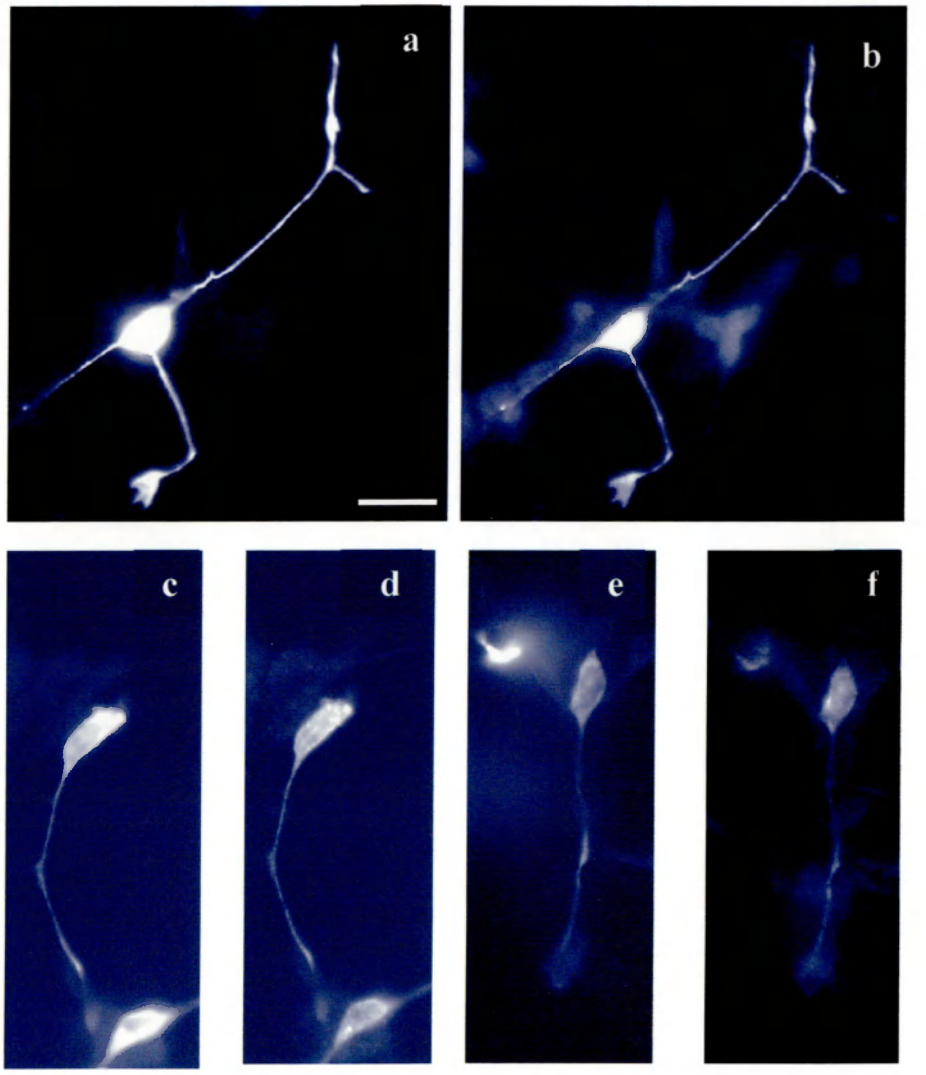

Fig. 4.27. Arf6 specifically regulates p95-C-mediated neurite extension.

Neuritogenesis is enhanced in cell coexpressing p-95C and w.t. Arf6 (a,b), while no effects could be observed in neurons coexpressing p95-C with w.t. Arf5 (c,d) or p95-C with w.t. Arf1 (e,f). Neurons were transfected with pFlag-p95C together with pBK-Arf6 (a,b), pBK-Arf5 (c,d), and pBK-Arf1 (e,f), respectively. Cells were stained with the anti-Flag antibody (a,c,e), with anti-Arf6 antibody (b) and with anti-HA antibody (d, f). (Bar in a, b, 10 μm; in c-f, 5 μm)

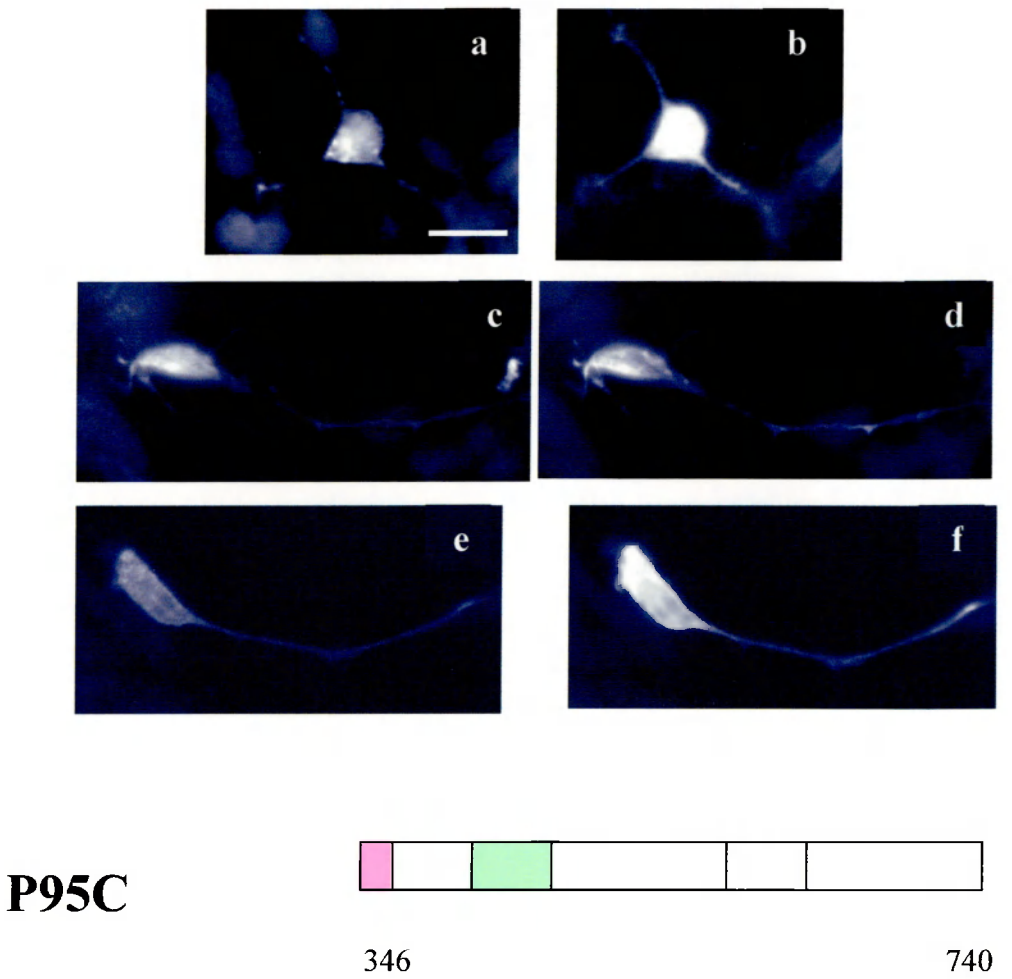

Fig. 4.28. Specific inhibition of N27Arf6 on p95C-mediated neuritogenesis.

Neuritogenesis is reduced in cells coexpressing p-95C and N27Arf6 (a,b), while no effects could be observed in neurons coexpressing p95-C with N31Arf1 (c,d) or N31Arf5 (e, f). Neurons were transfected with pFlag-p95C and pBK-N27Arf6 (a,b), pBK-N31Arf1 (c,d) and pBK-N31Arf5 (e,f) and stained with the anti-Flag antibody (b, d ,f), with anti-Arf6 antibody (a), and with anti-HA antibody (c, e). (Bar, 5 μm).

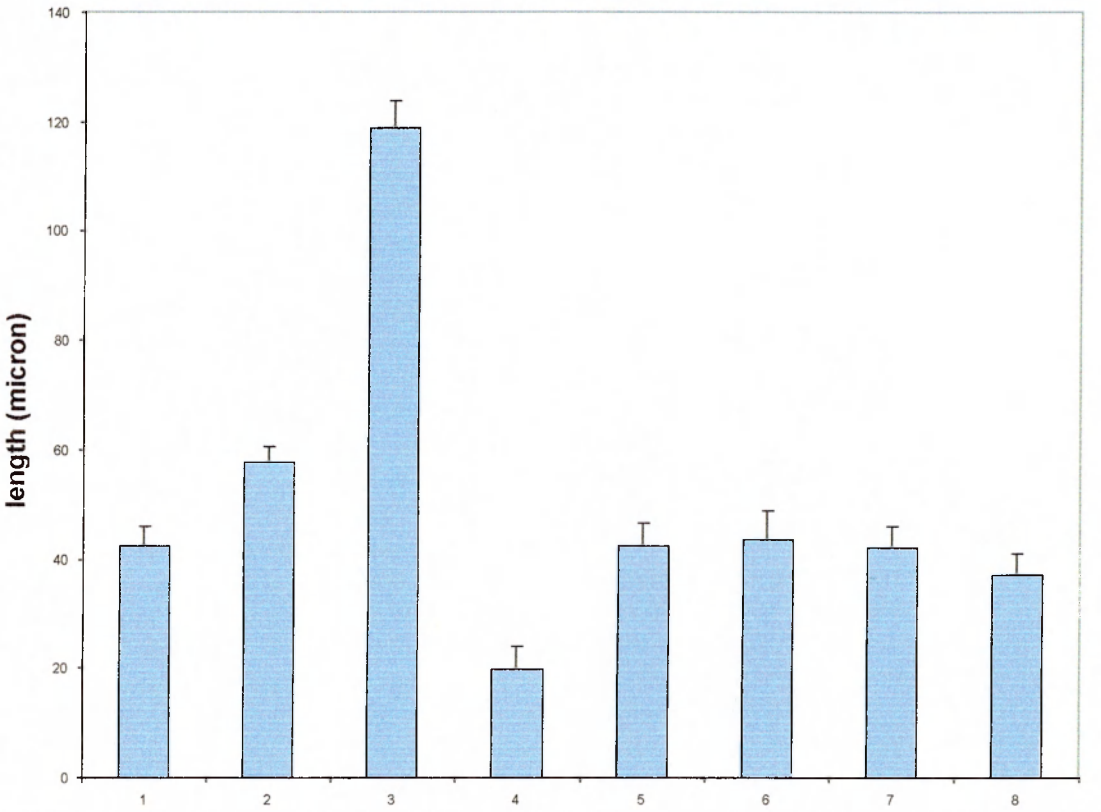

Fig. 4.29. Arf6 specifically enhances p95-C-mediated neurite extension.

Quantification of neurite length in transfected and cotransfected neurons was performed by measuring the total neurite length/cell in 30 neurons from two experiments. Bars represent SEM.

Coexpression of N27Arf6 with p95-C inhibits total neurite length/cell, which was not affected in cells coexpressing p95-C with either N31Arf1 or N31Arf5.

1: β-gal; 2: Arf6; 3: Arf6+p95-C; 4: N27Arf6+p95-C; 5: Arf1+p95-C; 6: N31Arf1+p95-C; 7: Arf5+p95-C; 8: N31Arf5+p95-C.

4.6 WILD-TYPE ARF6 AND P95-APP1 ARE REQUIRED FOR RAC1B-ENHANCED NEURITOGENESIS

E6 retinal neurons express Rac1 and Rac1B/Rac3 GTPases (Malosio et al., 1997). Low levels of endogenous Rac1B are required for the basal neurite extension on laminin 1, while the overexpression of Rac1B induces a potentiation of neuritogenesis and neurite branching (Albertinazzi et al., 1998). Cotransfection of wild-type Rac1B with p95-APP1 resulted in a small reduction of the percentage of neurons with branched neurites when compared to the cells transfected with Rac1B alone (Fig. 4.30, 4.31). Quantitation of the average number of primary neuritic branches/neuron was similar in neurons transfected with Rac1B alone (2,50+/- 0,19 (SEM), n=50), and in neurons coexpressing Rac1B and p95-APP1 (2,34+/- 0,18 (SEM), n=50).

The coexpression of the truncated construct p95-C2 strongly reduced Rac1B-potentiated neurite outgrowth (Fig. 4.31). It is interesting to note that wild-type Rac1B localized at the large p95-C2-positive vesicles (Fig. 4.30).

Rac1B induced neurite extension and branching was also reduced by the coexpression of the inactive N27Arf6 (Fig. 4.30), with a five-fold decrease in the percentage of neurons with branched neurites, and a 3.6-fold increase in neurons without neurites, compared to neurons expressing only Rac1B (Fig. 4.31).

These results suggest that both N27Arf6 and ArfGAP-defective p95-C2 have dominant negative effects on Rac1B-mediated neurite extension, and indicate a functional connection between these proteins in the process of neuritogenesis.

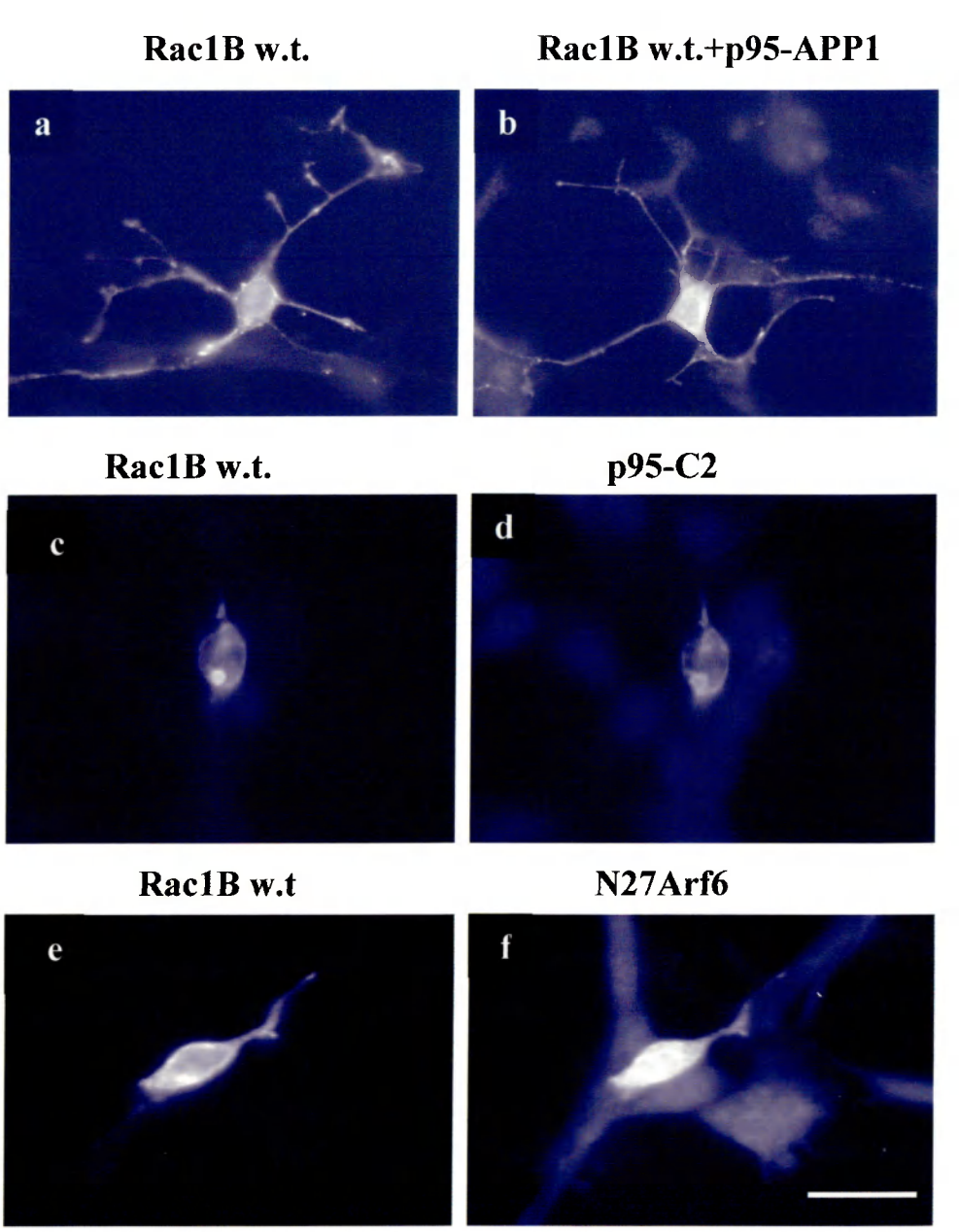

Fig. 4.30. p95-C2 and N27Arf6 inhibited Rac1B induced neuritogenesis.

Neuritogenesis is reduced in cells coexpressing Rac1B w.t. and p-95C2 (c,d), and in cells coexpressing Rac1B w.t. and N27Arf6 (e, f), while no striking effects could be observed in neurons coexpressing Rac1Bw.t. with p95-APP1 (a, b). Neurons transfected with pFlag-Rac1B and pBK-HA-p95-APP1 (a,b), pFlag-Rac1B and pBK-HA-p95-C2 (c,d), and pFlag-Rac1B and pBK-N27Arf6 (e,f), were fixed after 24 h and stained with the anti-Flag antibody (a, c, e), with anti-HA antibody (b, d), and with anti-Arf6 antibody (f). (Bar, 7 μm).

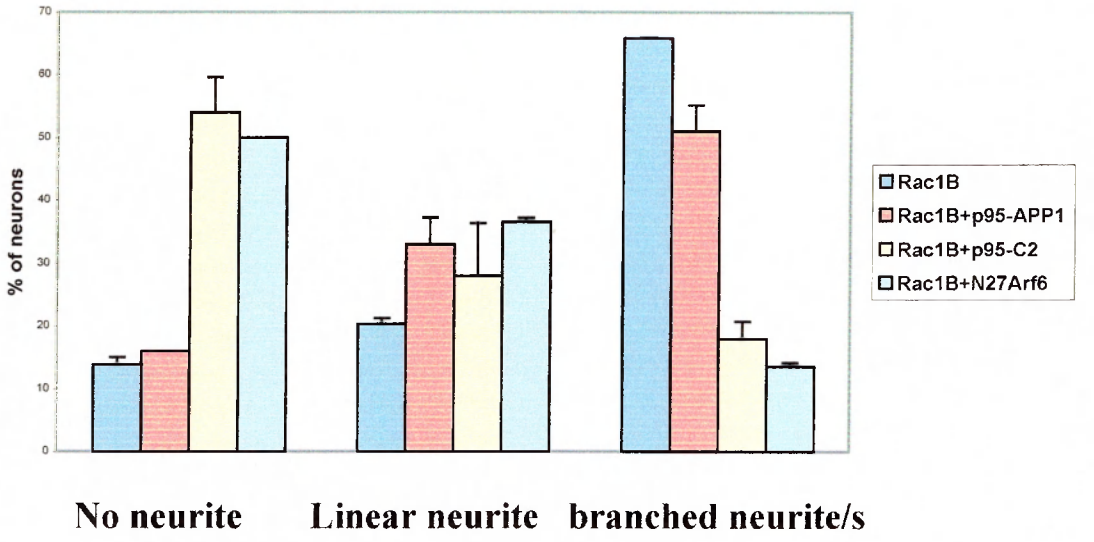

Fig. 4.31. Quantitative analysis of the inhibition of Rac1B-mediated neurite branching by p95-C2 and N27Arf6.

Data are expressed as percentage of cotransfected neurons with no neurite, with linear neurite, and with one or more branched neurites. Branching was evaluated in a total of 100 neurons from two independent experiments. Values are means +/- s.d. Dominant negative Arf6 and ArfGAP-deficient p95-C2 inhibit neurite branching induced by Rac1B.

4.7 THE PIX-SH3 DOMAIN AND DIMERIZATION ARE REQUIRED FOR NEURITE INHIBITION BY THE ARFGAP-DEFECTIVE P95-C2, AND FOR ACCUMULATION AT LARGE ENDOCYTIC VESICLES.

The data obtained suggest that PIX could be responsible for the recruitment of p95-C2 to the Rab11-positive compartment by binding to the SHD domain.

All the members of the PIX family have an SH3 domain highly specific for the binding of Pak, a DH domain (the GEF domain) and a PH domain, which could be involved in membrane targeting. The 85-kDa βPix, considered in this study, also contains an Arf-GAP binding domain and a leucine zipper domain at the C-terminal end, involved in dimerization (Kim et al., 2000) (Fig. 4.32).

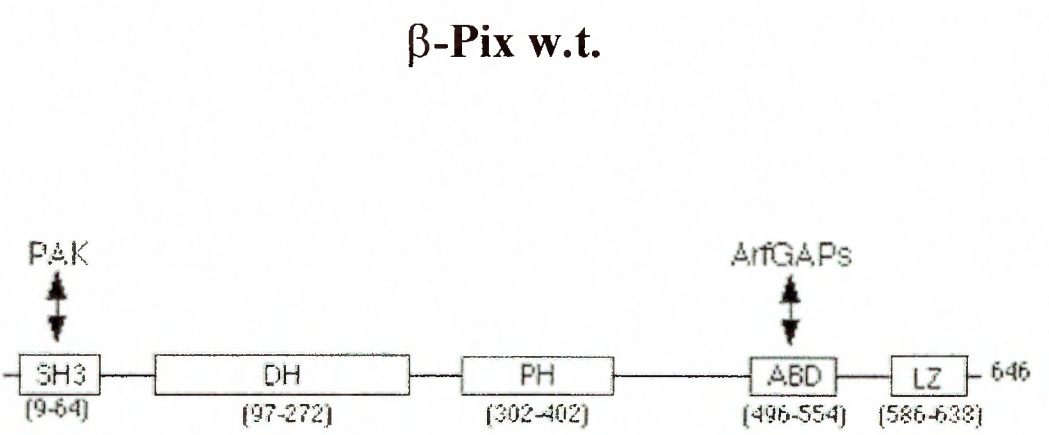

Fig. 4.32. Domain structure of βPix protein: schematic representation of βPix protein. It contains several domains: SH3 (Src Homology 3), DH (Dbl-homology), PH (Pleckstrin homology), ABD (the Arf-GAP binding domain), and LZ (Leucine zipper).

In order to study in detail the mechanism underlying the recruitment of the p95 complex to Rab11-positive recycling vesicles, the involvement of βPix was analysed. The leucine-zipper in the C-terminal portion of βPix can mediate homodimerization (Kim et al., 2000), and p95-APP1 also has a putative leucine-zipper domain in the coiled coil region (Fig. 1.5) which can form homodimers. A number of constructs were prepared including a monomeric form of p95-APP1, called p95-LZ, in which the leucine zipper was mutated (Fig. 4.33, upper panel). In particular, two central leucines of the leucine zipper were mutated into prolines (Leu 448 and 455). These substitutions abolished the ability of the protein to form dimers as shown in coimmunoprecipitation experiment (Fig. 4.33, lower panel) in which CEFs were cotransfected with pBK-HA-p95APP1 and with pFlag-p95-APP1. In cotransfected fibroblasts HA-p95 could be co-immunoprecipitated with FLAG-p95. The disruption of the leucine zipper of p95-APP1 abolished the ability of the resulting FLAG-p95-LZ protein to associate with the HA-p95 protein. The monomeric form of p95-C2, called p95-C2-LZ, was constructed with the same substitutions in the leucine zipper domain (Fig. 4.33, upper panel), and a set of dimeric and monomeric PIX mutants, in which specific domains had been deleted or mutated were made (Fig. 4.34, upper panel). In particular, a dimeric PIX-PG mutant was made in which two amino acid residues of the SH3 domain, tryptophans 43 and 44, were changed into proline 43 and glycine 44. From this construct the monomeric Pix-PG-ΔLZ mutant was derived. The mutation in the SH3 domain inhibits PAK binding (Manser et al., 1998), as confirmed by coprecipitation experiments (Fig. 4.34, lower panel). Another construct was generated, was the monomeric Pix-ΔPH-ΔLZ with a deletion of the Pleckstrin Homology domain (PH), that is involved in membrane interaction in several proteins. As a control, monomeric p95-C2-LZ protein was still

able to heterodimerize with monomeric Pix constructs. Coprecipitation showed the interaction of p95-C2-LZ with the monomeric SH3 mutant Pix-PG-ΔLZ (Fig. 4.35). The monomeric forms of Pix mutants and p95-C2 were used in order to eliminate the possible dimerization of the transfected proteins with the endogenous Pix and p95-APP1 in retinal neurons.

Combinations of these mutants were used to investigate the effects on the subcellular distribution of the Pix-p95 complex and on neurite extension. Wild type Pix, and the PixSH3 mutant PixPG showed a diffuse distribution and did not affect neurite extension (Fig. 4.36). Coexpression of Pix-PG with p95-C2 resulted in a phenotype similar to that observed upon expression of p95-C2 alone: neurites were strongly inhibited (Fig. 4.36) and both proteins colocalized at large vesicles.

Interestingly, the coexpression of monomeric Pix-PG-ΔLZ with monomeric p95-C2-LZ showed a diffuse distribution of the two proteins in transfected neurons, and the neuronal morphology was not affected (Fig. 4.37). In contrast the complexes including either dimeric p95-C2 with monomeric Pix-PG-ΔLZ, or monomeric p95-C2-LZ with dimeric Pix-PG were still able to induce both accumulation of the complex at the large vesicles, as well as strong neurite inhibition (Fig. 4.38). Therefore, complexes including either one of the two mutants in a dimeric form preserved the ability to affect the neuronal morphology, while heterodimers of monomeric proteins with a mutated Pix SH3 did not.

The specificity of the effects observed with the monomeric Pix SH3 mutant is supported by the finding that when monomeric Pix-ΔPH-ΔLZ was coexpressed with monomeric p95-C2-LZ, the proteins were still able to accumulate the complex at vesicles and to inhibit neurite extension (Fig. 4.39). Altogether, these data implicate the SH3 domain of Pix in the recruitment of p95-APP1 to the recycling compartment, and support a fundamental role of Pix and hetero-oligomerization in the regulation of p95-APP1

function during neuritogenesis. The quantitation of the effects of different combinations of mutants (Fig. 4.40) showed that there was an inverse relationship between the accumulation of the complexes at large vesicles and the ability of neurons to extend neurites.

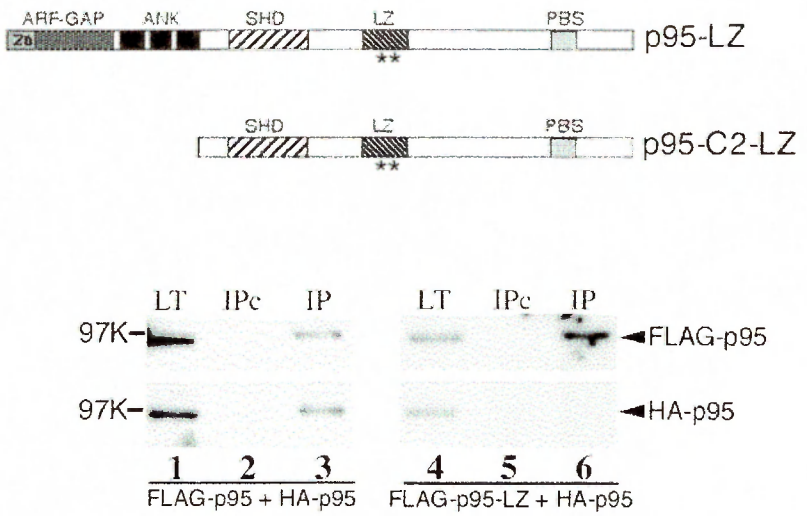

Fig. 4.33. The leucine zipper of p95-APP1 is required for dimerization.

Upper panel: constructs with mutated leucine zipper used in this study, in which two leucine residues in position 448 and 455 (asterisks) have been mutated into two prolines. Lower panel: CEFs were cotransfected with pFlag-p95-APP1 and pBK-HA-p95-APP1 (lanes 1-3), or with pFlag-p95-LZ and pBK-HA-p95-APP1 (lanes 4-6). Lysates were first incubated with beads only (IPc); the unbound fractions were loaded on beads coated with anti-Flag mAb (IP). After SDS-PAGE, one set (upper blot) was incubated with the anti-Flag mAb to detect the Flag-p95 (lanes 1-3) and Flag-p95-LZ (lanes 4-6) polypeptides. The second set (lower blot) was incubated with the anti-HA pAb to detect the HA-p95 polypeptide. LT (total lysate).

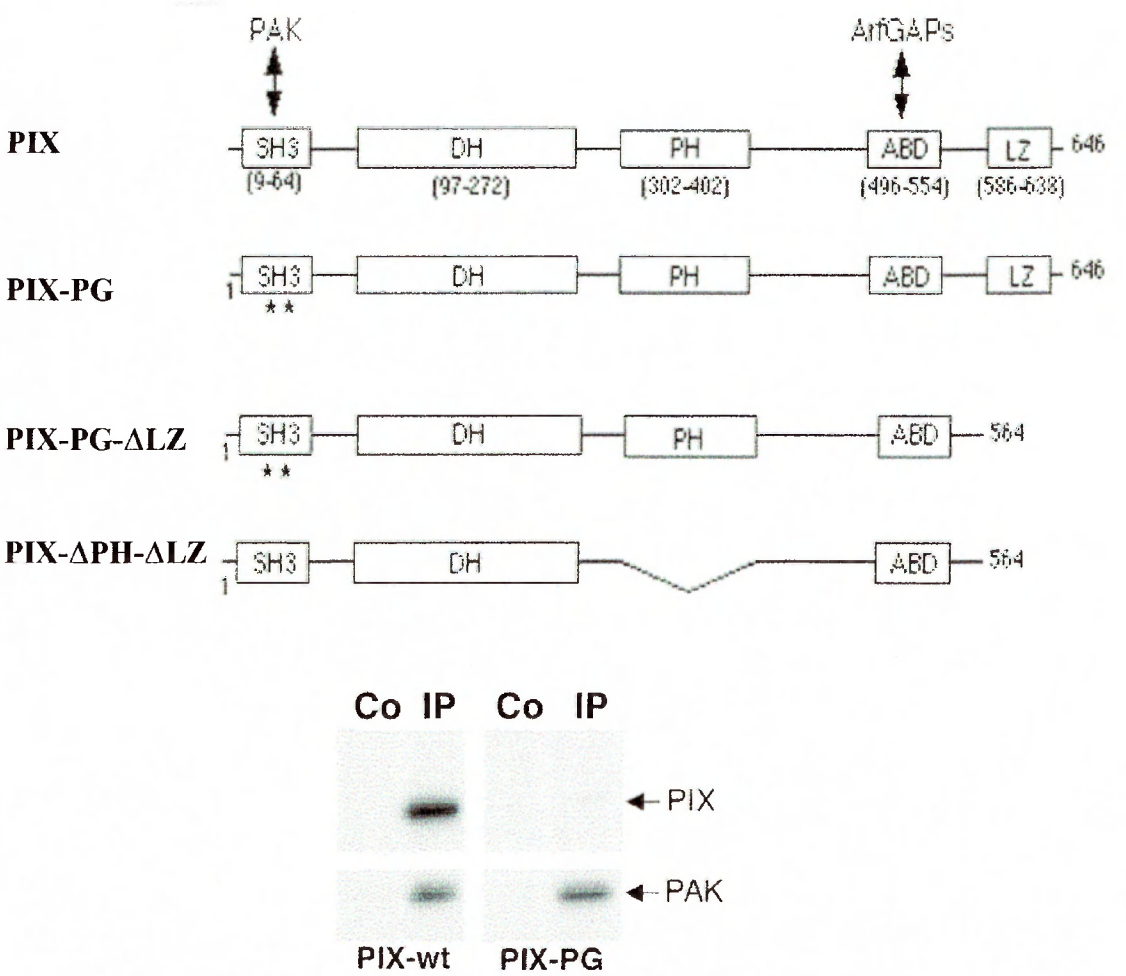

Fig. 4.34. The SH3 domain of βPIX is required for Pak binding.

Upper panel: constructs of βPIX used in this study. PIX-PG: two aminoacid residues of the SH3 domain, tryptophans 43 and 44 (asterisks), have been changed into proline 43 and glycine 44, respectively. PIX-PG-ΔLZ is the monomeric form obtained from the PIX-PG mutant. PIX-ΔPH-ΔLZ is the monomeric construct with a deletion of the PH domain. Lower panel: immunoprecipitates with anti-Myc antibody from lysate of CEFs cotransfected with HA-βPIX and Myc-Pak1 (PIX wt), or with HA-βPIX-PG and Myc-PAK (PIX-PG), were blotted with anti-Myc (lower blot) and anti-HA (upper blot) antibodies to detect Pak and PIX, respectively. Lysates were incubated with control beads (Co), before incubation with beads coated with anti-Myc antibodies.

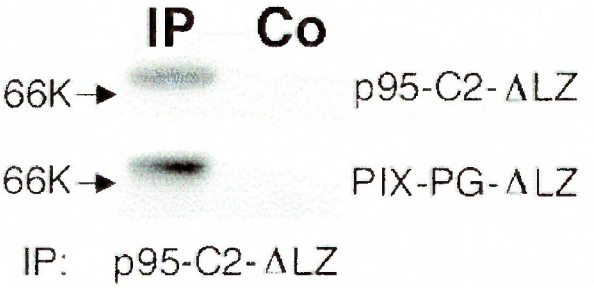

Fig. 4.35. Monomeric mutants of p95-APP1 and PIX can form heterodimers.

Immunoprecipitates with anti-Flag antibody from lysates of CEFs coexpressing monomeric p95-C2-LZ with monomeric PIX-PG-ΔLZ. Filters were blotted with anti-Flag mAb to detect Flag-p95-C2-LZ (upper blot), and with anti-HA pAb to detect the coprecipitating HA-PIX-derived construct (lower blot). The lysate was incubated with control beads (Co) before incubation with beads coated with specific antibody (IP).

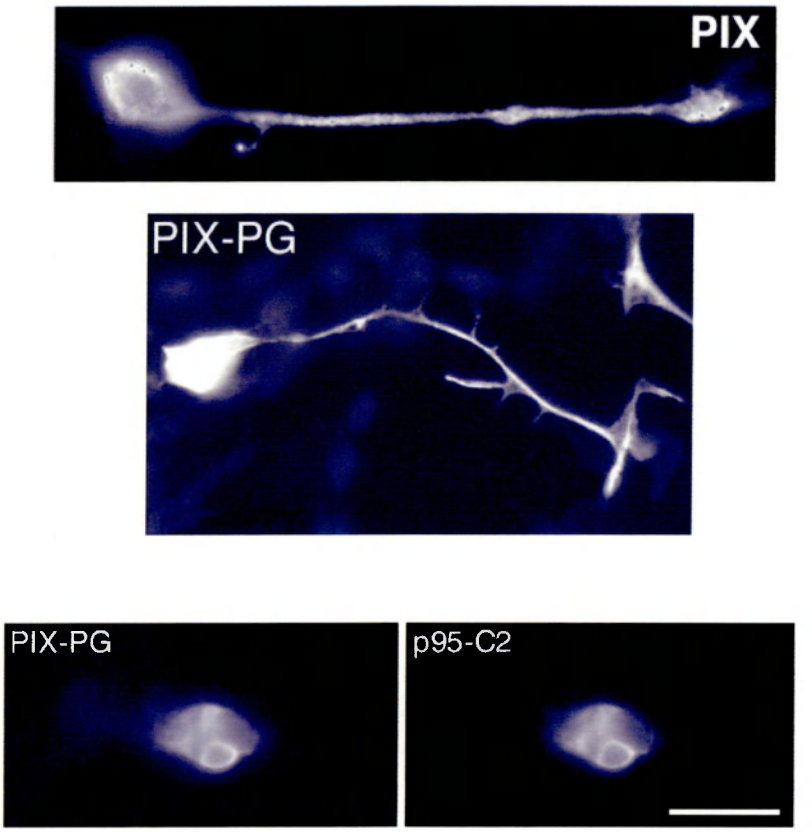

Fig. 4.36. Coexpression of dimeric p95-C2 and PIX-PG mutants results in localization at large vesicles and neurite inhibition.

Transfected neurons were fixed one day after transfection and stained with the anti-Flag mAb and anti-HA pAb to detect the indicated polypeptides. The expression of either HA-PIX, or HA-PIX-PG results in normal neuritogenesis. The coexpression of HA-PIX-PG and Flag-p95-C2 results in the inhibition of neurite extension. The two proteins localize at large vesicles. (Bar, 7 μm).

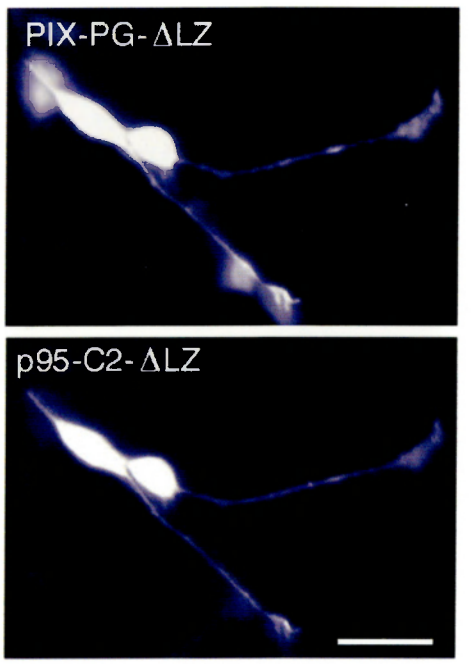

Fig. 4.37. Coexpression of the p95-C2-LZ and PIX-PG-ΔLZ mutants prevents the formation of large vesicles and neurite inhibition.

Neurons cotransfected with Flag-p95-C2-LZ and HA-PIX-PG-ΔLZ were fixed one day after transfection and treated for immunofluorescence with the anti-Flag mAb and anti-HA pAb to detect the indicated polypeptides. Coexpression of the monomeric mutants results in diffuse localization of the expressed polypeptides and normal neurites. (Bar, 10 μm).

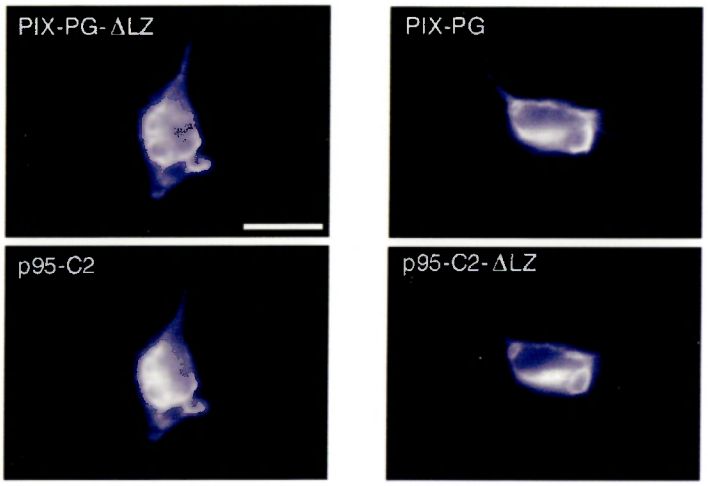

Fig. 4.38. Complexes including either one of the two mutants in a dimeric form preserve the ability to affect the neuronal morphology.

Neurons cotransfected either with Flag-p95-C2 and HA-PIX-PG-ΔLZ or with Flag-p95C2-LZ and HA PIX-PG were fixed one day after transfection and treated for immunofluorescence with the anti-Flag mAb and anti-HA pAb to detect the indicated polypeptides. The coexpression of any combination including at least one dimeric mutant results in localization of the proteins at large vesicles, and in neurite inhibition. (Bar, 5 μm).

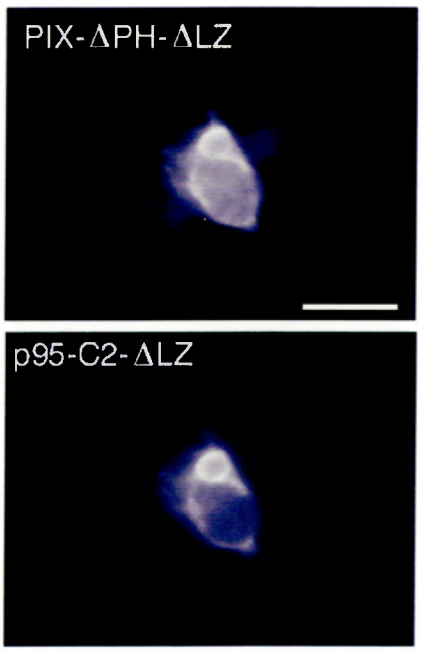

Fig. 4.39. Coexpressed monomeric Pix-ΔPH-ΔLZ and monomeric p95-C2-LZ are still able to accumulate at vesicles and to inhibit neurite extension.

Neurons cotransfected with the monomeric forms Flag-p95-C2-LZ and HA-PIX-ΔPH-LZ were fixed one day after transfection and treated for immunofluorescence with the anti-Flag mAb and anti-HA pAb to detect the indicated polypeptides. The coexpression of the indicated monomeric constructs results in localization at the large vesicles and in neurite inhibition. (Bar, 5 μm).

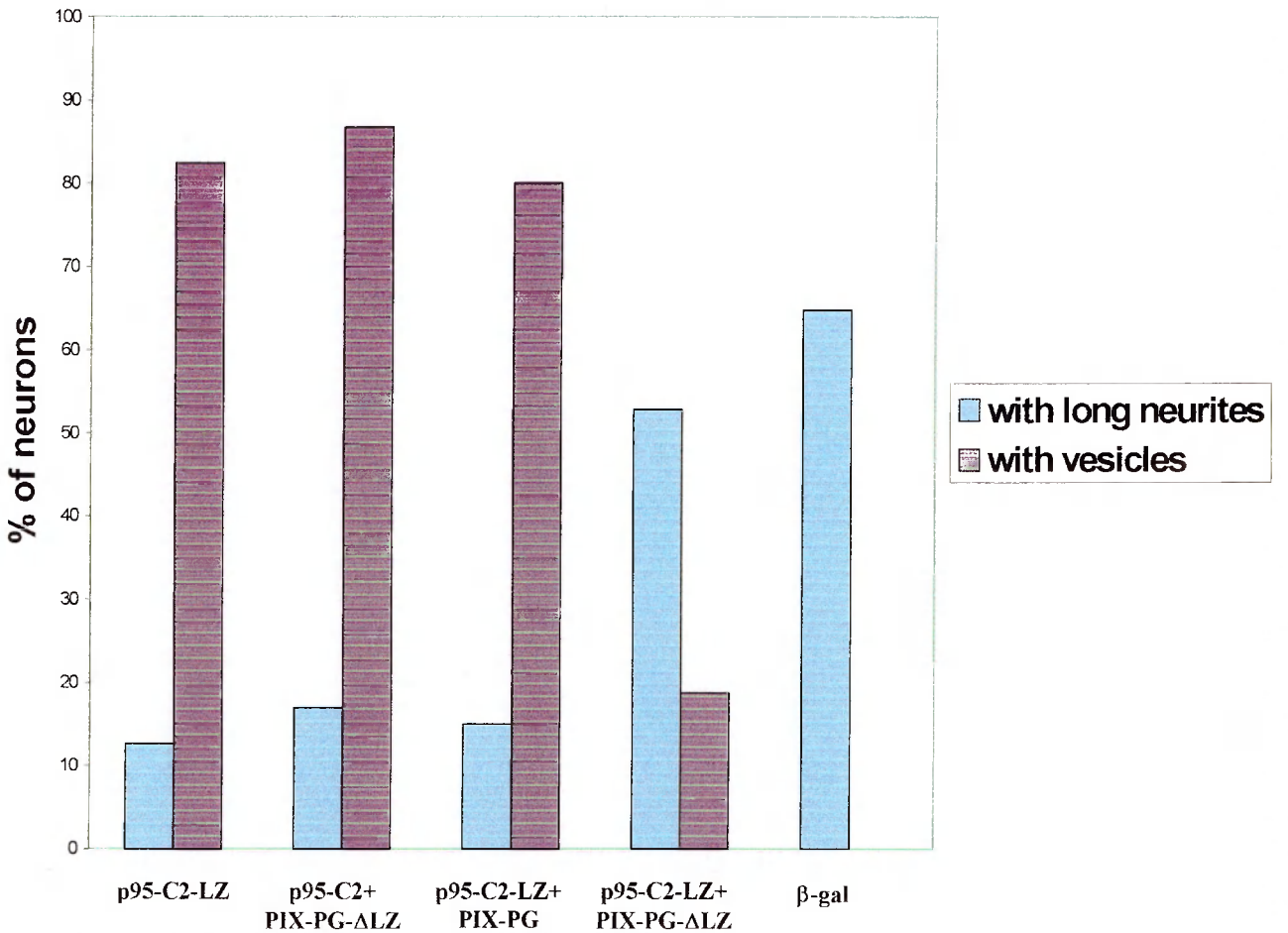

Fig. 4.40. An inversed relationship exists between the accumulation of p95 complexes at large vesicles and the ability of neurons to extend neurites.

Neurons from experiments as those shown in Fig. 4.37, 4.38 were utilized to quantify the effects of different p95-Pix mutants on neurite extension and on the localization of the transfected proteins to large vesicles. Each bar represents the percentage obtained from the analysis of 100 neurons from two experiments.

4.8 DISCUSSION

In the second part of my thesis I have analysed the intracellular mechanisms driving neurite extension in primary neurons, based on the previous observation that the neural-specific Rac1B GTPase is required and specifically enhances neurite outgrowth from embryonic retinal neurons (Albertinazzi et al., 1998). More recently, a protein complex was identified that specifically interacted with active GTP-bound Rac GTPases (Di Cesare et al., 2000), and included p95-APP1, a member of an ArfGAP family including the mammalian GIT1 protein (Donaldson and Jackson, 2000), corresponding to avian p95-APP1. The characterization of the complex in non-neuronal cells strongly suggests a role for this protein in connecting membrane traffic with actin dynamics during the process of cell motility (De Curtis, 2001).

Three major findings can be described from this work. First, mutation or deletion of the Arf-GAP domain of p95-APP1 leads to the accumulation of the p95 complex at large Rab11-positive vesicles, and to the concomitant inhibition of neurite extension. Second, Arf6 activity is specifically required for Rac1B-mediated neurite elongation, and morphological and functional analysis with different Arf proteins has shown a specific functional connection between Arf6 and the Arf-GAP p95-APP1 during neurite extension. Finally, the SH3 domain of PIX is required for the specific effects induced by the Arf-GAP mutants of p95-APP1.

4.8.1 The GAP activity is required for neurite extension

The complex structure of p95-APP1 has made it essential to use deletion mutants to explore its function. In neurons, overexpression of the full-length protein and of the carboxy-terminal p95-C protein did not affect neuronal morphology. In contrast, mutation or deletion of the ArfGAP domain in the presence of the PIX-binding site drastically inhibits neurite extension. Such inhibition is accompanied by the specific

accumulation of p95-complex at enlarged vesicles positive for Rab11, a functional marker of the endocytic recycling compartment (Ullrich et al. 1996; Ren et al. 1998). This indicates a functional connection between membrane recycling and neurite extension in these neurons. It is known that growth cones are sites of intense endocytosis, and require an equivalent membrane flow back to the surface to maintain equilibrium. Recent work has shown the existence of dynamic recycling endosomes in axons and dendrites of developing hippocampal neurons (Prekeris et al., 1999). The endocytic/exocytic mechanism may represent a dynamic reservoir of mobile membrane to respond to extracellular stimuli leading to growth cone-mediated neurite extension or retraction (Craig et al., 1995). The net addition of membrane during neurite elongation may derive from both the distant cell body and the extending neurite (Shea and Sapirstein, 1988; Popov et al., 1993; Craig et al., 1995; Dai and Sheetz, 1995; Vance et al., 1991). A contribution to neurite progression may come from endocytosed, recycled membranes: accordingly, membrane recycling at the growth cone has been demonstrated (Diefenbach et al., 1999). In non-transfected retinal neurons the Rab11 compartment consists of small structures distributed along the neurites. Moreover, recent work has shown the existence of a dynamic tubulovesicular recycling endosomal network in axons and dendrites of developing hippocampal neurons (Prekeris et al. 1999). These structures, which show bidirectional movement along the neurites, are regulated via the microtubule network. One possible interpretation of the results shown in this thesis is that the p95-APP1 ArfGAP mutants (the truncated mutant p95-C2 and the construct with the point mutation p95-K39) interfere with the recycling of vesicles back to the cell surface along the neurite, leading to accumulation of membrane in the cell bodies and preventing the elongation of neurites.

In the future it would be interesting to use the RNAi tecnique in order to confirm this hypothesis and to investigate how the loss of p95-APP1 could affect neurite extension.

4.8.2. Arf6 activity is required for Rac1B-mediated neurite elongation

Arf6 is implicated in membrane recycling at the plasma membrane (D'Souza-Schorey et al., 1995; Peters et al., 1995). Inhibition of both normal and Rac1B-enhanced neuritogenesis was observed by expressing mutants affecting the nucleotide cycle of Arf6. Corresponding mutants for Arf1 and Arf5, representatives of class I and class II Arfs respectively, showed weaker effects on the inhibition of neuritogenesis, indicating a prominent role of Arf6 in this process. The decrease in the percentage of neurons with a long neurite observed when the Arf1 and Arf5 mutants were transfected (Fig. 4.26), could be explained by the fact that mutants of Arf1 perturb the Golgi apparatus, leading to an indirect contribution in reduction of membrane addition to the membrane.

These data also show that a cycling GTPase is required for neurite extension, as already observed for other GTPases implicated in the regulation of neuritogenesis (see for a review Luo, 2000), including Rac1B (Albertinazzi et al., 1998), and may reflect the need for a cyclic mode of signalling, appropriate to a highly dynamic process such as neurite extension.

As with other Arf proteins, Arf6 has a very slow rate of GTP hydrolysis and requires a GAP to be inactivated (Welsh. et al, 1994). The Arf-GAP activity of GIT1 on different Arf proteins, including Arf6, has recently been demonstrated in vitro (Vitale et al., 2000). The strong homology between avian p95-APP1 and mammalian GIT1, the colocalization of the p95-APP1 mutants affecting neurite extension with Arf6 at endocytic vesicles in cotransfected neurons (Fig.4.18, 4.22), and the lack of colocalization of p95-APP1 with Arf1, suggest p95-APP1 as a candidate Arf6 regulator in retinal neurons. Accordingly, while GIT2 has recently been shown to specifically affect Arf1-mediated βCOP distribution (Mazaky et al., 2001), no effect on βCOP distribution by overexpressing p95-APP1 was detected in retinal cells. A direct prove

for the activity of p95-APP1 on Arf6 would come from in vitro GAP assay, which is an important experiment to perform in the future.

A partial overlap in localizations between p95-N and Arf5 was also observed. Like Arf1, Arf5 has been implicated in traffic regulation in the Golgi (Liang and Kornfeld, 1997), although Arf5 could also influence the same cellular pathways as Arf6 through common effectors (Arfophilin) (Shin et al., 2001).

Prove for the involvement of p95-APP1 in the specific regulation of Arf6 comes from the potentiation of neuritogenesis in cells coexpressing wild-type Arf6 with p95-C. This potentiation is not observed in neurons cotransfected with either Arf1 or Arf5 and p95-C. This cooperativity could be prevented by expressing either p95-C2 with wild-type Arf6, or the dominant negative N27Arf6 with p95-C. The data suggest that, for a dynamic morphogenetic process such as growth cone-driven neurite extension, an interplay is needed between a wild-type Arf6, able to dynamically cycle between the GTP- and GDP-bound form, and a p95-APP1 protein that can be dynamically recruited at, and relocalised away from the recycling compartment. Considering these findings, one could speculate that, like Arf1 in the Golgi (Roth, 1999), Arf6 regulates vesicle formation during recycling between endosomes and the plasma membrane, and that like the Arf1-specific ArfGAP protein in the Golgi (Goldberg, 1999), p95-APP1 could play a role in the regulation of these events at recycling endosomes.

The localization of the endogenous p95-APP1 is also fundamental. The preparation of a polyclonal antibody for the protein is in progress, and in the future subcellular localization analysis of the protein, and colocalization with the other components of the complex, will clarify the role of p95-APP1 in recycling membrane events in developing retinal neurons.

4.8.3 The Pix SH3 domain is required for neurite inhibition and vesicles formation by the ArfGAP defective mutant p95C2

By considering the differences between the p95-C and p95-C2 mutants in vesicle formation and neurite extension, the results show that both the lack of an active ArfGAP domain and the presence of the PIX-binding domain are necessary for the accumulation of the p95-complex on enlarged Rab11-positive endosomes, and for the subsequent inhibition of neurite extension. Since the difference between p95-C and p95-C2 consists of the presence of the PIX-binding domain in p95-C2 (Fig. 4.4), it is therefore reasonable to implicate PIX in the recruitment of the p95-APP1 complex at the Rab11 compartment. Support for this hypothesis comes from the finding that mutation of the SH3 domain of PIX specifically prevents the accumulation of the ArfGAP-defective p95-C2 protein at endocytic vacuoles, with concomitant restoration of neurite extension.

It would be important, for the future, to confirm biochemically the association of Rab11, and the other components of the complex, at the p95-C2 vesicles, with expreriments of cell fractionation after transfection of the ArfGAP-deficient mutant.

One complication in the analysis of the function of the PIX/p95 complex originates from the finding that both PIX (Kim et al., 2001) and p95-APP1 (Fig. 4.33) homo-dimerize. Moreover, the biochemical analysis presented here shows that in neural retinal cells p95-APP1 forms stable endogenous complexes with PIX (and paxillin) (Fig.4.3). These observations may explain why inhibition of the association of the p95 complex with endocytic vesicles could only be induced by coexpressing monomeric PIX-SH3 mutants together with monomeric ArfGAP-defective p95-APP1 polypeptides, preventing dimerization with endogenous proteins. In fact, the two mutants can form heterodimers (as shown biochemically). According to the proposed model, the monomeric mutants would not be able to compete with the endogenous complexes, thus

making it impossible for them to accumulate on the Rab11 compartment, and consequently inhibit neurite extension (Fig. 4.37). Any other combination of coexpressed polypeptides in which either the p95- or the PIX-derived mutant is able to form dimers with endogenous components, caused accumulation of ArfGAP-defective p95-C2 at the endocytic compartment, and therefore neurite inhibition (Fig. 4.36, 4.38).

The SH3 domain of PIX is known to bind PAK with high affinity (Manser et al., 1998). PAK is therefore a likely candidate responsible for the subcellular localization of the PIX/p95-APP1 complex, and for the regulation of p95-APP1 function in neuritogenesis. Interestingly, a kinase-independent, Rac/Cdc42 binding-independent role for PAK in both lamellipodium formation at growth cones and neurite-like structures in PC12 cells has already been demonstrated. This function can be inhibited by interfering with the interaction of PAK with PIX (Obermeier et al., 1998).

The analysis shown in this thesis identified a functional link between p95-APP1 and Arf6, which is required for normal and Rac1B-enhanced neurite extension, and provides evidence for an important role of the p95-APP1 complex in the regulation of membrane traffic during neuritogenesis. A model can be proposed in which p95-APP1, recruited at the recycling compartment by Pix, could contribute, by its GAP activity on Arf6, in the formation of membrane vesicles directed towards the growth cone of the elongating neurite (Fig. 4.41). At the growth cone, p95-APP1 would also be involved in the mechanisms of actin cytoskeleton reorganization mediated by Rac1B, and in the regulation of focal contacts formation, since p95 is able to directly interact with paxillin. If the GAP activity is blocked, with the overexpression of GAP-defective mutants of p95-APP1, the recycling event of membrane vesicles directed to the growth cone is not possible anymore, and the process of neurite extension is blocked (Fig. 4.41).

This strongly supports a functional connection between membrane recycling and neurite extension, and provides evidences for an important role of the p95-APP1 complex during the formation of a neurite.

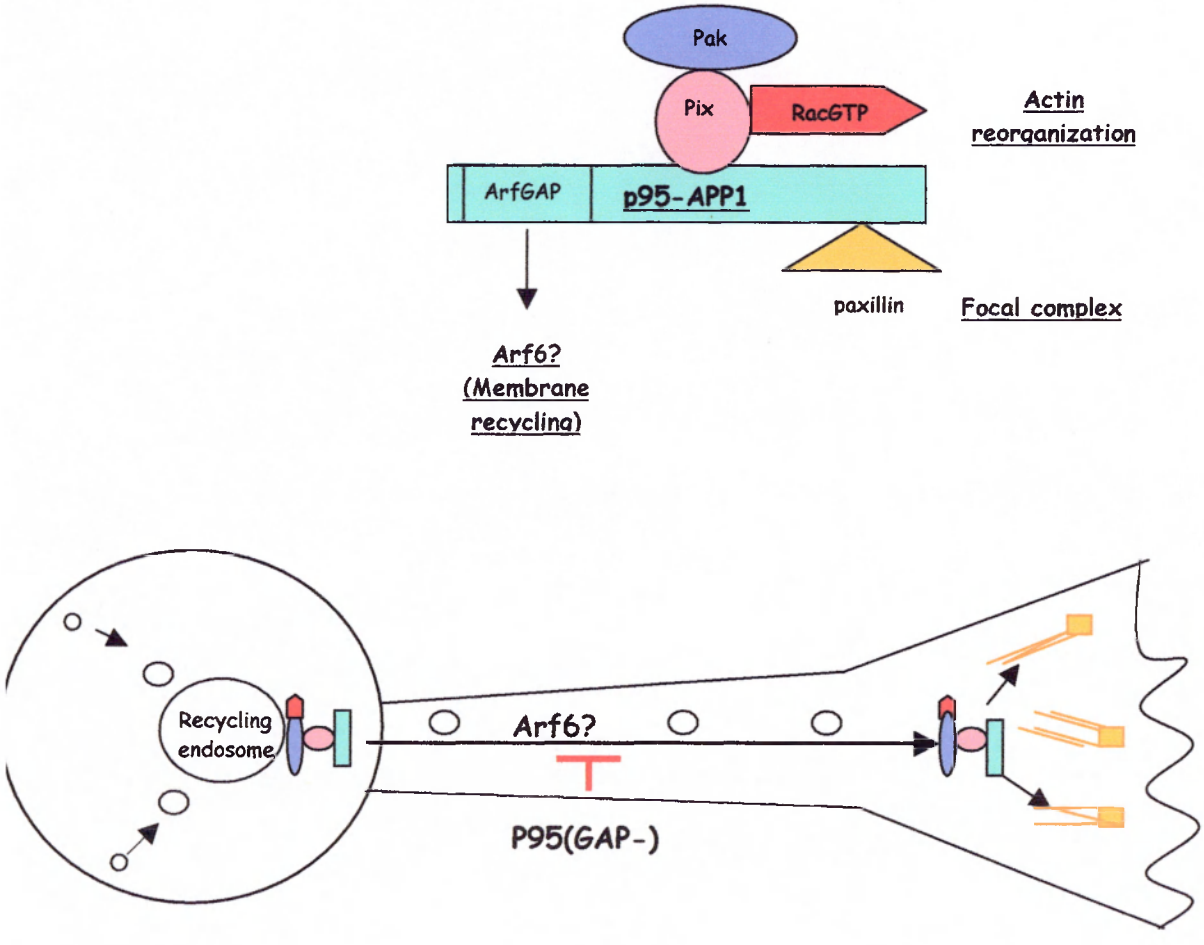

Fig 4.41 Model for p95-APP1 function.

References

Abdul-Manan, N., Aghazadeh, B., Liu, G. A., Majumdar, A., Ouerfelli, O., Siminovitch, K. A. and Rosen, M. K. 1999

Structure of Cdc42 in complex with the GTPase binding domain of the ' Wiskott-Aldrich syndrome ' protein.

Nature 399, 379-383.

Aberle H, Schwartz H, Kemler R. 1996

Cadherin-catenin complex: protein interactions and their implications for cadherin function.

J Cell Biochem. 61(4), 514-23.

Adler, R., Jerdan, J., and A. T. Hewitt. 1985.

Responses of cultured neural retinal cells to substratum-bound laminin and other extracellular matrix molecules.

Dev. Biol. 112,100-114.

Albertinazzi, C., D. Gilardelli, S. Paris, R. Longhi, and I. de Curtis. 1998. Overexpression of a neural-specific Rho family GTPase, cRac1B, selectively induces enhanced neuritogenesis and neurite branching in primary neurons.

J. Cell Biol. 142, 815-825.

Albertinazzi C., Cattelino A., de Curtis I. 1999

Rac GTPases localize at sites of actin reorganization during dynamic remodeling of cytoskeleton of normal embryonic fibroblasts.

Cell Sci. 112, 3821-3831.

Aoki, J., Katoh, H., Mori, K., Negushi, M.2000.

Rnd1, a novel rho family GTPase, induces the formation of neuritic processes in PC12 cells.

Biochem Biophy Res Commun 278, 604-608

Arber, S., Barbayannis, F. A., Hanser, H., Schneider, C., Stanyon, C. A., Bernard, O. and Caroni, P. 1998

Regulation of actin dynamics through phosphorylation of cofilin by LIM-kinase.

Nature 393, 805-809

Awasaki, T. et al. 2000.

The Drosophila Trio plays an essential role in patterning of axons by regulating their directional extension.

Neuron 26, 119–131

Bagrodia, S., Taylor, S. J., Creasy, C. L., Chernoff, J. and Cerione, R. A. 1995

Identification of a mouse p21Cdc42/Rac activated kinase.

J. Biol. Chem. 270, 22731-22737

Bagrodia, S. and Cerione, R. A. 1999

Pak to the future.

Trends Cell. Biol. 9,350-355

Bagrodia, S., Bailey, D., Lenard, Z., Hart, M., Guan, J. L., Premont, R. T., Taylor, S. J. and Cerione, R. A. 1999

A tyrosine-phosphorylated protein that binds to an important regulatory region on the Cool family of p21-activated kinase-binding proteins.

J. Biol. Chem. 274, 22393-22400.

Bateman, J., Shu, H. & Van Vactor, D. 2000

The guanine nucleotide exchange factor Trio mediates axonal development in the Drosophila embryo.

Neuron 26, 93–106

Bernard, V., B.P. Pohl, and G.M. Bokoch. 1999.

Characterization of Rac and Cdc42 activation in chemoattractant-stimulated human neutrophils using a novel assay for active GTPases.

J. Biol. Chem. 274:13198-13204.

Bixby JL, Zhang R 1990

Purified N-cadherin is a potent substrate for the rapid induction of neurite outgrowth.

J Cell Biol. 110(4),1253-60.

Bokoch, G. M., Wang, Y., Bohl, B. P., Sells, M. A., Quilliam, L. A. and Knaus, U. G. 1996

Interaction of the Nck adapter protein with p21-activated kinase (PAK1).

J. Biol. Chem. 271, 25746-25749

Bradke, F. & Dotti, C. G. 1999

The role of local actin instability in axon formation.

Science 283, 1931–1934

Bradke, F. & Dotti, C. G. 2000

Establishment of neuronal polarity: lessons from cultured hippocampal neurons.

Curr. Opin.Neurobiol. 10

Brown, M.T., Andrade, J., Radhakrishna, H., Donaldson, J.G., Cooper, J.A., randazzo, P.A. 1998.

ASAP1, a phospholipid-dependent Arf GTPase activating protein that associates with and is phosphorylated by Src.

Mol. Cell Biol. 18, 7038-7051.

Brown, M. D., Cornejo, B. J., Kuhn, T. B. & Bamburg, J. R. 2000

Cdc42 stimulates neurite outgrowth and formation of growth cone filopodia and lamellipodia.

J. Neurobiol. 43, 352–364

Brugnera E, Haney L, Grimsley C, Lu M, Walk SF, Tosello-Trampont AC, Macara IG, Madhani H, Fink GR, Ravichandran KS. 2002

Unconventional Rac-GEF activity is mediated through the Dock180-ELMO complex

Nat Cell Biol 4(8), 574-82

Caron, E. and Hall, A. 1998

Identifcation of two distinct mechanisms of phagocytosis controlled by different Rho GTPases.

Science 282, 1717-1721

Carpenter, C. L., Tolias, K. F., Van Vugt, A. and Hartwig, J. 1999

Lipid kinases are novel effectors of the GTPase Rac1.

Adv. Enzyme Regul. 39, 299-312.

Cattelino, A., Cairo, S., Malanchini, B. and de Curtis, I. 1997.

Preferential localization of tyrosine phosphorilated paxillin to focal adhesions.

Cell Adhes Commun 4, 457-467.

Cattelino, A., Albertinazzi, C., Bossi, M., Critchley, D.R., and de Curtis, I. 1999.

A cell-free system to study regulation of focal adhesions and of the connected actin cytoskeleton.

Mol Biol Cell 10, 373-391.

Cherfils J, Chardin P. 1999

GEFs: structural basis for their activation of small GTP-binding proteins.

Trends Biochem Sci 24(8), 306-11

Chomczynski, P. and N. Sacchi. 1987.

Single-step method of RNA isolation by acid guanidinium thiocyanate-phenol-chloroform extraction.

Anal. Biochem. 162,156-159.

Craig, A.M., R.J. Wyborski, and G. Banker. 1995.

Preferential addition of newly synthesized membrane protein at axonal growth cones.

Nature 375, 592–594.

D'Souza-Schorey, C., G. Li, M.I. Colombo, and P.D. Stahl. 1995.

A regulatory role for ARF6 in receptor-mediated endocytosis.

Science 267, 1175–1178.

D'Souza-Schorey, C., Boshans, R. L., McDonough, M., Stahl, P. D. and Van Aelst, L. 1997

A role for POR1, a Rac1-interacting protein, in ARF6-mediated cytoskeletal rearrangements.

EMBO J. 16, 5445-5454

D'Souza-Schorey, C., van Donselaar,E., Hsu, V.W., Yang, C., Stahl, P.D., Peters, P.J. 1998.

Arf6 targets recycling vesicles to the plasma membrane: insights from an ultrastructural investigation.

J. Cell Bio. 140, 603-616.

Dai, J., and M.P. Sheetz. 1995.

Axon membrane flows from the growth cone to the cell body.

Cell 83, 693–701.

Daniels, R. H., Hall, P. S. and Bokoch, G. M. 1998

Membrane targeting of p21-activated kinase 1 (PAK1) induces neurite outgrowth from PC12 cells.

EMBO J. 17,754-764

Davis JQ, Bennett V. 1994

Ankyrin binding activity shared by the neurofascin/L1/NrCAM family of nervous system cell adhesion molecules.

J Biol Chem. 1994 269(44), 27163-6.

Debant, A. et al. 1996

The multidomain protein Trio binds the LAR transmembrane tyrosine phosphatase, contains a protein kinase domain, and has separate Rac-specific and Rho-specific guanine nucleotide exchange factor domains.

Proc. Natl Acad. Sci. USA 93, 5466–5471

de Curtis, I. 2001.

Cell migration: GAPs between membrane traffic and the cytoskeleton.

EMBO Rep. 2, 277-281.

De Langhe, S., Haataja, L., Senadheera, D., Groffen, J., Heisterkamp, N. 2002.

Interaction of the small GTPase Rac3 with NRBP, a protein with a kinase-homology domain.

Int J Mol Med 9 (5), 451-9

Dharmawardhane, S., Sanders, L. C., Martin, S. S., Daniels, R. H. and Bokoch,

G. M. 1997

Localization of p21-activated kinase 1 (PAK1) to pinocytic vesicles and cortical actin structures in stimulated cells.

J. Cell. Biol. 138, 1265-1278

Di Cesare, A., S. Paris, C. Albertinazzi, S. Dariozzi, J. Andersen, M. Mann, R. Longhi, and I. de Curtis. 2000

p95-APP1 links membrane transport to Rac-mediated reorganization of actin. Nature Cell Biol. 2, 521-530.

Diefenbach, T.J., P.B. Guthrie, H. Stier, B. Billups, and S.B. Kater. 1999.

Membrane Recycling in the Neuronal Growth Cone Revealed by FM1–43 Labeling.

J. Neurosci. 19,9436–9444

Donaldson, J.G., and C.L. Jackson. 2000.

Regulators and effectors of the ARF GTPases.

Curr. Opin. Cell Biol. 12, 475-482.

Eden S, Rohatgi R, Podtelejnikov AV, Mann M, Kirschner MW. 2002

Mechanism of regulation of WAVE1-induced actin nucleation by Rac1 and Nck.

Nature 2002 418(6899), 790-3

Edwards, D. C., Sanders, L. C., Bokoch, G. M. and Gill, G. N. 1999

Activation of LIM-kinase by Pak1 couples Rac/Cdc42 GTPase signalling to actin cytoskeletal dynamics.

Nat. Cell Biol. 1, 253-259

Flynn, P., Mellor, H., Palmer, R., Panayotou, G. and Parker, P. J. 1998

Multiple interactions of PRK1 with RhoA. Functional assignment of the Hr1 repeat motif.

J. Biol. Chem. 273, 2698-2705

Forscher, P., and Smith, S.J. 1988.

Actions of cytochalasins on the organizations of actin filaments and microtubules in a neuronal growth cone.
J. Cell Biol. 107, 1505-1516.

Gaschet, J., and V.W. Hsu. 1999.
Distribution of ARF6 between membrane and cytosol is regulated by its GTPase cycle.
J. Biol. Chem. 274, 20040-20045.

Gauthier-Rouviere, C., Vignal, E., Meriane, M., Roux, P., Montcourier, P., Fort, P. 1998.
RhoG GTPase controls a pathway that independently activates Rac1 and Cdc42Hs.
Mol Biol Cell 9, 1379-1394.

Goldberg, J. 1999.
Structural and functional analysis of the ARF1-ARFGAP complex reveals a role for coatomer in GTP hydrolysis.
Cell 96, 893-902.

Haataja, L., Groffen, J., and Heisterkamp, N. 1997
Characterization of *RAC*3, a Novel Member of the Rho Family.
J Biol Chem 272, 20984-20988.

Haataja, L., Groffen, J., Heisterkamp, N. 1998.
Identification of a novel Rac3-interacting protein C1D.
Int J Mol Med 1(4), 665-70

Haataja, L., Kaartinen, V., Groffen, J., and Heisterkamp, N. 2002

The small GTPase Rac3 interacts with the Integrin-binding Protein CIB and promotes Integrin αIIbβ3-mediated adhesion and spreading.
J Biol Chem 277(10), 8321-8.

Habets, G.G.M., R.A. van der Kammen, J.C. Stam, F. Michiels, and J.C. Collard. 1995.
Sequence of the human invasion-inducing Tiam 1 gene, its conservation in evolution and its expression in tumor cell lines of different tissue origin
Oncogene. 10, 1371–1376.

Hall, A. 1994
Small GTP-binding poteins and the regulations of the actin cytoskeleton.
Annu Rev Cell Biol 10, 31-54.

Hall, A. 1998
Rho GTPases and the actin cytoskeleton.
Science 279, 509-514

Hart M.J., Sharma S., Elmasry N., Qiu R.G., McCabep, Polakis P, and Bollag G. 1996
Identification of a novel guanine nucleotide exchange factor for the Rho GTPase.
J Biol Chem 271, 25452–25458

Hartwig, J. H., Bokoch, G. M., Carpenter, C. L., Janmey, P. A., Taylor, L. A., Toker, A. and Stossel, T. P. 1995
Thrombin receptor ligation and activated Rac uncap actin filament barbed ends through

phosphoinositide synthesis in permeabilized human platelets.

Cell 82, 643-653

Heisterkamp, N., V. Kaartinen, S. van Soest, G.M. Bokoch, and J. Groffen. 1993.

Human ABR encodes a protein with GAPrac activity and homology to the

DBL nucleotide exchange factor domain.

J. Biol. Chem. 268,16903–16906.

Hoffman S, Sorkin BC, White PC, Brackenbury R, Mailhammer R, Rutishauser U, Cunningham BA, Edelman GM. 1982

Chemical characterization of a neural cell adhesion molecule purified from embryonic brain membranes.

J Biol Chem. 257(13), 7720-9.

Ihara, K., Muraguchi, S., Kato, M., Shimizu, T., Shirakawa, M., Kuroda, S., Kaibuchi, K. and Hakoshima, T. 1998

Crystal structure of human RhoA in a dominantly active form complexed with a GTP analogue.

J. Biol. Chem. 273, 9656-9666

Jackson, T. R., F.D. Brown, Z. Nie, K. Miura, L. Foroni, J. Sun, V.W. Hsu, J.G. Donaldson, and P.A. Randazzo. 2000.

ACAPs are ARF6 GTPase-activating proteins that function in the cell periphery.

J. Cell Biol. 151, 627-638.

Jin, Z. & Strittmatter, S. M. 1997

Rac1 mediates collapsin-1-induced growth cone collapse.

J. Neurosci. 17, 6256–6263

Joyal, J. L., Annan, R. S., Ho, Y. D., Huddleston, M. E., Carr, S. A., Hart, M. J. and Sacks, D. B. 1997

Calmodulin modulates the interaction between IQGAP1 and Cdc42. Identification of IQGAP1 by nanoelectrospray tandem mass spectrometry.

J. Biol. Chem. 272, 15419-15425

Joneson, T., McDonough, M., Bar-Sagi, D. and Van Aelst, L. 1996

RAC regulation of actin polymerization and proliferation by a pathway distinct from Jun kinase.

Science 274, 1374-1376

Kalman, D., Gomperts, S. N., Hardy, S., Kitamura, M. &

Bishop, J. M. 1999

Ras family GTPases control growth of astrocyte processes.

Mol. Biol. Cell 10, 1665–1683

Katoh, H., Yasui, H., Yamaguchi, Y., Aoki, J., Fujita, H., Mori, K., Negishi, M. 2000.

Small GTPase RhoG is a key regulator for neurite outgrowth in PC12 cells.

Mol Cell Biol 20, 7378-7387.

Kawachi H, Fujikawa A, Maeda N, Noda M. 2001

Identification of GIT1/Cat-1 as a substrate molecule of protein tyrosine phosphatase zeta /beta by the yeast substrate-trapping system.

PNAS 98(12), 6593-8.

Kim, A. S., Kakalis, L. T., Abdul-Manan, N., Liu, G. A. and Rosen, M. K. 2000

Autoinhibition and activation mechanisms of the Wiskott-Aldrich syndrome protein.
Nature 404, 151-158

Kim S, Lee SH, Park D. 2001.
Leucine zipper-mediated homodimerization of the p21-activated kinase-interacting factor, beta Pix. Implication for a role in cytoskeletal reorganization.
J. Biol. Chem. 276, 10581-10584.

King FJ, Hu E, Harris DF, Sarraf P, Spiegelman BM, Roberts TM. 1999
DEF-1, a novel Src SH3 binding protein that promotes adipogenesis in fibroblastic cell lines.
Mol Cell Biol. (3), 2330-7.

Kobayashi, K., Kuroda, S., Fukata, M., Nakamura, T., Nagase, T., Nomura, N., Matsuura, Y., Yoshida-Kubomura, N., Iwamatsu, A. and Kaibuchi, K. 1998
p140Sra-1 (specifically Rac1-associated protein) is a novel specific target for Rac1 small GTPase.
J. Biol. Chem. 273, 291-295

Kondo, A., Hashimoto, S., Yano, H., Nagayama, K., Mazaki, Y., Sabe, H. 2000
A new paxillin-binding protein, PAG3/PAPα/KIAA0400, bearing an ADP-ribosylation factor GTPase activating protein activity, is involved in paxillin recruitment to focal adhesions and cell migration.
Mol Biol Cell 11, 1315-1327.

Kozma, R., Ahmed, S., Best, A., and lim, L. 1995
The Ras-related protein Cdc42Hs and bradykinin promote formation of peripheral actin microspikes and filopodia in Swiss 3T3 fibroblasts.

Mol cell Biol 101, 2134-2144.

Kozma, R., Ahmed, S., Best, A. & Lim, L. 1996

The GTPaseactivating protein n-Chimaerin cooperates with Rac1 and Cdc42Hs to induce the formation of lamellipodia and filopodia.

Mol. Cell. Biol. 16, 5069–5080

Kozma, R., Sarner, S., Ahmed, S. & Lim, L. 1997

Rho family GTPases and neuronal growth cone remodelling: relationships between increased complexity induced by Cdc42Hs, Rac1, and acetylcholine and collapse induced RhoA and lysophosphatidic acid.

Mol. Cell. Biol. 17, 1201–1211

Lakso M, Pichel JG, Gorman JR, Sauer B, Okamoto Y, Lee E. 1996.

Efficient *in vivo* manipulation of mouse genomic sequences at the zygote stage.

PNAS 93, 5860-5865.

Lamarche, N. and Hall, A. 1994

GAPs for rho-related GTPases.

Trends Genet. 10, 436-440.

Lamarche, N., Tapon, N., Stowers, L., Burbelo, P. D., Aspenstrom, P., Bridges, T., Chant, J. and Hall, A. 1996

Rac and Cdc42 induce actin polymerization and G1 cell cycle progression independently of p65PAK and the JNK/SAPK MAP kinase cascade.

Cell 87, 519-529

Lamoureux, P., Altun-Gultekin, Z. F., Lin, C., Wagner, J. A. & Heidemann, S. R. 1997
Rac is required for growth cone function but not neurite assembly.
J. Cell Sci. 110, 635–641

Lee, T., Winter, C., Marticke, S. S., Lee, A. & Luo, L. 2000
Essential roles of Drosophila RhoA in the regulation of neuroblast proliferation and dendritic but not axonal morphogenesis.
Neuron 25, 307–316

Lehrach, H., D. Diamond, J.M. Wozney, and H. Boedtker. 1977.
RNA molecular weight determinations by gel electrophoresis under denaturing conditions, a critical reexamination.
Biochemistry 16, 4743-4751.

Liebl, E. et al. 2000
Dosage-sensitive, reciprocal genetic interactions between the Abl tyrosine kinase and the putative GEF trio reveal Trio's role in axon pathfinding.
Neuron 26, 107–118

Lu, W., Katz, S., Gupta, R. and Mayer, B. J. 1997
Activation of Pak by membrane localization mediated by an SH3 domain from the adaptor protein Nck.
Curr. Biol. 7, 85-94

Luo, L. et al. 1996

Differential effects of the Rac GTPase on Purkinje cell axons and dendritic trunks and spines.

Nature 379, 837–840

Luo, L., Liao, Y. J., Jan, L. Y. & Jan, Y. N. 1994

Distinct morphogenetic functions of similar small GTPases: Drosophila Drac1 is involved in axonal outgrowth and myoblast fusion.

Genes Dev. 8, 1787–1802

Luo, L., Jan, L. Y. and Jan, Y. N. 1997

Rho family GTP-binding proteins in growth cone signalling.

Curr. Opin. Neurobiol. *7*, 81-86

Luo, L. 2000.

Rho GTPases in neuronal morphogenesis.

Nat. Rev. Neurosci. 1, 173-180.

Malosio, M.L., D. Gilardelli, S. Paris, C. Albertinazzi, and I. de Curtis. 1997. Differential expression of distinct members of the Rho family of GTP-binding proteins during neuronal development: Identification of Rac1B, a new neural-specific member of the family.

J. Neurosci. 17, 6717-6728.

Mandiyan, V., J. Andreev, J. Schlessinger, and S.R. Hubbard. 1999.
Crystal structure of the ARF-GAP domain and ankyrin repeats of PYK2-associated protein beta.
EMBO J. 18, 6890-6898.

Manser, E., Leung, T., Salihuddin, H., Zhao, Z. S. and Lim, L. 1994
A brain serine/threonine protein kinase activated by Cdc42 and Rac1.
Nature 367, 40-46

Manser, E., Chong, C., Zhao, Z. S., Leung, T., Michael, G., Hall, C. and Lim, L.
1995
Molecular cloning of a new member of the p21-Cdc42/Rac-activated kinase
(PAK) family.
J. Biol. Chem. 270, 25070-25078

Manser, E., T.H. Loo, C.G. Koh, Z.S. Zhao, X.Q. Chen, L. Tan, I. Tan, T. Leung, and L. Lim. 1998.
PAK kinases are directly coupled to the PIX family of nucleotide exchange factors.
Molec. Cell 1, 183-192.

Matafora V., S. Paris, S. Dariozzi, and I. de Curtis. 2001.
Molecular mechanisms regulating the subcellular localization of p95-APP1 between the endosomal recycling compartment and sites of actin organization at the cell surface.
J. Cell Sci. 114, 4509-4520.

Miki, H., Miura, K. and Takenawa, T. 1996
N-WASP, a novel actin-depolymerizing protein, regulates the cortical cytoskeletal rearrangement in a PIP2-dependent manner downstream of tyrosine kinases.

EMBO J. 15, 5326-5335

Miki, H. and Takenawa, T. 1998

Direct binding of the verprolin-homology domain in N-WASP to actin is essential for cytoskeletal reorganization.

Biochem. Biophys.Res. Commun. 243, 73-78

Miki H, Yamaguchi H, Suetsugu S, Takenawa T. 2000

IRSp53 is an essential intermediate between Rac and WAVE in the regulation of membrane ruffling

Nature 2000,408(6813), 732-5

Mira, J.P., Benard, V., Groffen, J., Sanders, L.C.and Ulla G. Knaus. 1999

Endogenous, hyperactive Rac3 controls proliferation of breast cancer cells by a p21-activated kinase-dependent pathway.

PNAS 97, 185-189.

Mott, H. R., Owen, D., Nietlispach, D., Lowe, P. N., Manser, E., Lim, L. and Laue, E. D. 1999

Structure of the small G protein Cdc42 bound to the GTPase-binding domain of ACK.

Nature 399, 384-388

Murphy, G.A., Solski, P.A., Jillian, S.A., Perez de la Ossa, P., d'eustachio, P., Der, C.J., Rush, M.G. 1999.

Cellular functions of TC10, a Rho family GTPase: regulation of morphology, signal transduction and cell growth.

Oncogene 18, 3831-3845.

Nakayama, A. Y., Harms, M. B. & Luo, L. 2000

Small GTPases Rac and Rho in the maintenance of dendritic spines and branches in hippocampal pyramidal neurons.

J. Neurosci. 20, 5329–5338

Nassar, N., Hoffman, G. R., Manor, D., Clardy, J. C. and Cerione, R. A. 1998

Structures of Cdc42 bound to the active and catalytically compromised forms of Cdc42GAP.

Nat. Struct. Biol. 5, 1047-1052

Neudauer, C.L., Joberty, G., Tatsis, N., Macara, I.G. 1998.

Distinct cellulare effects and interactions of the Rho-family GTPase TC10.

Curr Biol 8 1151-1160.

Neugebauer KM, Tomaselli KJ, Lilien J, Reichardt LF. 1988

N-cadherin, NCAM, and integrins promote retinal neurite outgrowth on astrocytes in vitro.

J Cell Biol. 107(3), 1177-87.

Newsome, T. et al. 2000

Trio combines with Dock to regulate Pak activity during photoreceptor axon pathfinding in Drosophila.

Cell 101, 283–294

Nobes, C.D., and Hall, A. 1995.

Rho, Rac and Cdc42 GTPases regulate the assembly of multimolecular focal complexes associated with actin stress fibers, lamellipodia and filopodia.

Cell 81: 53-62.

Nobes, C. D. and Hall, A. 1999

Rho GTPases control polarity, protrusion, and adhesion during cell movement.

J. Cell Biol. 144, 1235-1244

Nobes, C.D., Lauritzen, I., Mattei, M.G., Paris, S., Hall, A., Chardin, P. 1998

A new member of the Rho family, Rnd1, promotes disassembly of actin filament structures and loss of cell adhesion.

J Cell Biol 141, 187-197.

Obermeier, A., S. Ahmed, E. Manser, S.C. Yen, C. Hall, and L. Lim. 1998.

PAK promotes morphological changes by acting upstream of Rac.

EMBO J. 17, 4328-4339.

Peck, J., Douglas, G., Wu C., Burbelo P. 2002

Human RhoGAP domain-containing proteins: structure, function and evolutionary relationships.

FEBS Lett 528, 1-3

Peters, P.J., V.W. Hsu, C.E. Ooi, D. Finazzi, S.B. Teal, V. Oorschot, J.G. Donaldson, R.D. Klausner. 1995.

Overexpression of wild-type and mutant ARF1 and ARF6: distinct perturbations of nonoverlapping membrane compartments.

J. Cell Biol. 128, 1003-1017.

Popov, S., A. Brown, and M.M. Poo. 1993.

Forward plasma membrane flow in growing nerve processes.

Science 259, 244 –246.

Prekeris R., D.L. Foletti, and R.H. Scheller. 1999.

Dynamics of tubulovesicular recycling endosomes in hippocampal neurons.

J Neurosci. 19, 10324-10337.

Prokopenko, S. N., Saint, R. and Bellen, H. J. 2000

Untying the gordian knot of cytokinesis : role of small g proteins and their regulators. J. Cell Biol. 148, 843-848

Radhakrishna, H., R.D. Klausner, and J.G. Donaldson. 1996.

Aluminum fluoride stimulates surface protrusions in cells overexpressing the ARF6 GTPase.

J. Cell Biol. 134, 935-947.

Radhakrishna, H., O. Al-Awar, Z. Khachikian, and J.G. Donaldson. 1999.

ARF6 requirement for Rac ruffling suggests a role for membrane trafficking in cortical actin rearrangements.

J. Cell Sci. 112, 855-866.

Rameh, L. E., Arvidsson, A., Carraway, K. L. R., Couvillon, A. D., Rathbun, G., Crompton, A., VanRenterghem, B., Czech, M. P., Ravichandran, K. S., Burakoff, S. J.

et al. 1997

A comparative analysis of the phosphoinositide binding specificity of pleckstrin homology domains.

J. Biol. Chem. 272, 22059-22066

Randazzo, P. A., J. Andrade, K. Miura, M.T. Brown, Y.-Q. Long, S. Stauffer, P. Roller, P. and J.A. Cooper. 2000.

The ARF GAP ASAP1 regulates the actin cytoskeleton.

Proc. Natl. Acad. Sci. *USA* 97, 4011-4016.

Ren, M., G. Xu, J. Zeng, C. De Lemos-Chiarandini, M. Adesnik, and D.D. Sabatini. 1998.

Hydrolysis of GTP on rab11 is required for the direct delivery of transferrin from the pericentriolar recycling compartment to the cell surface but not from sorting endosomes.

Proc. Natl. Acad. Sci. *USA* 95, 6187-6192.

Rhom, B., Rahim, B., Kleiber, B., ovatta, I., Pushel, A.W. 2000.

The semaphorin 3A receptor may directly regulate the activity of small GTPases.

FEBS Lett 486, 68-72.

Ridley, A. J. 2001

Rho GTPases and cell migration

Journal of Cell Science 114, 2713-2722

Ridley, A. J., Paterson, H. F., Johnston, C. L., Diekmann, D. and Hall, A. 1992

The small GTP-binding protein rac regulates growth factor-induced membrane ruffling.

Cell 70, 401-410

Ridley A.J., and A. Hall 1992.

The small GTP-binding protein Rho regulates the assembly of focal adhesion and actin stress fibers in response to growth factors.

Cell 70, 389-399.

Rittinger, K., Walker, P. A., Eccleston, J. F., Nurmahomed, K., Owen, D., Laue, E., Gamblin, S. J. and Smerdon, S. J. 1997

Crystal structure of a small G protein in complex with the GTPase- activating protein rhoGAP.

Nature 388, 693-697

Rittinger, K., Walker, P. A., Eccleston, J. F., Smerdon, S. J. and Gamblin, S. J. 1997

Structure at 1.65 A/ of RhoA and its GTPase-activating protein in complex with a transition-state analogue.

Nature 389, 758-762

Rivero-Lezcano, O. M., Marcilla, A., Sameshima, J. H. and Robbins, K. C. 1995

Wiskott-Aldrich syndrome protein physically associates with Nck through Src homology 3 domains.

Mol. Cell Biol. 15, 5725-5731

Rohatgi, R., Ma, L., Miki, H., Lopez, M., Kirchhausen, T., Takenawa, T. and Kirschner, M. W. 1999

The interaction between N-WASP and the Arp2/3 complex links Cdc42-dependent signals to actin assembly.

Cell 97, 221-231

Roth, M.G. 1999.

Snapshots of ARF1: Implications for Mechanisms of Activation and Inactivation.

Cell . 97, 149–152.

Ruchhoeft, M. L., Ohnuma, S., McNeill, L., Holt, C. E. & Harris, W. A. 1999

The neuronal architecture of Xenopus retinal ganglion cells is sculpted by Rho-family GTPases in vivo.

J. Neurosci. 19, 8454–8463

Ruppert, C., Kroschewski, R., Bahler, M. 1993

Identification, characterization and cloning of myr1, a mammalian myosin-I

J Cell Biol 120, 1393-1403.

Sahai, E., Alberts, A. S. and Treisman, R. 1998

RhoA effector mutants reveal distinct effector pathways for cytoskeletal reorganization, SRF activation and transformation.

EMBO J. 17, 1350-1361

Sanders, L. C., Matsumura, F., Bokoch, G. M. and de Lanerolle, P. 1999

Inhibition of myosin light chain kinase by p21-activated kinase.

Science 283, 2083-2085

Schmidt A, Hall A. 2002

Guanine nucleotide exchange factors for Rho GTPases: turning on the switch.

Genes Dev 16(13), 1587-609

Seabra, M. C. 1998.

Membrane association and targeting of prenylated Ras-like GTPases.

Cell Signal. 10, 167-172.

Sells, M. A., Knaus, U. G., Bagrodia, S., Ambrose, D. M., Bokoch, G. M. and

Chernoff, J. 1997

Human p21-activated kinase (Pak1) regulates actin organization in mammalian cells.

Curr. Biol. 7, 202-210

Serafini, T., S.A. Colamarino, E.D. Leonardo, H. Wang, R. Beddington, W.C. Skarnes, and M. Tessier-Lavigne. 1996.

Netrin-1 is required for commissural axon guidance in developin vertebrate nervous system.

Cell 87, 1001-1014.

Settleman, J. 1999

Rho GTPases in development.

Prog. Mol. Subcell. Biol. *22*, 201-229

Shea, T.B., and V.S. Sapirstein. 1988.

Vesicle-mediated delivery of membrane to growth cones during neuritogenesis in embryonic rat primary neuronal cultures.

Exp.Cell Biol. 56, 67–73.

Shin O.H., A.D. Couvillon, and J.H. Exton. 2001.

Arfophilin is a common target of both class II and class III ADP-ribosylation factors.

Biochemistry 40, 10846-10852.

Simonsen, A., Lippe, R., Christoforidis, S., Gaullier, J. M., Brech, A., Callaghan, J., Toh, B. H., Murphy, C., Zerial, M. and Stenmark, H.1998.
EEA1 links PI(3)K function to Rab5 regulation of endosome fusion.
Nature 394, 494-498.

Sone, M. et al. 1997
Still life, a protein in synaptic terminals of Drosophila homologous to GDP–GTP exchangers.
Science 275, 543–547

Sonnichsen, B., S. De Renzis, E. Nielsen, J. Rietdorf, and M. Zerial. 2000.
Distinct membrane domains on endosomes in the recycling pathway visualized by multicolor imaging of Rab4, Rab5, and Rab11.
J. Cell Biol. 149, 901-914.

Steven, R. et al.1998
UNC-73 activates the Rac GTPase and is required for cell and growth cone migrations in C. elegans.
Cell 92, 785–795

Szafer, E., E. Pick, M. Rotman, S. Zuck, I. Huber, and D. Cassel. 2000.
Role of coatomer and phospholipids in GTPase-activating protein-dependent hydrolysis of GTP by ADP-ribosylation factor-1.
J. Biol. Chem. 275, 23615-23619.

Tanabe, K., Tachibana, T., Yamashita, T., Che, Y.H., Yoneda, Y., Ochi, T., Tohyama, M., Yoshikawa, H., Kiyama, H. 2000

The small GTP-binding protein TC10 promotes nerve elongation in neuronal cells, and its expression is induced durino nerve regeneration in rats.
J Neurosci 20, 4138-4144

Tanaka, E., and J. Sabry. 1995.
Making the connection: cytoskeletal rearrangements during growth cone guidance.
Cell 83:171-176.

Threadgill, R., Bobb, K. & Ghosh, A. 1997
Regulation of dendritic growth and remodeling by Rho, Rac, and Cdc42.
Neuron 19, 625–634

Timpl, R., H. Rhode, P. Gehron-Robey, S. Rennard,, J.M. Foidart, and G. Martin. 1979.
Laminin, a glycoprotein from basement membrane.
J. Biol. Chem. 254, 9933-9937.

Tolias, K. F., Hartwig, J. H., Ishihara, H., Shibasaki, Y., Cantley, L. C. and Carpenter, C. L. 2000
Type ialpha phosphatidylinositol-4-phosphate 5-kinase mediates rac dependent actin assembly.
Curr. Biol. 10, 153-156

Tu, H. and Wigler, M. 1999
Genetic evidence for Pak1 autoinhibition and its release by Cdc42.
Mol. Cell. Biol. 19, 602-611

Turner, C.E., M.C. Brown, J.A. Perrotta, M.C. Riedy, S.N. Nikolopoulos, A.R. McDonald, S. Bagrodia, S. Thomas, and P.S. Leventhal. 1999.
Paxillin LD4 motif binds PAK and PIX through a novel 95-kD ankyrin repeat, ARF-GAP protein: A role in cytoskeletal remodeling.
J. Cell Biol. 145, 851–863.

Ullrich, O., S. Reinsch, S. Urbe, M. Zerial, and R.G. Parton. 1996.
Rab11 regulates recycling through the pericentriolar recycling endosome.
J. Cell Biol. 135, 913-924

Van Aelst, L., Joneson, T. and Bar-Sagi, D. 1996
Identification of a novel Rac1-interacting protein involved in membrane ruffling.
EMBO J. 15, 3778-3786

Van Aelst L, D'Souza-Schorey C. 1997
Rho GTPases and signaling networks.
Genes Dev. 11(18), 2295-322.

van Leeuwen, F. N. et al. 1997
The guanine nucleotide exchange factor Tiam1 affects neuronal morphology; opposing roles for the small GTPases Rac and Rho.
J. Cell Biol. 139, 797–807

Vance, J.E., D. Pan, D.E. Vance, and R.B. Campenot. 1991.
Biosynthesis membrane lipids in rat axons.
J. Cell Biol. 115, 1061–1068.

Vastrik, I., Eickholg, B. J., Walsh, F. S., Ridley, A. & Doherty, P. 1999

Sema3A induced growth-cone collapse is mediated by Rac1 amino acids 17–32.

Curr. Biol. 9, 991–998

Vikis HG, Li W, Guan KL 2002

The plexin-B1/Rac interaction inhibits PAK activation and enhances Sema4D ligand binding.

Genes Dev 16(7), 836-45

Vitale, N., W.A. Patton, J. Moss, M. Vaughan, R.J. Lefkowitz, and R.T. Premont. 2000.

GIT proteins, a novel family of phosphatidylinositol 3,4,5-trisphosphate-stimulated GTPase-activating proteins for ARF6.

J. Biol. Chem. 275, 13901–13906.

Wei, Y., Zhang, Y., Derewenda, U., Liu, X., Minor, W., Nakamoto, R. K., Somlyo, V., Somlyo, A. P. and Derewenda, Z. S. 1997

Crystal structure of RhoA-GDP and its functional implications.

Nat. Struct. Biol. 4, 699-703

Welsh, C.F., J. Moss, and M. Vaughan. 1994.

Isolation of recombinant ADP-ribosylation factor 6, a -20-kDa guanine nucleotide-binding protein, in an activated GTP-bound state.

J. Biol. Chem. 269, 15583-15587

Weston, C., Yee, B., Hod, E. & Prives, J. 2000

Agrin-induced acetylcholine receptor clustering is mediated by the small guanosine triphosphatases Rac and Cdc42.

J. Cell Biol.150, 205–212

Wolf, E., P.S. Kim, and B. Berger. 1997.

MultiCoil: a program for predicting two- and three-stranded coiled coils.

Protein Sci. 6, 1179–1189.

Wong, W. T., Faulkner-Jones, B., Sanes, J. R. & Wong,

R. O. L. 2000

Rapid dendritic remodeling in the developing retina: dependence on neurotransmission and reciprocal regulation by Rac and Rho.

J. Neurosci. 20, 5024–5036

Yamada, K. M., Spooner, B. S. & Wessells, N. K. 1970

Axon growth: roles of microfilaments and microtubules.

Proc. Natl Acad. Sci. USA 66, 1206–1212

Yamashita, T., Ticker, K. L. & Barde, Y.-A. 1999

Neurotrophin binding to the p75 receptor modulates Rho activity and axonal outgrowth.

Neuron 24, 585–593

Zhao, Z. S., Manser, E., Loo, T.H., Lim, L. 2000

Interaction between Pak-interacting exchange factor Pix to Git1 promotes focal complex disassembly

Mol Cell Biol 20, 6354-6363.

Zipkin, I. D., Kindt, R. M. & Kenyon, C. J.1997

Role of a new Rho family member in cell migration and axon guidance in C. elegans.

Cell 90, 883–894

List of illustrations

List of abbreviations

AD: adult

CEFs: Chichen Embryo Fibroblasts

DMEM: Dulbecco's Modified Eagle's Medium

DMSO: Dimethyl Sulphoxide

EDTA: Ethylenediaminetetra-acetic acid

EEA1: Early Endosome Antigen 1

ES: Embryonic Stem

FCS: Fetal Calf Serum

GAP: GTPase Activating Protein

GEF: Guanine Exchange Factor

kD: kiloDalton

K.O.: Knock-Out

mAb: monoclonal antibody

nf: neurofilament

pAb: polyclonal antibody

PI: pre-immune

PBS: Phosphate Buffer Saline

PBS domain: Paxillin Binding Domain

RGM: Retinal Growth Medium

SDS: Sodium-Dodecyl-Sulphate

SHD: Spa2 Homology Domain

Tris: Tris(hydroxymethyl)methylamine

VPM: Ventral Plasma Membrane